MAREES TERRESTRES

BULLETIN D'INFORMATIONS

N° 90

15 SEPTEMBRE 1983

Association Internationale de Geodesie

Commission Permanente des Marees Terrestres

Editeur Prof. Paul MELCHIOR

Observatoire royal de Belgique

Avenue Circulaire 3

1180 Bruxelles

TABLE DES MATIERES

Traduction

PARAMETRES DE LA MAREE ELASTIQUE DANS LA REGION DE LA DEPRESSION DNIEPR-DONETZ

V.G. Balenko

Etude de la Terre comme planète par les méthodes
de l'Astronomie, de la Géophysique et de la Géodésie.

Académie des Sciences d'Ukraine,
Observatoire Astronomique Principal, Kiev 1982.

Un des problèmes essentiels dans l'étude des marées terrestres consiste à déterminer les amplitudes et les phases des ondes de la marée élastique qu'il est convenu d'appeler globales. On n'a pas réussi jusqu'à présent à résoudre ce problème avec une précision de quelques pourcents, malgré de grands efforts. Même pour l'onde la plus importante, M_2, les valeurs obtenues pour le facteur d'amplitude γ dans ces stations présentent une divergence de 0,3 à 1,0 tandis que l'écart de phases entre la marée théorique et observée atteint des dizaines de degrés.

On pourrait considérer à priori que cette divergence n'a pas de cause géophysique puisque la marée élastique concerne tout le corps de la Terre jusqu'en son centre. Cependant les observations clinométriques se font à la surface de l'écorce terrestre constituée de blocs distincts avec une géologie et une topographie variables. C'est pourquoi les résultats de ces observations sont troublés par des perturbations d'origine locale : couverture, topographie, géologie et tectonique. Le calcul de ces effets, sauf conditions particulières, montre qu'ils ne sont pratiquement pas importants. C'est pourquoi un bon choix du site des observations clinométriques, pour lequel on peut négliger les effets locaux, est important et est une condition nécessaire de succès.

Au début des années 60 on a conçu, à l'Observatoire gravimétrique de Poltava, sous la direction de Z.N. Aksentieva, un plan de recherches clinométriques couvrant les 10 à 20 dernières années au cours desquelles un

groupe de collaborateurs a étudié la possibilité d'obtenir des valeurs régionales des constantes harmoniques des ondes de marées avec une précision d'au moins 1 % pour une région de quelques centaines de kilomètres. Ce travail a été accompli avec succès de 1963 à 1980.

Dans les années soixante on a montré que les résultats des observations clinométriques dépendent de la structure tectonique de la région. Un travail de P.S. Matveyev présentait un grand intérêt, car il examinait l'influence de l'affaiblissement de zones de large étendue dans l'écorce terrestre sur la déformation de marée. Le choix de la région pour l'installation des clinomètres doit satisfaire à deux exigences principales :

1) se trouver à l'intérieur du continent afin que l'influence des zones proches de la marée océanique soit tout à fait négligeable;
2) éliminer l'influence des fractures et, pour cela, se trouver sur une plateforme recouverte d'une épaisseur de plusieurs kilomètres de roches sédimentaires, loin des structures mobiles.

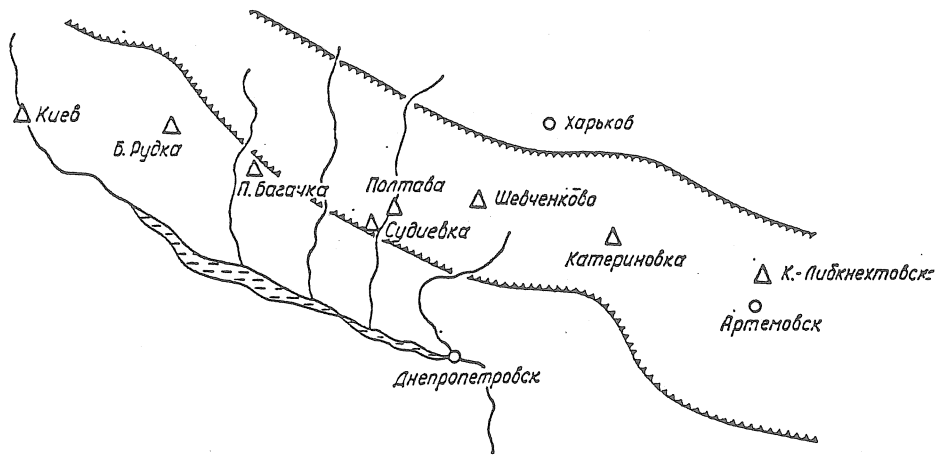

Fig. 1 : Schéma du profil clinométrique Kiev-Artemovsk.
1 - Stations clinométriques; 2 - fractures larges limitant la dépression Dniepr-Donetz.

Les socles cristallins, les sites montagneux, les zones côtières conviennent bien pour les travaux de détermination des caractéristiques de marées régionales et par conséquent globales.

Sur le territoire de l'Ukraine, la région de la dépression du Dniepr-Donetz correspondait à ces conditions. Partant des possibilités de l'Observatoire de Poltava on a décidé de placer les stations clinométriques le long de la dépression Kiev-Artemovsk (Fig. 1). A la station de Kiev les observations ont été faites en deux points et dans les stations [illegible] Berezovka

Roudka, Pokrovskaïa, Bagatchka, Schevtchenkov et Katerinovka dans des puits d'une profondeur de 12 à 15 m et, dans la station Karlo-Libknechtovsk, dans une mine de sel à une profondeur de 120 m et dans quatre salles d'après un petit profil d'une longueur d'environ 600 mètres. Les observations clinométriques sont déjà terminées en trois points : Soudievka, Velikie Boudicha et Poltava par un second groupe de collaborateurs sous la direction de P.S. Matveyev et au point de Poltava I par Z.N. Aksentieva (série de 11 années).

Dès la première étape des travaux il a fallu définir les conditions pour la construction des stations clinométriques qui diminueraient au maximum les perturbations provenant les effets locaux. Dans les années 60 il n'y avait pas encore de recommandations théoriques à cet effet et il a fallu se baser uniquement sur les représentations de l'influence perturbatrice de la zone affaiblie.

Dès l'abord l'attention a été attirée sur le relief voisin du site d'installation des appareils et, dans la station de Karlo-Libknechtovsk, sur la possibilité de perturbations venant des volumes vidés de sel.

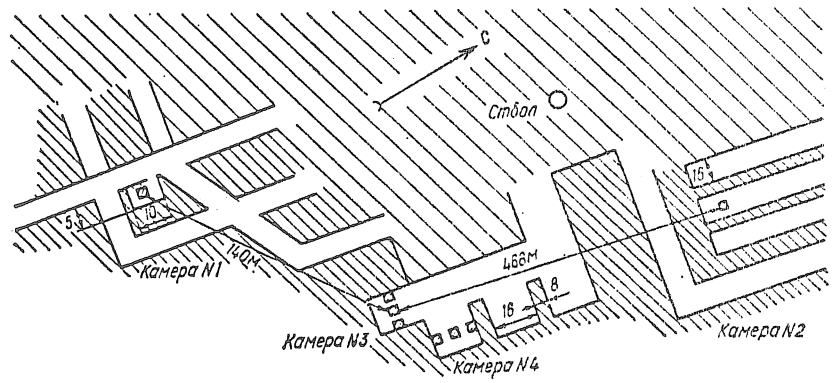

Fig. 2 : Schéma de disposition des salles clinométriques dans la mine N° 1 "Artemsol".

Les premières observations clinométriques du profil Kiev-Artemovsk ont été faites dans des cavernes de la réserve Lavro-Petcherski dans des conditions de topographie complexe. Les résultats obtenus ont montré que le relief trouble sensiblement les caractéristiques de marées et toutes les dernières stations ont été placées dans un endroit plat, loin de ravins, de constructions massives et d'édifices.

Dans la seconde moitié des années 70, Lecolazet, Harrisson, Chassiliev et des co-auteurs ont créé en une première approximation la théorie

TABLE 1 : Constantes harmoniques de l'onde M_2 obtenues dans les stations clinométriques de la dépression Dniepr-Donetz.

Station clinométrique	Observations				Corrigé de la topographie				Corrigé de la topographie et de la marée océanique			
	NS		EW		NS		EW		NS		EW	
	γ	Δφ (degrés)	γ	Δφ (degrés)	γ	Δφ (degrés)	γ	Δφ (degrés)	γ	Δφ (degrés)	γ	Δφ (degrés)
Kiev	0,704	±1,62	0,718	—5,48								
	±0,026	±2,26	±0,046	±2,51								
Beresovaïa Boudicha	0,712	—1,20	0,718	—4,23	0,703	—1,13	0,717	—4,28	0,740	+0,35	0,735	—1,34
	0,005	0,78	0,005	0,51								
Pokrovskaïa	0,684	—1,00	0,717	—4,90	0,658	—0,63	0,710	—5,30	0,693	+1,03	0,728	—2,48
	0,008	0,62	0,008	0,74								
Bagatchka	0,699	+0,57	0,710	—4,18	0,699	+0,57	0,710	—4,18	0,735	+2,11	0,728	—1,90
	0,008	0,94	0,007	1,08								
Schevtchenko	0,689	—1,12	0,714	—0,53								
	0,009	0,94	0,006	0,48								
Katerinovka	0,688	—0,32	0,718	—1,11	0,688	—0,32	0,718	—1,11	0,725	+1,22	0,735	+0,64
	0,003	1,26	0,003	1,39								
Karlo-Likknechtovsk	0,686	—2,38	0,702	—0,46	0,684	—1,47	0,701	—1,36	0,720	+0,06	0,721	+1,11
	0,019	1,42	0,012	1,50								
Poltava	0,679	+0,78	0,719	—3,92	0,671	+0,77	0,717	—3,91	0,707	+2,30	0,727	—1,44
	0,002	0,12	0,002	0,15								
Soudievka	0,693	—0,38	0,714	—3,10								
	±0,004	±0,53	±0,002	±0,68								

mathématique des effets de cavité, de topographie et de géologie. C'est pourquoi on a vu la possibilité de calculer les corrections de l'effet de topographie pour les stations du profil Kiev-Artemovsk. Nous donnons dans la table 1 les valeurs du facteur d'amplitude γ et de la phase $\Delta\phi$ avant et après l'introduction de ces corrections. En analysant la méthode de calcul des perturbations dues à la zone affaiblie et les résultats obtenus dans les stations du profil Kiev-Artemovsk, les auteurs sont arrivés à la conclusion que le calcul des corrections de topographie et de géologie, avec la précision nécessaire, exige des recherches complémentaires tellement coûteuses que c'est pratiquement irréalisable. C'est pourquoi, dans la suite, les stations clinométriques devront être établies dans un endroit plat sur un rayon de 100 m, dont l'inclinaison ne doit pas dépasser 1° et où ravins et collines ne doivent pas se trouver plus près que 500 à 1000 m.

Les observations clinométriques à la station de Karlo-Libnechtovsk dans la mine de sel n° 1 "Artemsol" ont été exécutées depuis 1967, pendant 10 ans, dans quatre salles et sur huit socles. Le schéma de disposition des salles est représenté sur la figure 2. Les observations dans la salle n° 1 avait comme but, outre de déterminer γ et $\Delta\phi$, d'expliquer le degré de perturbation possible provenant de l'influence des travaux de mine (effet de cavité). Pour cela les clinomètres ont été installés dans une grande niche de dimensions 10 x 5 x 4 m taillée en entier à la limite du sol de la mine. Dans ces conditions il fallait s'attendre a une valeur sensible de l'effet de cavité, s'il existe. Pour ces ondes semi-diurnes dans la salle n° 1 on a obtenu $\gamma = 0{,}47$. Ainsi, l'effet de cavité peut altérer les constantes harmoniques des ondes de marées de dizaines et même de centaines de pourcents. Dans une seconde étape des recherches dans la mine n° 1 on s'est posé le problème d'obtenir les paramètres γ et $\Delta\phi$ affranchis de l'effet perturbateur de cavité qui seraient représentatifs pour le point Karlo-Libknechtovsk. Partant des représentations générales sur l'influence de la zone affaiblie on a décidé d'installer les appareils suivant une ligne axiale dans la galerie orientée dans la direction nord-sud et séparée de l'ensemble par deux à trois galeries qui y sont parallèles. Cet endroit a reçu le nom de salle n° 2. En 1972, les observations y ont donné des paramètres γ et $\Delta\phi$ affranchis de l'effet de cavité et pouvant être considérés comme représentatifs pour le point Karlo-Libknechtovsk. Après cela on a pu entreprendre l'étude de l'effet de cavité. Dans la mine n° 1, sur la ligne qui relie les salles n° 1 et 2, on a trouvé deux longues galeries réciproquement perpendiculaires et orientées dans les directions nord-sud et est-ouest (salles n° 3 et 4). On y a placé six socles.

TABLE 2 : Paramètres de l'onde M_2 à la station de Karlo-Libnechtovsk.

Salle	Socle	Le long de la mine et sur son axe				En travers de la mine sous ses murs			
		NS		EW		*NS*		*EW*	
		γ	$\Delta\phi$ (degrés)	γ	$\Delta\phi$ (degrés)	φ	$\Delta\phi$ (degrés)	γ	$\Delta\phi$ (degrés)
2	—	0,696 ±0,004	±2,70 ±0,25	0,717 ±0,004	—3,16 ±0,26	—	—	—	—
3	1	0,679 ±0,004	—2,89 ±0,21	0,714 ±0,006	+0,16 ±0,32	—	—	—	—
3	2	0,679	—1,56	—	—	—	—	0,665 ±0,010	+2,01 ±0,90
3	3	0,699	—0,91	—	—	—	—	0,700 ±0,007	—3,03 ±0,61
4	4	—	—	0,720 ±0,005	—1,04 ±0,40	0,814 ±0,007	—1,32 ±0,51	—	—
4	5	0,692 ±0,009	±1,08 ±0,73	—	—	—	—	—	—
4	6	—	—	—	—	0,648 ±0,014	+0,12 ±1,27	—	—
Moyenne vectorielle		0,688 ±0,004	—0,32 ±1,26	0,718 ±0,003	—1,11 ±1,39	—	—	—	—

Les observations dans la salle n° 3 devaient donner une réponse à la question de l'influence de cavité sur la phase des ondes de marées et dans la salle n° 4, sur le paramètre γ. Les facteurs d'amplitude et de phase de l'onde M_2 obtenus dans les salles n° 2 et 3 et 4 sont donnés dans la table 2. Les observations dans la salle n° 3 ont commencé en 1970.

Les considérations qui ont présidé au choix du site des observations dans la mine n° 1, concordent avec les déductions théoriques : sur l'axe longitudinal des galeries et dans les directions qui leur sont parallèles, l'effet de cavité n'existe pas. Dans la direction perpendiculaire on décèle brusquement l'effet de cavité qui s'amortit rapidement avec la distance. Dans la salle n° 4 l'influence perturbatrice des galeries n° 5 et 6 est sensible uniquement sur le socle n° 6. L'effet maximum de cavité s'observe pour l'installation d'appareils dans une niche. Comme pour le cas de l'effet de topographie sur un lieu compliqué, le calcul de l'effet de cavité est pratiquement irréalisable avec une précision nécessaire même pour le cas le plus simple des mines de section rectangulaire.

Il résulte des observations à Karlo-Libknechtovsk que, pour obtenir des caractéristiques de marées régionales, dans les mines et tunnels il faut choisir pour l'installation des appareils de longues galeries de section géométrique simple avec des murs unis. Il faut placer les socles rigoureusement dans la ligne axiale des galeries.

Les observations clinométriques suivant le profil Kiev-Artemovsk permettent de tirer les conclusions suivantes.

1. En six points on a obtenu les constantes harmoniques pour les ondes semi-diurnes (M_2, N_2) avec une dispersion ne dépassant pas 3 % dans la direction nord-sud et 1 % dans la direction est-ouest.
   Ceci montre que dans les régions de plate-formes recouvertes de plusieurs kilomètres de roches sédimentaires, à l'intérieur des continents, on peut obtenir les caractéristiques de marées régionales avec une précision atteignant 1 %.

2. Les effets de cavité, de topographie, de géologie et de tectonique doivent être pris en considération avant que les observations clinométriques effectuées soient utilisées pour la déduction des caractéristiques de marées globales. Les observations dans les montagnes, près des failles, dans les endroits d'un relief découpé, avec des nappes d'eaux souterraines, dans des mines et salles de section géométrique irrégulière, ne sont pas valables

TABLE 3 : Constantes harmoniques de l'onde M_2 tirées des observations des variations de la force de pesanteur à Poltava.

Etape des observations	Appareils Askania	Utilisateur	Durée des observations	Avant l'introduction des corrections de marée océanique		Après l'introduction des corrections de marée océanique	
				δ	Δφ degrés	δ	Δφ degrés
1	GS 3	Z.N. Aksentieva	8.09. 1955—4.11.1955	1,17	—8,9	—	—
2	GS 11	I.A. Ditchko	6.11. 1961—1.01.1964	1,181 ±0,005	+0,80 ±0,20	—	—
3	GS 11	V.G. Balenko V.G. Boulatsen V.P. Schliachovoi P.S. Korba I.A. Ditchko	27.12.1973—24.12.1974	1,1754 ±0,0024	+0,33 ±0,12	—	—
			25.09.1974—29.09.1975	1,1897 ±0,0020	+0,38 ±0,10	—	—
			16.11.1975—26.12.1976	1,1970 ±0,0024	+0,57 ±0,11	—	—
3	GS 12		25.11.1973—13.04.1974	1,1755 ±0,0059	+0,08 ±0,21	—	—
			8.01.1976—8.11.1976	1,1957 ±0,0029	+0,28 ±0,14	—	—
4	GS 12	V.G. Balenko V.G. Boulatsen	12.02.1980 (продолжаются)	1,164	—0,38	1,147	—0,40

sauf si les clinomètres sont installés sur la ligne axiale des mines et non dans des niches aménagées dans leurs parois. La plupart des observations clinométriques qui ont été faites ne répondent pas à ces exigences.

Dans le centre de la dépression Dniepr-Donetz on a fait également de longues séries d'observations des marées de la pesanteur. Les résultats obtenus sont donnés dans la table 3. On peut les répartir d'après leur précision en quatre étapes :

1ère étape : La précision des résultats n'est pas grande.

2ème étape : Les résultats se caractérisent par une augmentation sensible de la précision.

3ème étape : On a atteint une précision maximum d'après la méthode généralement adoptée des observations et du contrôle de la sensibilité. On a fait des recherches instrumentales et on a constaté que la vis micrométrique du gravimètre (Askania) ne convient pas pour les observations des marées terrestres car elle introduit dans le paramètre δ, pour une série annuelle, une erreur systématique atteignant 3 %.

4ème étape : Le gravimètre Askania GS-12 a été modernisé, on a élaboré une nouvelle méthode de mesure de la sensibilité qui exclut la vis micrométrique. Les résultats obtenus après l'introduction des corrections nécessaires doivent être considérés comme représentatifs pour Poltava et la région de la dépression du Dniepr-Donetz.

Sur le territoire de l'URSS on a utilisé les gravimètres Askania GS-11 et GS-12. Les défauts de la vis micrométrique de ces gravimètres par rapport aux exigences actuelles ont deux conséquences négatives fondamentales :

1) pour approcher la précision réelle du paramètre δ de la précision indiquée par la convergence interne, il faut faire la moyenne de dix séries annuelles d'observations obtenues par quelques appareils;

2) la comparaison des paramètres de marées en différentes régions perd son sens puisque les différences en δ se trouvent dans les limites de leurs erreurs systématiques.

Les observations ultérieures des variations de la force de pesanteur en utilisant la vis micrométrique des gravimètres du type GS-11 et GS-12 ne sont pas souhaitables. Il faut les moderniser, après avoir remplacé la cellule photoélectrique, ou appliquer un émetteur photoélectrique fabriqué à l'Observatoire Gravimétrique de Poltava.

Les résultats des observations clinométriques et gravimétriques dans la zone de la dépression Dniepr-Donetz, bien qu'ils soient obtenus dans l'intérieur du continent, sont troublés par l'influence des zones éloignées de la marée océanique. Les corrections de cet effet ont été calculées à l'Institut de Physique de la Terre de l'Académie des Sciences d'URSS par B.P. Pertsev. Les paramètres de la marée terrestre corrigés de l'influence des zones lointaines de la marée océanique sont donnés dans la troisième colonne de la table 1 et dans la deuxième colonne de la table 3. La précision des corrections introduites n'est pas grande. On peut tirer les conclusions suivantes :

1. L'introduction des corrections a diminué la valeur de la différence $\gamma_{NS}-\gamma_{EW}$ qui devient comparable à son erreur. Par conséquent dans les limites de la dépression Dniepr-Donetz cette différence est déterminée non par les particularités de la structure de l'écorce terrestre mais par les effets indirects locaux et régionaux. L'onde météorologique diurne n'est pas la cause de l'inégalité $\gamma_{NS}-\gamma_{EW}$.

2. Pour la direction ouest-est on a éliminé le retard de la marée observée par rapport à la théorie qui se note dans toutes les stations clinométriques

de l'Ukraine. De façon indirecte cela témoigne de ce que les corrections calculées par B.P. Pertsev et les cartes cotidales utilisées ont des caractéristiques de phases satisfaisantes.

3. Il est difficile d'évaluer la précision relative des corrections sur γ et δ. On peut en obtenir une certaine représentation, après avoir calculé les nombres de Love par les valeurs γ et δ prises avant et après introduction des corrections de l'influence des zones lointaines de la marée océanique. Elles sont données dans la table 4. Les données de cette table témoignent de ce que les corrections en γ et δ sont calculées avec une précision insuffisante, ce qui témoigne de façon indirecte de la faible précision des caractéristiques d'amplitude des cartes cotidales.

TABLE 4 : Nombres de Love déterminés par les observations de marées terrestres dans la région de la dépression Dniepr-Donetz.

Appareils	Direction	Avant l'introduction des corrections à la marée dans l'océan.		Après l'introduction des corrections à la marée dans l'océan.	
		k	h	k	h
Clinomètres	Nord-Sud	0,307	0,614	0,277	0,554
	Ouest-Est	0,286	0,572	0,270	0,540
Gravimètres		0,328	0,656	0,294	0,588
Gravimètres et Clinomètres	Nord-Sud	0,286	0,593	0,260	0,537
Gravimètres et Clinomètres	Ouest-Est	0,244	0,530	0,246	0,516

En conclusion il faut dire quelques mots sur la valeur de la résonance $\gamma_{01} - \gamma_{K1}$ obtenue à partir de quatre séries annuelles d'observations des inclinaisons dans la station Karlo-Libknechtovak. On a obtenu : $\gamma_{01} - \gamma_{K1} = -0,043 \pm 0,011$. Le groupe de collaborateurs de l'Institut de Physique de la Terre sous la direction de N.N. Pariiskii ont obtenu par l'analyse de toutes les observations gravimétriques en URSS (16.136 jours d'appareils) : $\delta_{01} - \delta_{K1} = 0,025 \pm 0,011$. On considère d'habitude que les gravimètres ont une prédominance sur les clinomètres lors de l'étude de la structure interne de la Terre. Or les clinomètres installés dans ce même but, dans des mines de sel ne le cèdent en rien aux gravimètres.

A time-variant tidal estimator : the Kalman predictor

F. De Meyer
Royal Meteorological Institute
Av. Circulaire 3, 1180 Brussels, Belgium.

Abstract. A multi input - single output model is applied to observed hourly tilt readings for the time interval 1969 - 1980, measured with two Verbaandert-Melchior pendulums at the tidal station Dourbes (Belgium). The model expresses the tide as a weighted sum of present and past values of the tidal functions and other subsystems, which incorporate the effects of background noise. The Kalman filter scheme is used to verify possible non-stationarity of the system model. It is found that the model weights are time-dependent, but the tidal parameters γ and κ are interpreted as being constant over the observation interval. The amplitude responses of barometric pressure, atmospheric temperature and ocean tide in the main tidal wave bands are concluded to be time-variable.

1. Introduction

The aim of an Earth tidal analysis is to estimate the response function of the Earth by comparing it with a theoretical physical model. The traditional harmonic approach describes the tidal oscillations by amplitude ratios γ (or δ) and phase lags κ for a finite, predetermined set of sinusoidal functions of precisely known frequencies, but this framework suffers from the apparent incapability of accounting for noise contributions which are inevitably present in the tidal records.

Unlike the conventional harmonic procedure of tidal analysis, the multi input-single output or MISO model (De Meyer, 1982), expresses the tide as a weighted sum of present and past values of a relatively small number of time-varying input functions. This multichannel model aims to take account of the theoretical tidal variations, meteorological perturbations and ocean tide influences, thus allowing freely for the presence of extraneous noise. The method is based on the same principles as the response algorithm of Munk and Cartwright (1966) in the sense that the results of the analysis are expressed as transfer (admittance) functions, which reveal directly the frequency responses of the physical system to the various inputs.

The first four input channels are used to describe the response of the Earth to the tidal gravitational potential. Since the analysis of Earth tide data should include inputs representing effects

of local and global nature, the essential objective of this approach is to isolate the linear part of the response of the Earth to the purely gravitational forces at the tidal periods from the contributions of other influences that are ultimately the result of atmospheric loading, on-site temperature fluctuations and non-linear sea level interaction.

Separate transfer functions can then be calculated for distinct, sufficiantly uncorrelated inputs, whose spectral lines are not normally separable from one another by a conventional least squares analysis. However, since the transfer functions depend on a limited number of model parameters, the computed admittances will be continuous and smooth and are consequently uncapable of showing resonance effects.

The impulse response weigths of the MISO model generate directly the transfer functions associated with the different inputs by the discrete Fourier transform. The model parameters can be estimated by simple least squares, but when the time series data have time-variant statistical characteristics then this numerical estimation method may fail to provide reliable results. In order to asses whether there is evidence of significant parametric variations over the observation interval, it is necessary to carry out statistical tests on the residuals to check model adequacy. In this context non-stationarity of the system model would entail time-variant amplitudes γ (or δ) and phase differences κ .

The problem of estimating a set of time variable parameters is very similar to the problem of estimating the state of a linear system. The Kalman filter was introduced in the control literature by Kalman (Kalman,1960,1963; Kalman and Bucy,1961) and is particularly suitable for tracking the behaviour of time-variant parameters in discrete time.Kalman filtering is a sophisticated and flexible estimation method which is used for detecting paremeter variations in real-time. The application of this method to discrete and non-linear systems is described briefly in Section 2.

2. Parametric variations of a linear model

We consider the problem of estimating the value of the dependent variable y on the basis of information on n a priori chosen variates $h_1,\ldots,h_n$. If there is no apparent mathematical or physical relation between the noisy quantities y and h_j the linear algebraic regression model is often postulated

$$y = \sum_{j=1}^{n} h_j x_j + v = \sum_{j=1}^{n} h_j \hat{x}_j + \hat{v} \qquad (2.1)$$

in terms of the unknown parameters $x_1,\ldots,x_n$. The first relationship in Eq.(2.1) expresses the linear model in terms of the true parameters x_j and the true, although commonly unknown, model error v, which describes the various disturbing elements of the model description, including systematic and random measurement errors as well as imperfect model specification by the presence of 'ignored' variables. The second relationship in Eq.(2.1) concerns the estimates $\hat{x}_j$ of the x_j and the observed residual $\hat{v}$.

Treating t as a discrete time index the value of the observation y_t of the dependent variable at time t is thus assumed to be given by

$$y_t = \sum_{j=1}^{n} h_{tj} x_j + v_t = \sum_{j=1}^{n} h_{tj} \hat{x}_j + \hat{v}_t \qquad (2.2)$$

in terms of the simultaneous observations h_{tj} on the independent variables h_j. Writing lower case letters with an underbar to designate column vectors and capital letters to denote matrices, the transpose of any vector $\underline{a}$ and matrix A will be represented by $\underline{a}^T$ and A^T, respectively. Equation (2.2) is consequently written in the convenient shorthand

$$y_t = \underline{h}_t^T \underline{x} + v_t = \underline{h}_t^T \underline{\hat{x}} + v_t \quad , \qquad (2.3)$$

where $\underline{h}_t^T = (h_{t1},\ldots,h_{tn})$ is the n-dimensional vector of explanatory variables at time t and $\underline{x} = (x_1,\ldots,x_n)^T$ is the parameter vector.

To denote possible time dependence of the parameters the measurement equation at time t now reads

$$y_t = \underline{h}_t^T \underline{x}_t + v_t = \underline{h}_t^T \underline{\hat{x}}_t + \hat{v}_t \qquad (2.4)$$

and we require a model to reproduce the continuous transitions of the parameter vector over time. The general non-stationary filtering problem is essentially solved in the work of Kalman (1960,1963), Kalman and Bucy (1961) and Jazwinsky (1970). The word 'filter' is a relic from the early history of control engineering. Nowadays the terms 'predictor, state estimator, forecastor, signal-noise separator' are more appropriate.

In general it is supposed that any parameter variation over time of discrete, linear, sampled-data systems can be modelled by a stochastic vector-matrix difference equation

$$\underline{x}_t = F_{t-1}\underline{x}_{t-1} + G_{t-1}\underline{w}_{t-1} \quad , \tag{2.5}$$

which is termed the system or state equation. Equation (2.5) has the form of a Markov chain and represents the system behaviour in terms of well defined quantities and a system error, which reflects the imperfect representation of the system properties by the model. The matrices F_{t-1} and G_{t-1} are assumed to be known and arise from the formulation of the physical problem. The n-vector $\underline{w}_{t-1}$ is a random forcing vector or model error of serially uncorrelated variables with zero mean.

To complete the state representation of the system it is supposed that observations y_t are available by the measurement equation (2.4), where v_t is a zero-mean observation noise. The model specification (2.5) is complemented by the statistical description of the noise terms $\underline{w}_t$ and v_t. Their means and covariance matrices are assumed to be given by

$$\begin{aligned} E\{\underline{w}_t\} &= \underline{0} \quad , & E\{\underline{w}_t\underline{w}_s^T\} &= Q_t\,\delta_{ts} \quad , \\ E\{v_t\} &= 0 \quad , & E\{v_t v_s\} &= r_t\,\delta_{ts} \quad , \end{aligned} \tag{2.6}$$

where E stands for the mathematical expectation operator and δ_{ts} is the Kronecker symbol: $\delta_{ts} = 1$ if $t=s$ and $\delta_{ts} = 0$ if $t \neq s$. The matrix Q_t and the variance r_t of the measurement noise are supposed to be known at the outset. Often $\underline{w}_t$ and v_t are assumed to have Gaussian distributions and to be uncorrelated in time

$$E\{\underline{w}_t v_s\} = 0 \quad , \quad \text{for all } t \text{ and } s. \tag{2.7}$$

The matrix Q_t is usually taken to be constant and diagonal, i.e., $Q_t = \text{diag}\,(q_{11},\ldots,q_{nn})$.

3. The discrete Kalman algorithm

The problem now consists of estimating the parameter vector $\underline{x}_t$ from the sequence of noisy measurements y_t, while attempting to overcome the influence of the observation noise v_t. Before taking the measurement y_t at time t, the parameter vector $\underline{x}_{t-1}$ at time t-1

is assumed to be estimated by $\underline{\hat{x}}_{t-1,t-1}$, which is based on information up to and including time t-1. The a priori prediction of $\underline{x}_t$ from $\underline{\hat{x}}_{t-1,t-1}$ to time t, using only the information up to time t-1, results from Eq.(2.5)

$$\underline{\hat{x}}_{t,t-1} = F_{t-1}\underline{\hat{x}}_{t-1,t-1} \quad , \tag{3.1}$$

since the transition matrix F_{t-1} is supposed to be known explicitely. Given the extrapolation $\underline{\hat{x}}_{t,t-1}$, an updated estimate $\underline{\hat{x}}_{t,t}$ of $\underline{x}_t$ at time t is sought, which is based on the observations prior to time t and the new measurement y_t.

The estimation errors are defined by the difference between the predicted and the true parameter vectors

$$\underline{\tilde{x}}_{t,t-1} = \underline{\hat{x}}_{t,t-1} - \underline{x}_t \quad , \quad \underline{\tilde{x}}_{t,t} = \underline{\hat{x}}_{t,t} - \underline{x}_t \quad . \tag{3.2}$$

The uncertainty of the estimates $\underline{\hat{x}}_{t,t-1}$ and $\underline{\hat{x}}_{t,t}$ is measured by their respective error covariance matrices

$$P_{t,t-1} = E\left\{\underline{\tilde{x}}_{t,t-1}\underline{\tilde{x}}_{t,t-1}^T\right\} \quad , \quad P_{t,t} = E\left\{\underline{\tilde{x}}_{t,t}\underline{\tilde{x}}_{t,t}^T\right\} \quad . \tag{3.3}$$

The estimate $\underline{\hat{x}}_{t,t}$ of $\underline{x}_t$, using the predictable portion of $\underline{x}_t$ and the new observation y_t, is postulated in the linear, recursive form

$$\underline{\hat{x}}_{t,t} = K_t\underline{\hat{x}}_{t,t-1} + \underline{k}_t y_t \quad , \tag{3.4}$$

where K_t and $\underline{k}_t$ are a time-varying weighting matrix and vector, respectively, as yet unspecified. Substitution of Eqs. (2.4) and (3.2) into (3.4) gives

$$\underline{\hat{x}}_{t,t} = K_t(\underline{x}_t+\underline{\tilde{x}}_{t,t-1}) + \underline{k}_t(\underline{h}_t^T\underline{x}_t+v_t)$$

and

$$\underline{\tilde{x}}_{t,t} = (K_t+\underline{k}_t\underline{h}_t^T-I)\underline{x}_t + K_t\underline{\tilde{x}}_{t,t-1} + \underline{k}_t v_t \quad . \tag{3.5}$$

If $E\{v_t\} = 0$ and $E\{\underline{\tilde{x}}_{t,t-1}\} = \underline{0}$, the estimator $\underline{\hat{x}}_{t,t}$ will be unbiased, i.e., $E\{\underline{\tilde{x}}_{t,t}\} = 0$ for any parameter vector only if $K_t+\underline{k}_t\underline{h}_t^T-I = 0$. The unbiasedness requirement of the updated estimate $\underline{\hat{x}}_{t,t}$ therefore

imposes the choice $K_t = I - \underline{k}_t \underline{h}_t^T$ for the matrix K_t and the estimator (3.4) simplifies to

$$\hat{\underline{x}}_{t,t} = \hat{\underline{x}}_{t,t-1} + \underline{k}_t(y_t - \underline{h}_t^T \hat{\underline{x}}_{t,t-1}) \quad , \tag{3.6}$$

where the vector $\underline{k}_t$ still has to be specified. The resulting estimation error then follows from Eq.(3.5)

$$\tilde{\underline{x}}_{t,t} = (I - \underline{k}_t \underline{h}_t^T)\tilde{\underline{x}}_{t,t-1} + \underline{k}_t v_t \quad . \tag{3.7}$$

From Eqs.(3.2), (3.1) and (2.5) we obtain

$$\tilde{\underline{x}}_{t,t-1} = F_{t-1}\tilde{\underline{x}}_{t-1,t-1} - G_{t-1}\underline{w}_{t-1} \quad . \tag{3.8}$$

Taking expected values of both sides of Eq.(3.8) it is concluded that $\hat{\underline{x}}_{t,t-1}$ is unbiased provided that $E\{\tilde{\underline{x}}_{t-1,t-1}\} = E\{\underline{w}_{t-1}\} = \underline{0}$. In combination with Eq.(3.7) this result entails that the unbiasedness property of the updated estimate $\hat{\underline{x}}_{t,t}$ is generated directly by the unbiasedness property of $\hat{\underline{x}}_{t-1,t-1}$. Equation (3.6) consequently allows extrapolation of the parameter vector estimate from time t-1 to time t without introducing bias.

It remains to specify the weighting vector $\underline{k}_t$. Using the definition (3.3) an update from $P_{t,t-1}$ to $P_{t,t}$ can be constructed. Substitution of Eq.(3.7) into (3.3) gives

$$P_{t,t} = E\left\{[(I - \underline{k}_t \underline{h}_t^T)\tilde{\underline{x}}_{t,t-1} + \underline{k}_t v_t][\tilde{\underline{x}}_{t,t-1}^T (I - \underline{k}_t \underline{h}_t^T)^T + v_t \underline{k}_t^T]\right\}$$

or

$$P_{t,t} = (I - \underline{k}_t \underline{h}_t^T) P_{t,t-1} (I - \underline{k}_t \underline{h}_t^T)^T + r_t \underline{k}_t \underline{k}_t^T \quad , \tag{3.9}$$

where it is implicitely assumed that the estimation error $\tilde{\underline{x}}_{t,t-1}$ and the measurement noise v_t are uncorrelated.

The optimal choice of the gain vector $\underline{k}_t$ is obtained from minimizing the total variance

$$S_t^2 = \text{Trace } P_{t,t} = E\left\{\tilde{\underline{x}}_{t,t}^T \tilde{\underline{x}}_{t,t}\right\} \quad . \tag{3.10}$$

This is equivalent to minimizing the length of the estimation error vector. In this respect $\hat{\underline{x}}_{t,t}$ is a linear minimum variance estimator. Taking the partial derivatives of S_t^2 with respect to $\underline{k}_t$ and equating

the result to zero yields $-2(I-\underline{k}_t\underline{h}_t^T)P_{t,t-1}\underline{h}_t+2r_t\underline{k}_t=0$. Solving for $\underline{k}_t$ we obtain the Kalman gain vector

$$\underline{k}_t = P_{t,t-1}\underline{h}_t(\underline{h}_t^T P_{t,t-1}\underline{h}_t+r_t)^{-1} \quad . \tag{3.11}$$

Note that the term between brackets is simply a scalar quantity so that only simple division is required.

The optimized value of the updated error covariance matrix is obtained from substituting Eq.(3.11) into (3.9)

$$P_{t,t} = P_{t,t-1} - \underline{k}_t\underline{h}_t^T P_{t,t-1} - P_{t,t-1}\underline{h}_t\underline{k}_t^T + \underline{k}_t(\underline{h}_t^T P_{t,t-1}\underline{h}_t+r_t)\underline{k}_t^T$$

$$= P_{t,t-1} - \underline{k}_t\underline{h}_t^T P_{t,t-1} - P_{t,t-1}\underline{h}_t\underline{k}_t^T + P_{t,t-1}\underline{h}_t\underline{k}_t^T$$

or

$$P_{t,t} = (I-\underline{k}_t\underline{h}_t^T)P_{t,t-1} \quad . \tag{3.12}$$

The extrapolation from $P_{t-1,t-1}$ to $P_{t,t-1}$ finally results from Eqs. (3.3) and (3.8)

$$P_{t,t-1} = E\left\{(F_{t-1}\underline{\tilde{x}}_{t-1,t-1}-G_{t-1}\underline{w}_{t-1})(\underline{\tilde{x}}_{t-1,t-1}^T F_{t-1}^T-\underline{w}_{t-1}^T G_{t-1}^T)\right\}$$

Therefore

$$P_{t,t-1} = F_{t-1}P_{t-1,t-1}F_{t-1}^T + G_{t-1}Q_{t-1}G_{t-1}^T \tag{3.13}$$

since $\underline{\tilde{x}}_{t-1,t-1}$ and w_{t-1} are assumed to be uncorrelated.

The filter computations can proceed as follows:

(1) Store the filter state $\underline{\hat{x}}_{t-1,t-1}$, $P_{t-1,t-1}$;
(2) Compute the predicted parameter vector $\underline{\hat{x}}_{t,t-1}$ by Eq.(3.1);
(3) Compute the predicted error covariance matrix $P_{t,t-1}$ by Eq.(3.13)
(4) Compute the Kalman gain vector $\underline{k}_t$ by Eq.(3.11);
(5) Process the observation y_t and compute the updated estimate $\underline{\hat{x}}_{t,t}$ by Eq.(3.6);
(6) Compute the updated error covariance matrix $P_{t,t}$ by Eq.(3.12) or (3.9);
(7) Set t=t+1 and return to step (1).

The Kalman algorithm is very flexible and allows recursive computations with a limited data storage, whereby parameter and measurement noise statistics are explicitely incorporated. Since the computational requirements are minimal the Kalman filter design offers great generality and facilitates the derivation of the minimum variance unbiased estimate of the parameter vector once initial values for the model parameters and the error covariance matrix are specified. However, in the general Kalman filter approach the dynamical model matrices (F_{t-1}, G_{t-1}, H_t) and the noise statistics (Q_t, r_t) must be known in advance.

In view of the sequential nature of the Kalman procedure the equations have to be initiated at time t=0. If a reliable a priori estimate $\hat{\underline{x}}_{o,o}$ with error covariance matrix $P_{o,o}$ is available (e.g., by least squares), then these provide adequate starting conditions. Alternatively, the Kalman filter may be started with very little information and sequentially adapted as data become available. If the initial parameter estimate $\hat{\underline{x}}_{o,o}$ is known very poorly, it is possible to start with an arbitrary finite valued vector (e.g., $\hat{\underline{x}}_{o,o}=\underline{0}$) and select $P_{o,o}$ as a diagonal matrix with large elements (e.g., $P_{o,o}=10^5$ I). This choice reflects small confidence in the initial estimates and simulates no prior information; large starting standard errors for the diagonal elements of $P_{o,o}$ accelerate convergence of the algorithm (Lee,1964).

In Eq.(3.6), $\hat{\underline{x}}_{t,t-1}$ is the prediction of the parameter vector $\underline{x}_t$ at time t based on the observations $y_1,\ldots,y_{t-1}$ and $\hat{y}_t=\underline{h}_t^T\hat{\underline{x}}_{t,t-1}$ may be interpreted as a prediction of the measurement $y_t=\underline{h}_t^T\underline{x}_t+v_t$ using information up to time t-1. Therefore the innovation

$$\hat{v}_t = y_t - \underline{h}_t^T\hat{\underline{x}}_{t,t-1} = y_t - \hat{y}_t \tag{3.14}$$

represents the error observed in forecasting y_t from its previous values. Since

$$\hat{v}_t = v_t - \underline{h}_t^T\tilde{\underline{x}}_{t,t-1} \tag{3.15}$$

this predicted measurement residual error results in part from the observation noise v_t, but also from the error $\tilde{\underline{x}}_{t,t-1}$ in the estimate $\hat{\underline{x}}_{t,t-1}$ of the parameter vector at time t.

Since it is assumed that $E\{\tilde{\underline{x}}_{t,t-1}\} = \underline{0}$ and $E\{v_t\} = 0$ it follows that

$$E\{\hat{v}_t\} = 0 \tag{3.16}$$

and the variance of the innovation is given by

$$\hat{r}_t = E\left\{\hat{v}_t^2\right\} = \underline{h}_t^T P_{t,t-1}\underline{h}_t + r_t \qquad (3.17)$$

in view of Eqs.(2.6) and (3.3).

In Eq.(3.6) the correction to the estimate $\hat{\underline{x}}_{t,t-1}$ is proportional to the innovation, the factor of proportionality being the filter gain $\underline{k}_t$, thus allowing for corrections of the erring parameter estimates. Since $\underline{k}_t = P_{t,t-1}\underline{h}_t/\hat{r}_t$ we note that the filter gain vector is proportional to $1/\hat{r}_t$. Therefore the predicted residuals $\hat{v}_t$ provide us with a useful tool for judging the performance of the Kalman filter in a practical situation. By checking the statistical properties of the innovations against their theoretical expectations as given by Eqs.(3.16) and (3.17), we are able to asses the performance of the Kalman filter.

The gain vector can intuitively be interpreted as being 'proportional to the errors in the parameter estimates' and 'inversily proportional to the measurement noise'. If the observation noise is large (r_t large) and parameter uncertainties are small ($P_{t,t-1}$ small), $\underline{k}_t$ will be small and Eq.(3.6) shows that only small changes in the parameter estimates will result. In this case the innovations are due chiefly to the noise and large measurement noise provides a small decrease in the error covariance matrix. On the other hand, small observation noise (r_t small) and large uncertainties in the parameter estimates ($P_{t,t-1}$ large) indicate that $\hat{v}_t$ will contain important information about errors in the estimate and since $\underline{k}_t$ is relatively large, strong corrections to the parameter estimates may be expected. In conclusion the Kalman gain vector is operating in a way which agrees with an intuitive scheme to improving the estimate.

If the Kalman filter is constructed on the basis of an erroneous or incomplete dynamic model, the inexact filter model may degrade the filter performance in the sense that it may cause the filter to diverge (Jazwinsky,1970). This problem is particularly important when the noise input Q_t and the measurement noise variance r_t are small. Equation (3.11) shows that, when the error covariance matrix $P_{t,t-1}$ becomes unrealistically small, the gain $\underline{k}_t$ may become very small and Eq.(3.6) shows that the parameter update evolves nearly according to $\hat{\underline{x}}_{t,t} \simeq \hat{\underline{x}}_{t,t-1}$ so that subsequent observations will have negligible effects on the parameter estimates. The estimates may consequently diverge, which manifests itself in the inconsistency of the innovations with their predicted statistics. Innovations may become biased and larger in magnitude than their standard deviations as predicted by Eq.(3.17). The impact of filter diver-

gence is further enlarged for small observation noise, since the variance r_t then becomes small. From Eq.(3.11) it then follows that $\underline{k}_t\underline{h}_t^T \simeq I$ and Eq.(3.12) reduces to $P_{t,t} \simeq 0$.

4. The random walk model

Although the algorithm in Section 3 has theoretical appeal it may be exceedingly difficult in practice to specify a parameter variation model as defined in Eq.(2.5) because the transition matrix F_{t-1} is supposed to be known explicitely. In absence of such knowledge the multi-variable random walk model ($F_{t-1} = G_{t-1} = I$)

$$\underline{x}_t = \underline{x}_{t-1} + \underline{w}_{t-1} \tag{4.1}$$

assumes that the parameter variations are driven by white noise $\underline{w}_{t-1}$. The resulting parameter equations reduce to a simple form, which requires nevertheless the specification of the covariance matrix Q_t of the random parameter variations and the variance r_t of the measurement noise.

The model (4.1) merely states that the parameters undergo random fluctuations between samples. The elements of Q_{t-1} reflect the expected rate of variations of the parameters between successive observations. In this case the prediction equations (3.1) and (3.13) become simply

$$\hat{\underline{x}}_{t,t-1} = \hat{\underline{x}}_{t-1,t-1} \quad , \tag{4.2}$$

$$P_{t,t-1} = P_{t-1,t-1} + Q_{t-1} \tag{4.3}$$

and the update equations are given in Eqs.(3.6) and (3.12), with the Kalman gain vector defined in Eq.(3.11). The resulting Kalman filter procedure for random variations of the parameters of a linear model is summarized in Table 1. The Kalman filter scheme provides a reasonable approach to the estimation of slowly variable parameters, i.e., parameters whose percentage change per sampling instant is small.

The initial estimate $\hat{\underline{x}}_{o,o}$ may be taken to be zero or any better estimate available as obtained by a least squares analysis using a predetermined number of observations. The initial error covariance matrix $P_{o,o}$ may be a large multiple of the unit matrix (e.g., $P_{o,o} = 10^5\ I$), indicating low confidence in the initial estimate $\hat{\underline{x}}_{o,o}$. If $P_{o,o}$ is chosen to be too small, this would imply great confidence in the initial estimates, which leads to slow convergence

Table 1. Kalman filter for random parametric variations

System equation	$\underline{x}_t = \underline{x}_{t-1} + \underline{w}_{t-1}$
Measurement equation	$y_t = \underline{h}_t^T \underline{x}_t + v_t$
Parameter forecast	$\hat{\underline{x}}_{t,t-1} = \hat{\underline{x}}_{t-1,t-1}$
Measurement prediction	$\hat{y}_t = \underline{h}_t^T \hat{\underline{x}}_{t,t-1}$
Innovation	$\hat{v}_t = y_t - \hat{y}_t$
Parameter covariance forecast	$P_{t,t-1} = P_{t-1,t-1} + Q_{t-1}$
Kalman gain vector	$\underline{k}_t = P_{t,t-1}\underline{h}_t(\underline{h}_t^T P_{t,t-1}\underline{h}_t + r_t)^{-1}$
Parameter update	$\hat{\underline{x}}_{t,t} = \hat{\underline{x}}_{t,t-1} + \underline{k}_t \hat{v}_t$
Parameter covariance update	$P_{t,t} = (I - \underline{k}_t \underline{h}_t^T) P_{t,t-1}$

in the recusive algorithm because of insufficiant gain in the Kalman gain vector.

Inaccurate a priori estimates $\hat{\underline{x}}_{o,o}$ and $P_{o,o}$ and incorrect estimates of Q_{t-1} and r_t can lead to misspecification errors on the computed parameters; erratic estimates of these quantities will all affect the rate of convergence and the accuracy of the algorithm in Table 1. The random walk model has been proposed by Lee(1964), but Young(1970) and Jazwinsky(1970) suggest that the main problem is the adequate choice of the parameter error covariance matrix Q_{t-1} when this is not known a priori.

In general the choice of the appropriate level of the elements of Q_{t-1} is largely heuristic. A reasonable approach is that the parameters change with independent random increments, that is $F_{t-1} = G_{t-1} = I$ and $Q_{t-1}=\text{diag}(q_{11},\ldots,q_{nn})$, where q_{jj} is the assumed constant average rate of change of the parameter x_j. Any known time invariant parameter can be handled simply by setting the appropriate diagonal element of Q_{t-1} to zero.

The effect of Q_{t-1} in Eq.(4.3) is to keep $P_{t,t-1}$ from becoming unreasonably small. This has the consequence that the gain vector is prevented from going to zero which would end the updating of the parameter estimates. A large gain means that new innovations are weighted more at the expense of old ones and increases the rate

at which old data are 'forgotten'. The matrix Q_{t-1} therefore affects the speed with which the estimator (3.6) is able to follow changing parameters.

In consequence, to some extent the accuracy of the estimation procedure is a matter of choice. Large values of Q_{t-1} increase the tracking capacity of the random walk model, but this also gives rise to increased variability of the computed parameters due to the feedback of noise. The estimates then become erratic and $P_{t,t-1}$, indicating this behaviour, has large values. If Q_{t-1} decreases, so will both the fluctuations in the parameter estimates and the error covariance matrix. When Q_{t-1} becomes small, then the estimates become biased; since $\hat{\underline{x}}_{t,t-1}$ will be lagging behind $\underline{x}_t$, the bias is not included in $P_{t,t-1}$.

Therefore the matrix Q_{t-1}, specifying the average rate of change of the parameters, is a design parameter which affects the estimation accuracy and controls the tracking ability of the Kalman filter since it determines the rate at which old data are forgotten.

5. The multi input-single output (MISO) model

Suppose that the noisy output y(t) of a linear dynamic system is generated by m deterministic input signals $u_1(t),\ldots,u_m(t)$. Discrete dynamic systems can frequenctly be described by the linear convolution equation

$$y_t = \sum_{k=1}^{m} \sum_{j=0}^{p_k} a_{kj}\, u_{t-j\Delta t_k,k} + v_t \qquad (5.1)$$

of which the dynamic character is as far as possible identical with the true system response, In Eq.(5.1) t is treated as a discrete index and it represents a transfer function model (Box and Jenkins, 1970), where the dynamical behaviour of the output is explained in terms of the present and past observations of the inputs. The use of positive lags is avoided since it obviously violates causality. The parameter Δt_k denotes an appropriate time lag for input (channel) number k.

The weights $(a_{k0},a_{k1},\ldots,a_{kp_k})$ are the ordinates of the impulse response function for the input channel number k. In practice one very seldom has a priori information concerning the orders $p_1,\ldots,p_m$ of the numerical scheme (5.1). Box and Jenkins(1970) and Bennet(1979) discuss this problem of identification. Besides 'ignored' variables the model noise v_t includes input and output disturbances. Defining the row vectors

$$\underline{h}_t^T = [u_{t,1},\ldots,u_{t-p_1\Delta t_1,1},\ldots,u_{t,m},\ldots,u_{t-p_m\Delta t_m,m}]$$

and $$\underline{x}_t^T = (a_{10},\ldots,a_{1p_1},\ldots,a_{m0},\ldots a_{mp_m})$$

it is easily verified that the model (5.1) is a special case of the general shorthand relation (2.4).

Let z be the backward shift operator (Robinson,1980), that is

$$z^j u_{t,k} = u_{t-j\Delta t_k,k} \quad , \; j=0,1,2,\ldots \tag{5.2}$$

and define the z-transform of the impulse response of the kth channel

$$A_k(z) = \sum_{j=0}^{p_k} a_{kj} z^j \quad . \tag{5.3}$$

Then the basic deterministic equation (5.1) can be expressed in the convenient shorthand

$$y_t = \sum_{k=1}^{m} A_k(z) u_{t,k} + v_t \quad . \tag{5.4}$$

Knowledge of the transfer function operator $A_k(z)$ completely determines the dynamic response of the linear system to the input in the kth channel. The z-transform evaluated on the unit circle of the complex z-plane corresponds to the discrete Fourier transform of the impulse response

$$A_k(f) = \sum_{j=0}^{p_k} a_{kj} e^{-2\pi i j f \Delta t_k} \quad , \tag{5.5}$$

where f denotes frequency. The complex transfer function $A_k(f)$ is commonly expressed in polar form

$$A_k(f) = G_k(f) e^{i\Phi_k(f)} \quad . \tag{5.6}$$

Munk and Cartwright(1966) refer to $A_k(f)$ as the admittance function. The gain or amplitude response $G_k(f)$ represents the amplification by the system on passing an input harmonic wave of frequency f through the channel number k and the phase response $\Phi_k(f)$ determines the phase shift that will be observed in the output at the frequency f.

The backward difference operator ∇ is defined by

$$\begin{aligned} \nabla y_t &= y_t - y_{t-\Delta t} = (1 - z) y_t \quad , \\ \nabla u_{t,k} &= u_{t,k} - u_{t-\Delta t,k} \quad , \end{aligned} \tag{5.7}$$

with $zy_t = y_{t-\Delta t}$ and Δt the sampling interval of the output observations. On differencing both sides of Eq.(5.4) we obtain the following parametrization of the MISO model

$$\nabla y_t = \sum_{k=1}^{m} A_k(z)\, \nabla u_{t,k} + \nabla v_t \quad , \tag{5.8}$$

which shows that the incremental changes ∇y_t and $\nabla u_{t,k}$ satisfy the same transfer function model as do y_t and $u_{t,k}$.

If the non-stationary part (drift) of y_t is mainly concentrated at the low frequencies, its effect can be greatly attenuated by fitting the model (5.8) instead of (5.4), since the operator (1-z) essentially has the properties of a high-pass filter. In consequence, differencing the data allows limited removal of non-stationary effects of a stochastically varying bias or trend in time series, but it must be considered that differencing amplifies the high-frequency noise contributions and that the model error ∇v_t in Eq.(5.8) becomes even more autocorrelated than the original model error v_t. However, this procedure does not provide for more general non-stationary behaviour of the MISO model in which the parameters a_{kj} themselves vary as functions of time.

6. The MISO model and Earth tide observations

The Earth is now considered as a linear system where many forces act as input to generate the particular observed signal as the output of this system (i.e., gravity, tilt,strain). The MISO model parametrizes the relation between the various input channels and the output in the sense that the associated transfer functions reveal directly the frequency responses of the system concerned. The principle advantage of this method apparently lies in the fact that several inputs can be included a priori in the analysis and that separate transfer functions can be constructed for sufficiently uncorrelated inputs.

Effective use of the MISO model requires that we need a consistent procedure for deciding on the relevant non-gravitational (apart from the tidal) input signals to be included in the analysis and for choosing the appropriate number of parameters to fit the impulse response for each input function. One approach to the problem of deciding upon the inclusion of a particular input is to introduce a priori all workable channels in a lumped response analysis. An input is then rejected on the basis of unacceptably large confidence limits produced in the transfer function.

In order to suppress the long-period contributions associated with the 'drift' of the instrumental zero of Earth tide instruments, the MISO model in the form of Eq.(5.8) is selected. This means that the model is expressed in terms of the differences of the input and output observations.

The first four channels evidently correspond to the main frequency bands of the gravitational potential. In consequence the input functions $u_{t,1}$, $u_{t,2}$, $u_{t,3}$ and $u_{t,4}$ are confined to the long-period (LP), diurnal (D), semi-diurnal (SD) and ter-diurnal(TD) signals, respectively. These functions are computed hour by hour from the theoretical, time-harmonic expansions of the Cartwright-Tayler-Edden (1971,1973) model; they are calculated in the true azimuth (-8.00° E-S) of the pendulum. In this way the computed transfer functions are directly interpetable in terms of the amplitude (γ or δ) and phase (κ) factors of the tidal constituents as a function of frequency.

Noise is generated in the tidal wave bands as a result of atmospheric pressure fluctuations, which produce a S_2 meteorological component and as a result also of temperature variations acting on the instruments, which combine their effect into a S_1 meteorological wave. However, since these perturbations cannot be described by pure harmonic waves it is argued that their effects are spread out over the tidal wave bands concerned. As a result the inputs $u_{t,5}$ and $u_{t,6}$ respectively correspond to the interpolated hourly means of the barometric pressure (in millibar) and air temperature (in degrees centigrade), measured at the synoptic station Florennes (λ = 04°39' E, φ = 50°14' N), situated about 18 km north of the station Dourbes (λ = 04°36' E, φ = 50°06' N), Belgium.

Since the tidal station Dourbes is situated 170 km from the North Sea, the distortion of the Earth tide records by oceanic influences cannot be ignored and the MISO model should include shallow water interaction and radiational inputs from oceanic tides. To simulate sea level response the channel $u_{t,7}$ is added, which consists of the hourly tide readings (in meter) at the station Ostende (λ = 02°55' E, φ =51°14' N).

Geophysical considerations and experience indicate a rather smooth response of the Earth to body forces within the main tidal frequency bands. This implies a severe truncation of the impulse response functions. A fundamental decision is to be made about each time operator concerning its length $q_k = p_k + 1$ and the lag interval Δt_k. Increasing the sampling rate Δt_k defines a smaller bandwidth to which $A_k(f)$ is restricted and increasing the length q_k of the impulse response number k entails a more pronounced oscillatory aspect of the

transfer function.

The Fourier series (5.5) has periodicity $1/\Delta t_k$ in frequency, which is unrealistic from the physical point of view because of the periodic repetition of the transfer function. However, since the tidal information is restricted to a few narrow frequency bands this effect is acceptable, provided that $1/\Delta t_k \geq 2\Delta f_k$, with Δf_k the bandwidth within which $A_k(f)$ is confined. Considering that the LP-band extends from 0 to 0.0061 cph (cycles per hour), the D-band from 0.0341 to 0.0464 cph, the SD-band from 0.0744 to 0.0867 cph and the TD-band from 0.1177 to 0.1239 cph, the effective bandwidths $\Delta f_1 = 0.0061$, $\Delta f_2 = 0.0123$, $\Delta f_3 = 0.0123$ and $\Delta f_4 = 0.0062$ cph are obtained. The choises of the sampling rates of the impulse responses $\Delta t_1 = 82$ h, $\Delta t_2 = 43$ h, $\Delta t_3 = 40$ h and $\Delta t_4 = 81$ h confine the computed transfer functions to the frequency intervals (0,0.0061) cph, (0.0349,0.0465) cph, (0.0750,0.0875) cph and (0.1173,0.1235) cph, respectively (De Meyer, 1982). For the perturbation inputs we have chosen a priori $\Delta t_k = 3$ hours, k=5,6,7, thus restricting the associated spectra to the frequency interval $0 \leq f \leq 1/6$ cph.

The smoothness of the transfer function $A_k(f)$ actually depends on the number of weights a_{kj} used in Eq.(5.5). If the number of lags is increased there is a danger that the frequency curves will become unrealistically distorted in their attempt to adapt to the smaller tidal constituents. Writing $q_k \Delta t_k = 1/f_k$, truncation of the impulse response at the lag p_k implies that any change of the spectrum with a frequency larger than f_k will not be incorporated in the Fourier series representation. Trial an error indicated the following convenient choises: $p_1 = p_2 = 3$, $p_3 = 5$ and $p_4 = 2$. For the three perturbation channels we have chosen a priori $p_5 = p_6 = p_7 = 3$.

The foregoing discussion deliberately neglects the existence of sharp resonance peaks and therefore does not take account of the influence of the Earth's liquid core which has the effect of introducing a resonance in the diurnal band. Fitting Earth tide observations with only a few impulse response coefficients inevitably smoothes out the core effect, which distorts the amplitudes of the diurnal Earth tide constituents by a few percent over a narrow band centered on the frequency of resonance. However it may be expected that this resonance phenomenon is hopelessly contaminated by the extraneous noise in tilt observations. Accepting a large truncation value for p_2 could introduce very spurious information about the minor tidal waves (especially ψ_1).

7. Kalman filtering of EW pendulum data

A multi-response analysis was performed on a 4383 days series of hourly observations for the time interval 1/1/1969 - 31/12/1980, recorded with the Verbaandert-Melchior pendulum no° 28 at the station Dourbes. Since the instrument is an EW inclinometer the deviations of the vertical are taken to be positive to the East. For the station concerned the sensitivity determination is based on the measurement of the free period of the instrument; the non-uniformly distributed sensitivities are interpolated using a spline fit program for non-uniform sampling. Table 2 summarizes the impulse response coefficients a_{kj}, $2 \leqslant k \leqslant 7$, together with their estimated standard errors Δa_{kj}, for the MISO model in the form of Eq.(5.8). The weights are obtained with the least squares algorithm and the estimation of the confidence bands of the amplitude and phase response curves is discussed by De Meyer (1982).

Table 2
Impulse response weights HP 28 VM (least squares estimation)

j	Tidal channels					
	a_{2j}	Δa_{2j}	a_{3j}	Δa_{3j}	a_{4j}	Δa_{4j}
0	0.6696	0.011	0.8037	0.015	0.7450	0.353
1	0.0588	0.011	-0.0633	0.015	0.2500	0.193
2	-0.0555	0.011	0.0473	0.019	-0.0739	0.353
3	-0.0193	0.011	-0.0686	0.018		
4			-0.0051	0.012		
5			-0.0491	0.013		

j	Non-tidal channels					
	pressure		temperature		sea level	
	a_{5j}	Δa_{5j}	a_{6j}	Δa_{6j}	a_{7j}	Δa_{7j}
0	-0.1128	0.024	0.0077	0.016	-0.0870	0.050
1	-0.0989	0.024	-0.0160	0.015	0.0015	0.050
2	-0.0721	0.024	-0.0179	0.015	-0.1488	0.050
3	-0.0329	0.024	-0.0143	0.016	0.1528	0.051

The total sum of squares TSS = $1.304\ 10^6$ $mseca^2$ refers to the sum of squares of the differences $\nabla y_t = y_t - y_{t-\Delta t}$, with Δt = 1 hour, yielding an estimated variance of 12.7 $mseca^2$ for the observations ∇y_t in the output channel. Since the sum of squares due to the regression is SSR=$1.286\ 10^6$ $mseca^2$ a residual sum of squares RSS = TSS - SSR = $1.746\ 10^4$ $mseca^2$ and an estimated variance of 0.17 $mseca^2$ for the differences ∇v_t are obtained. A measure of the overall fit

of the MISO model is given by the multiple correlation coefficient R^2 = SSR/TSS = 0.9866, which yields the percentage explained sum of squares ESS = 100 R^2 = 98.66 %.

The amplitude and phase response curves, along with the 98 % confidence bands, for the diurnal and semi-diurnal wave bands are shown in Fig.1. Because the transfer functions, derived from the impulse response weights, can be directly interpreted in terms of the familiar ratios γ of the observed to the theoretical amplitudes and the differences κ between the observed and theoretical phases at the frequencies of the tidal waves, the comparison between the γ- and κ-factors, obtained with the MISO model and Venedikov's harmonic analysis, is represented in Table 3 for the main tidal constituents. Note that the resultscorrespond to the true azimuth of the pendulum.

Table 3

Comparison MISO and harmonic analysis HP 28 VM (EW)

Tidal wave	MISO model				Venedikov method			
	γ	$\Delta\gamma$	κ	$\Delta\kappa$	γ	$\Delta\gamma$	κ	$\Delta\kappa$
Q_1	0.6089	0.0016	6.08°	0.17°	0.6100	0.0124	7.26°	1.17°
O_1	0.6579	0.0015	0.03	0.13	0.6585	0.0023	8.45	0.20
NO_1	0.7158	0.0010	6.53	0.09	0.6818	0.0262	3.77	2.20
P_1	0.7443	0.0010	3.06	0.07	0.7133	0.0048	4.31	0.39
K_1	0.7460	0.0010	2.34	0.08	0.7501	0.0016	2.14	0.12
J_1	0.7288	0.0011	-2.02	0.09	0.6062	0.0293	2.93	2.77
OO_1	0.6784	0.0024	-3.41	0.22	0.5358	0.0479	-7.00	5.13
μ_2	0.8381	0.0029	9.47	0.19	1.1973	0.0201	-3.46	0.96
N_2	0.8478	0.0022	3.66	0.15	0.8299	0.0031	6.12	0.22
ν_2	0.8428	0.0020	3.25	0.14	0.7991	0.0163	9.00	1.17
M_2	0.8306	0.0016	3.25	0.11	0.8206	0.0006	5.37	0.04
L_2	0.8591	0.0018	1.21	0.12	0.8567	0.0174	14.93	1.16
S_2	0.8179	0.0012	-1.71	0.09	0.8279	0.0012	-0.88	0.08
K_2	0.8050	0.0012	-1.63	0.09	0.8219	0.0045	-0.84	0.31
M_3	0.8897	0.0186	14.04	1.20	0.8704	0.0171	13.67	1.12

This table apparently shows that the confidence limits of the tidal parameters of the principal waves K_1, M_2 and M_3 in each frequency band, computed in the two methods, are of the same order of magnitude. As expected, the confidence interval of the amplitude and phase factors of the minor tidal waves are largely underestimated

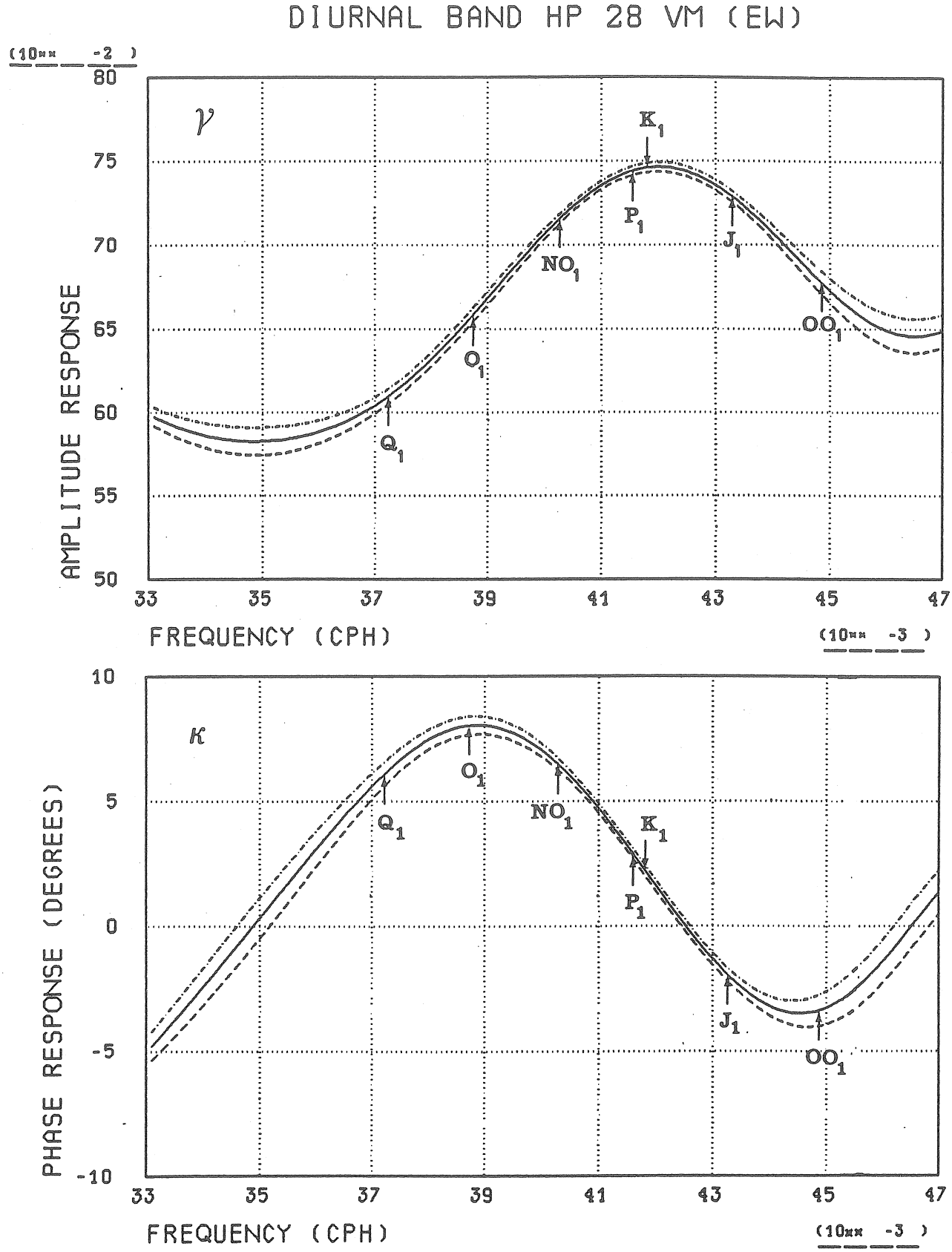

Fig.1.a. Transfer function in the diurnal band corresponding to $H_2(f)$; EW component.

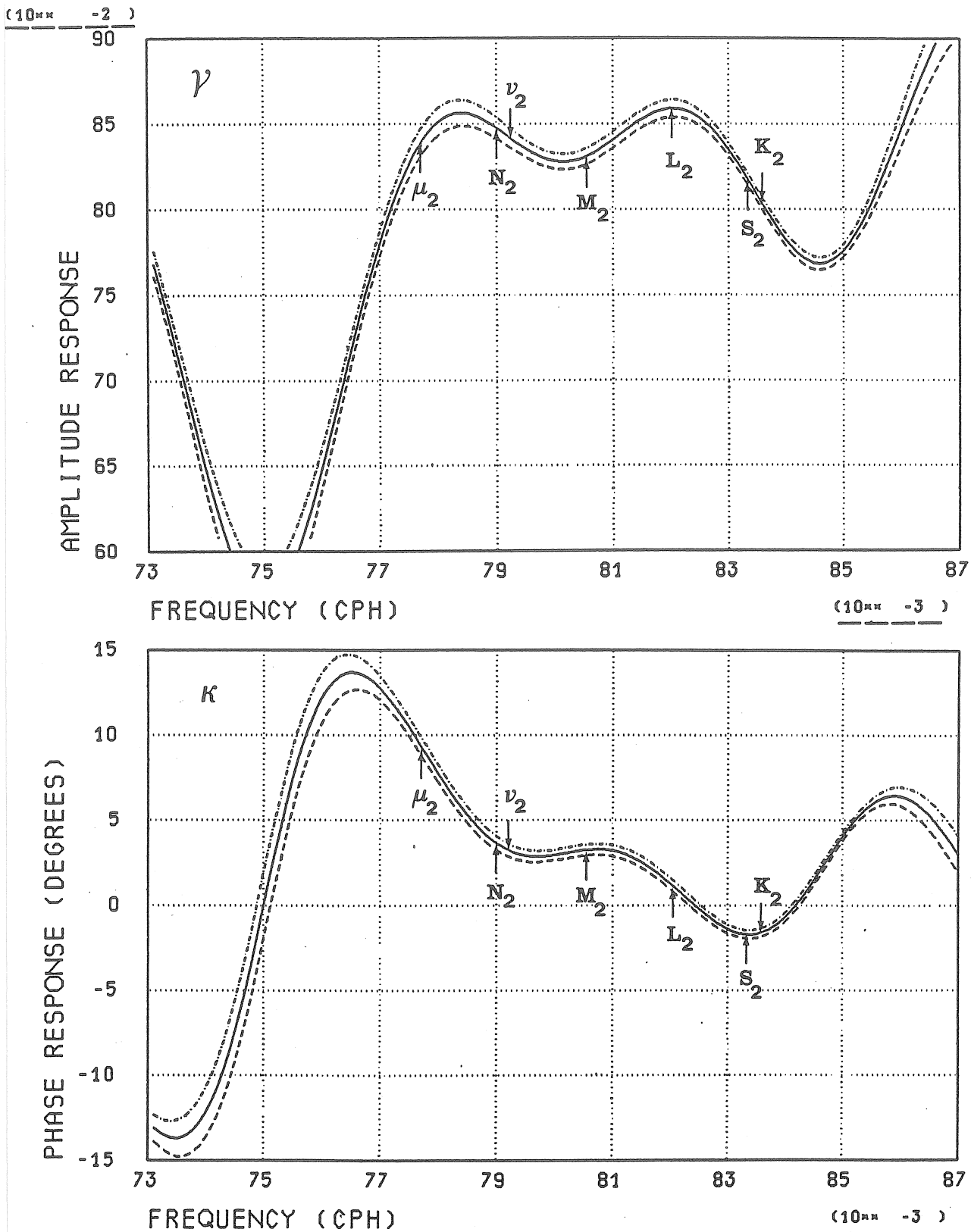

Fig.1.b. Transfer function in the semi-diurnal band corresponding to $H_3(f)$; EW component.

by the MISO model because these standard errors are strongly influenced by the corresponding values of the dominant waves. So to speak the confidence bands in Fig.1.a and Fig.1.b (dashed lines) are essentially generated by the estimated standard errors of the tidal parameters of K_1 and M_2.

The transfer function for the ter-diurnal input and the perturbation channels are not shown, although they can readily be computed from Eq.(5.5) and the impulse response coefficients in Table 2. Barometric pressure produces an estimated tilt effect of 0.07 mseca/mbar in the SD-band of the EW component. Also an amplitude response of 0.03 mseca/degree centigrade in the D-band and 0.02 mseca/degree centigrade in the SD-band, corresponding to atmospheric temperature variations, is observed. Expressing sea level variations in meter, an effect of the order of 0.15 mseca/meter in the D- and SD-bands, according to the chanell u_7, is obtained.

Figure 2 shows the residual power spectrum estimate, obtained with the periodogram technique (Jenkins and Watts,1968), in the frequency intervals $0 \leqslant f \leqslant 0.18$ cph and $0 \leqslant f \leqslant 0.03$ cph. A coloured noise spectrum with important contributions at the low frequencies and increased noise levels in the tidal bands (especially the SD-band) are observed. The diurnal group of lines appears to be adequately represented by the MISO model, but important residual power remains in the semi-diurnal interval, which can be explained by an incomplete representation of ocean tide effects by the corresponding channel u_7 of the model. In the quarter-diurnal (QD) band the lines MN_4 and MS_4, surrounding M_4, can be identified; these waves are related to shallow water loading influences because the station is only 170 km away from the North Sea. In the low-frequency interval the residual spectral peaks are associated with irregular oscillations of atmospheric pressure and ocean tide variations of long period. Lines near the annual and semi-annual periods are noted.

The important issue of parameter stability of the MISO model is further adressed using the recursive Kalman filtering method as an estimation framework. The measurements of the input and output channels are now treated as being given in a sequential manner; as a new set of observations is accounted for, the parameters are readjusted. For this on-line estimation the Kalman filtering procedure provides a convenient perspective.

As dynamic equation we consider the random walk model (4.1) for parameter variations with time; the measurement equation is (2.4), with the row vector $\underline{h}_t^T$ composed of observations of the input variates

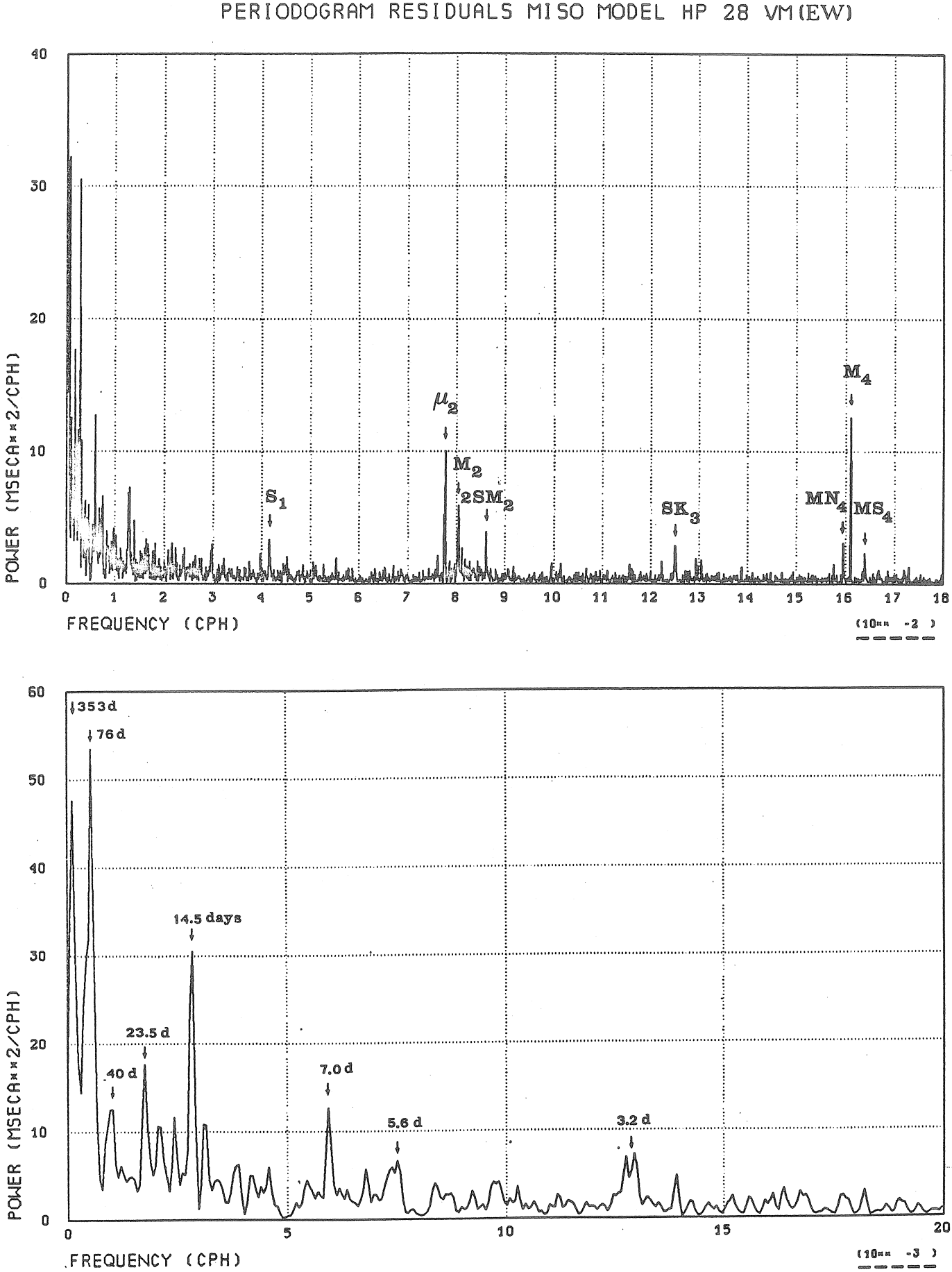

Fig.2. Residual power spectrum (least squares estimation); EW component.

as defined in Section 5. As initial conditions $\underline{x}_{o,o}$ and $P_{o,o}$ the values obtained by the preliminary least squares analysis are introduced, thereby indicating relatively great confidence in the a priori estimates of the model parameters. In the Kalman filter approach the variance r_t of the measurement noise is assumed to be known. An estimated variance of the order of 0.17 mseca^2 for the observed residuals was obtained as a result of the least squares analysis. Since Fig. 2 shows that the residual sequence has an autocorrelated structure, the residual variance will be underestimated (Johnstone,1972). For this reason the variance of the observation noise is taken to be constant and a value r_t=0.5 mseca^2 is selected.

The error covariance matrix Q_t is chosen to be constant and diagonal, i.e., Q_t=Q=diag($q_{11},\ldots,q_{nn}$), with the diagonal elements reflecting the expected rate of variation of the parameters between samples. For example, if the jth element x_j of the parameter vector at time t is expected to vary by an amount Δx_j between successive samples, then the jth diagonal element q_{jj} of Q should be set to $q_{jj}=(\Delta x_j)^2/\Delta t$, where Δt is the time interval between samples. In this respect different expected rates of change may be specified for different parameters.

In this context it is not possible to choose the elements of the matrix Q on the basis of the criterion of the expected rates of variation of the parameters since no objective information on possible time-dependence of the tidal parameters is available. After some preliminary tests the following values for the elements q_{jj}, corresponding to the individual inputs were selected: u_2:q_{jj} = 10^{-6}; u_3: q_{jj} = 10^{-6}; u_4: q_{jj} = 10^{-4}; u_5, u_6 and y_7: q_{jj}=10^{-2}. It was found that the final results were practically insensitive to the exact levels of the elements of the matrix Q and the value of r_t, as long as they had these orders of magnitude.

The recursive estimates of the impulse response coefficients a_{kj}, with r_t and Q set to the afore-said quantities, are shown in Fig.3 for the theoretical tidal inputs and in Fig.4 for the non-tidal channels concerned. The means $\bar{a}_{kj}$ and the standard deviations $\Delta\bar{a}_{kj}$ of the impulse response weights are summarized in Table 4.

It may be concluded that the model parameters a_{kj} of the D- and SD-input channels vary insignificantly over time, while the impulse responses of the other inputs seem to be time dependent over the observing interval. Since the sum of squares explained by the Kalman filter model is SSR = 1.288 10^6 mseca^2, whereas the total sum of squares is TSS = 1.304 10^6 mseca^2, a residual sum of squares RSS = 1.574 10^4 mseca^2 and an estimated variance 0.15 mseca^2 of the observed residuals are obtained. This gives a percentage explained sum of

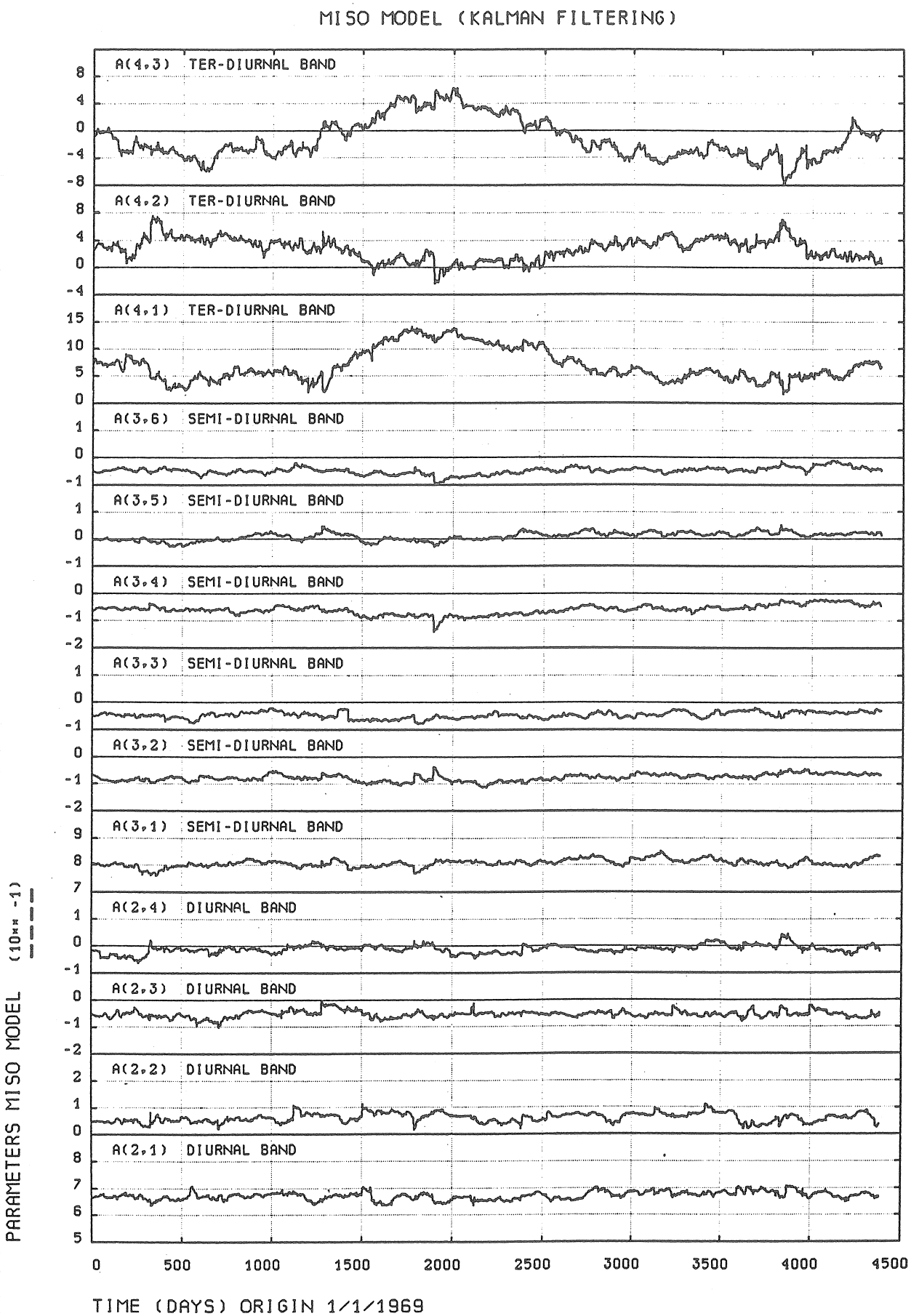

Fig.3. Time evolution of the impulse response weights associated with the tidal inputs (Kalman filtering); EW component.

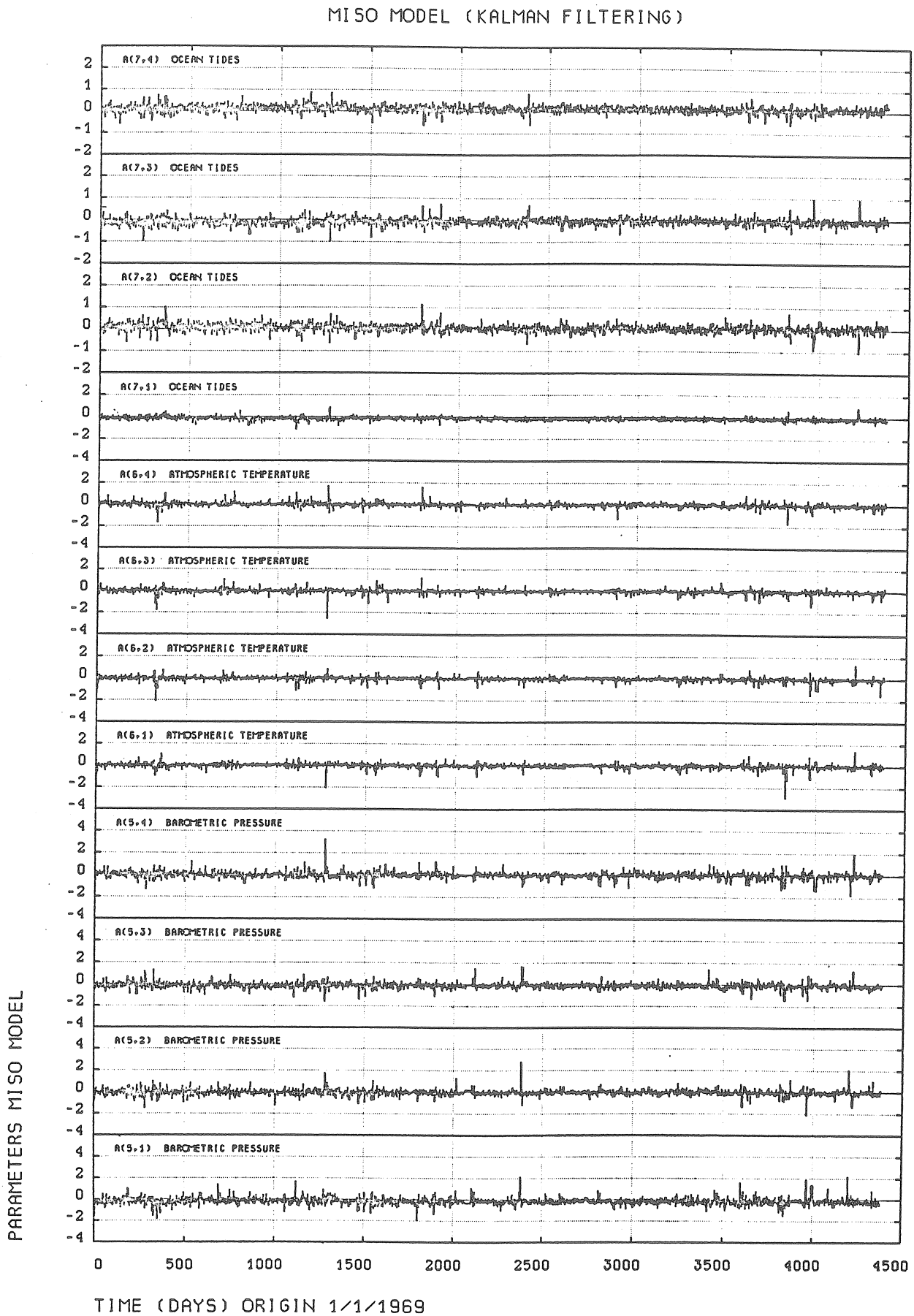

Fig.4. Time evolution of the impulse response weights associated with the non-tidal inputs (Kalman filtering); EW component.

squares ESS = 98.79 %.

Table 4
Means and standard deviations of the recursive impulse response weights (Kalman filtering)

j	$\bar{a}_{2j}$	$\Delta\bar{a}_{2j}$	$\bar{a}_{3j}$	$\Delta\bar{a}_{3j}$	$\bar{a}_{4j}$	$\Delta\bar{a}_{4j}$
0	0.6716	0.014	0.8072	0.013	0.6926	0.290
1	0.0605	0.053	-0.0770	0.013	0.2723	0.159
2	-0.0539	0.013	-0.0464	0.012	-0.1288	0.291
3	-0.0116	0.015	-0.0601	0.017		
4			0.0099	0.015		
5			-0.0485	0.013		
j	$\bar{a}_{5j}$	$\Delta\bar{a}_{5j}$	$\bar{a}_{6j}$	$\Delta\bar{a}_{6j}$	$\bar{a}_{7j}$	$\Delta\bar{a}_{7j}$
0	-0.1697	0.279	-0.0053	0.170	-0.1477	0.140
1	-0.0372	0.245	-0.0232	0.169	0.0514	0.145
2	-0.1099	0.236	-0.0203	0.169	-0.0887	0.141
3	-0.0053	0.258	0.0024	0.172	0.1155	0.140

From the recursive estimates of the coefficients a_{kj} the transfer function $A_k(f)$ for input channel number k can be computed at each time instant t using Eq.(5.5). Figure 5 shows the behaviour of the amplitude responses $G_2(f)$, $G_3(f)$ and $G_4(f)$ as a function of time at the main tidal constituents in each tidal wave band. A more detailed view of the time evolution of these γ-factors is given in Fig. 6 and Fig. 7 represents the variation of the associated phase differences κ . Table 5 summarizes the mean values and standard deviations of the γ and κ parameters, viewed as functions of time.

Table 5
Means and standard deviations of the tidal parameters γ and κ

	γ		κ	
	mean	st.dev.	mean	st.dev.
Q_1	0.6078	0.022	7.19°	2.21°
O_1	0.6630	0.025	8.58	1.60
K_1	0.7437	0.023	2.74	1.33
M_2	0.8399	0.025	5.27	0.95
S_2	0.8247	0.021	-1.67	1.13
K_2	0.8136	0.021	-1.57	1.09
M_3	0.8990	0.123	14.32	8.09

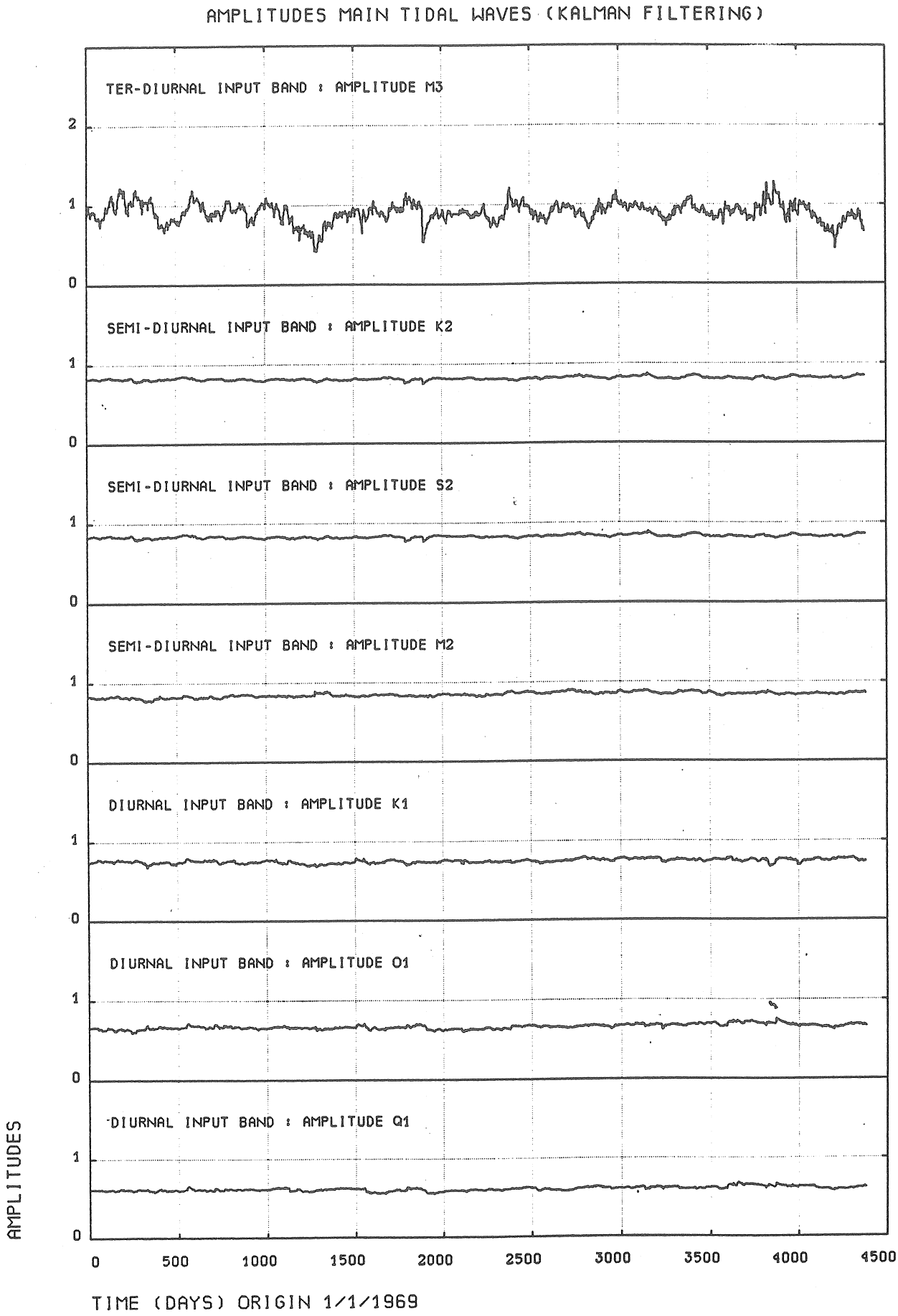

Fig.5. Time evolution of the γ-factors for the main tidal waves (Kalman filtering); EW component.

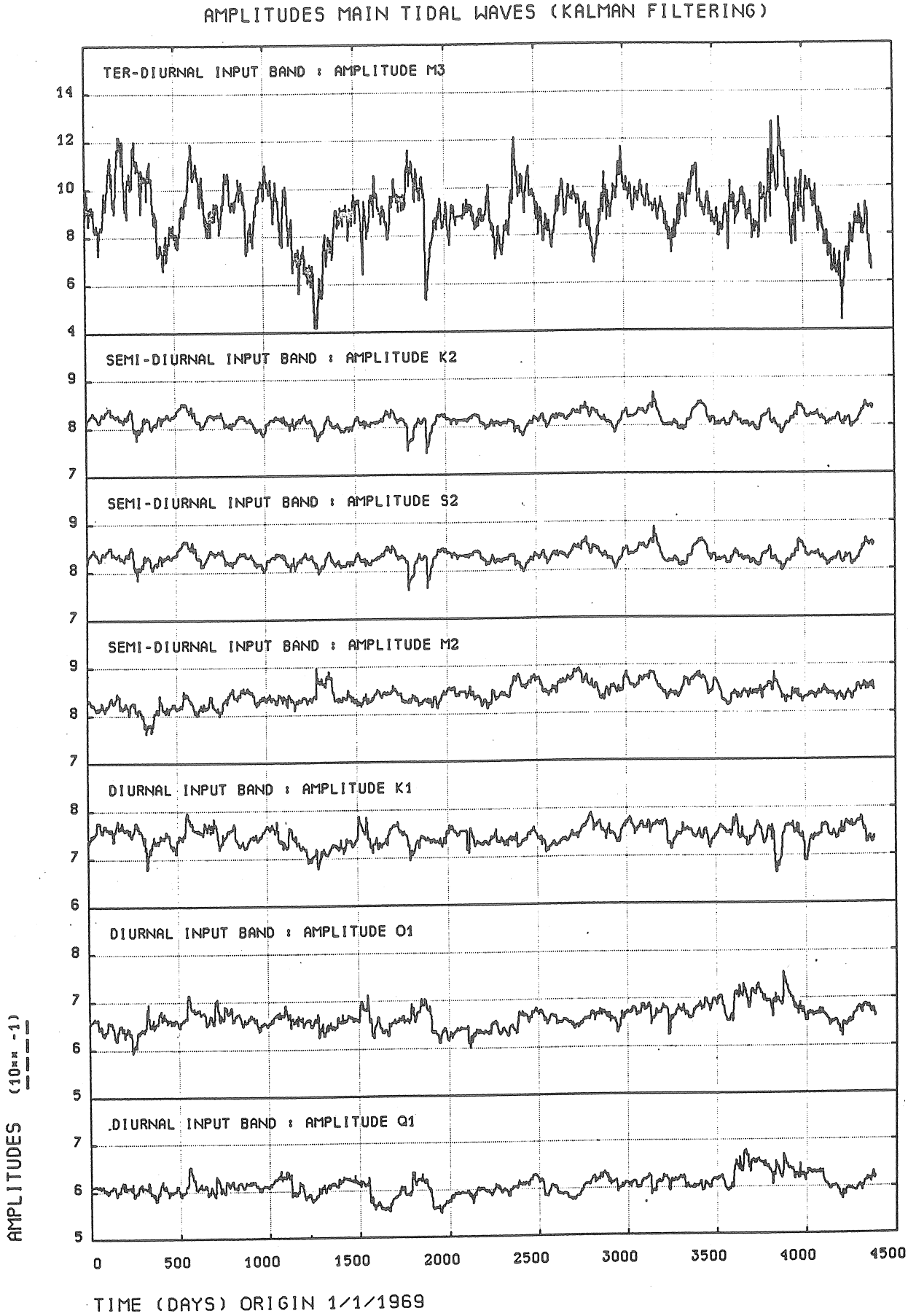

Fig.6. Time evolution of the γ-factors for the main tidal waves (Kalman filtering); EW component.

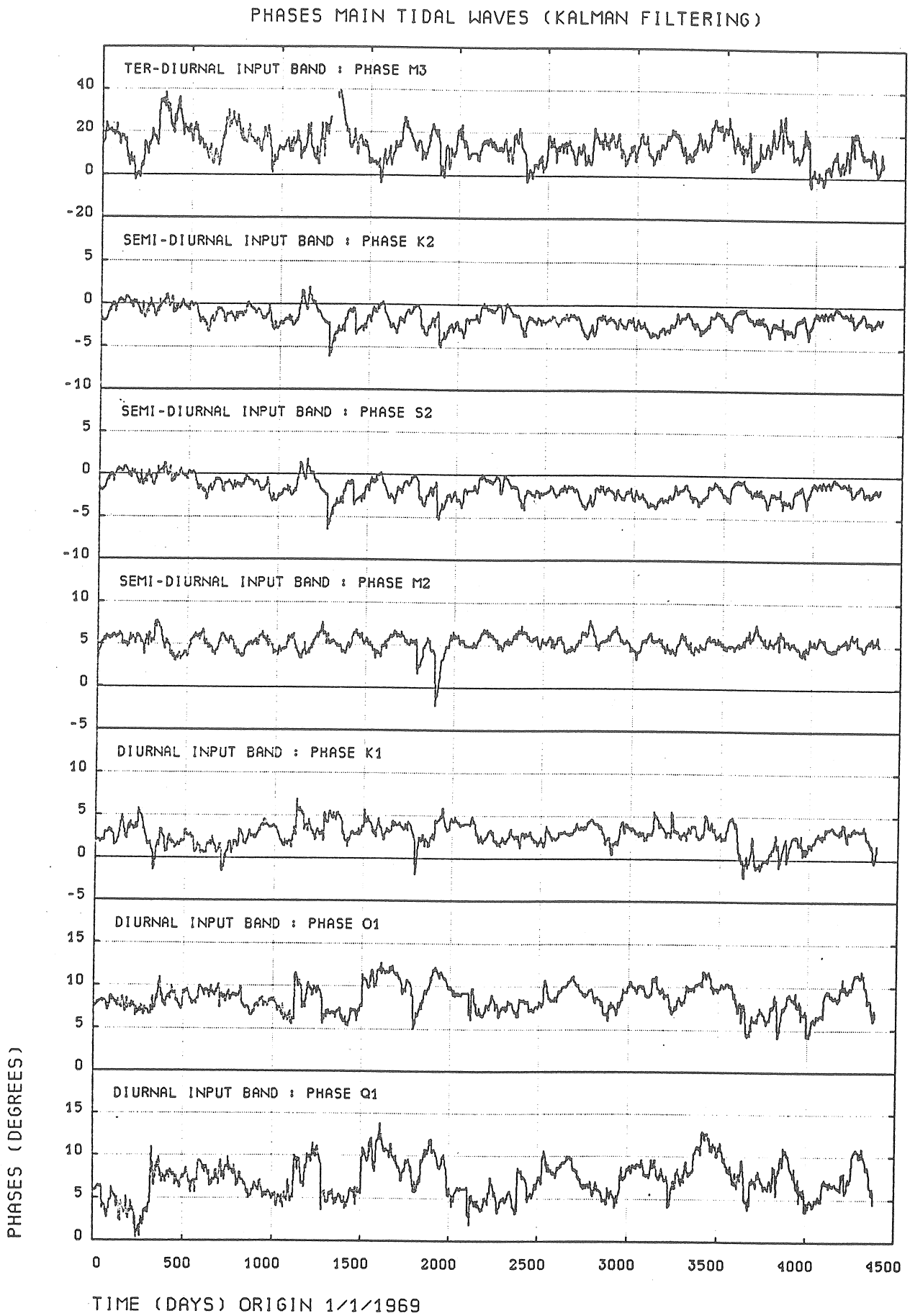

Fig.7. Time evolution of the phase differences κ for the main tidal waves (Kalman filtering); EW component.

It is concluded that there is no apparent indication of a significant time variation in the amplitude factors of the tidal waves considered. For the phase differences an identical conclusion is less affirmative.

Figure 8 represents the time variation of the amplitude responses of the three perturbation inputs at the frequencies of the principlal tidal waves K_1, M_2 and M_3. It is clear that these noisy input effects cannot be considered to be time-independent. Table 6 shows the means and standard deviations of the amplitude responses considered as functions of time; the means may be interpreted as an average of the estimated tilt effects of the disturbing phenomena in the tidal wave bands.

Table 6

Amplitude responses non-tidal inputs

	u_5 mseca/mbar		u_6 mseca/deg.cent.		u_7 mseca/meter	
	mean	st.dev.	mean	st.dev.	mean	st.dev.
K_1	0.51	0.41	0.27	0.30	0.30	0.17
M_2	0.37	0.32	0.22	0.20	0.23	0.16
M_3	0.36	0.27	0.21	0.20	0.30	0.19

Figure 9 shows the periodogram of the innovations in the Kalman filtering approach. It is interesting to see that there is no residual power left in the semi-diurnal band. It is concluded that this residual power, which remained unexplained by the constant parameter estimation of the MISO model, is now absorbed by the recursive estimation approach of the Kalman filtering procedure of the disturbing inputs and especially the channel u_7. In the quarter-diurnal band the same lines reappear, since these non-linear effects are not adequately incorporated in the model. In the low-frequency interval some residual spectral peaks are present, although the amplitudes of the associated oscillations are somewhat smaller in comparison with Fig. 2. This spectral power can be made to disappear, such that the innovations are nearly completely whitened, by taking larger values for the diagonal elements q_{jj} of the covariance matrix Q, which would result in more erratic behaviour of the model parameters and the amplitude and phase responses as functions of time. This is the compromise we have to make when applying the Kalman filtering technique.

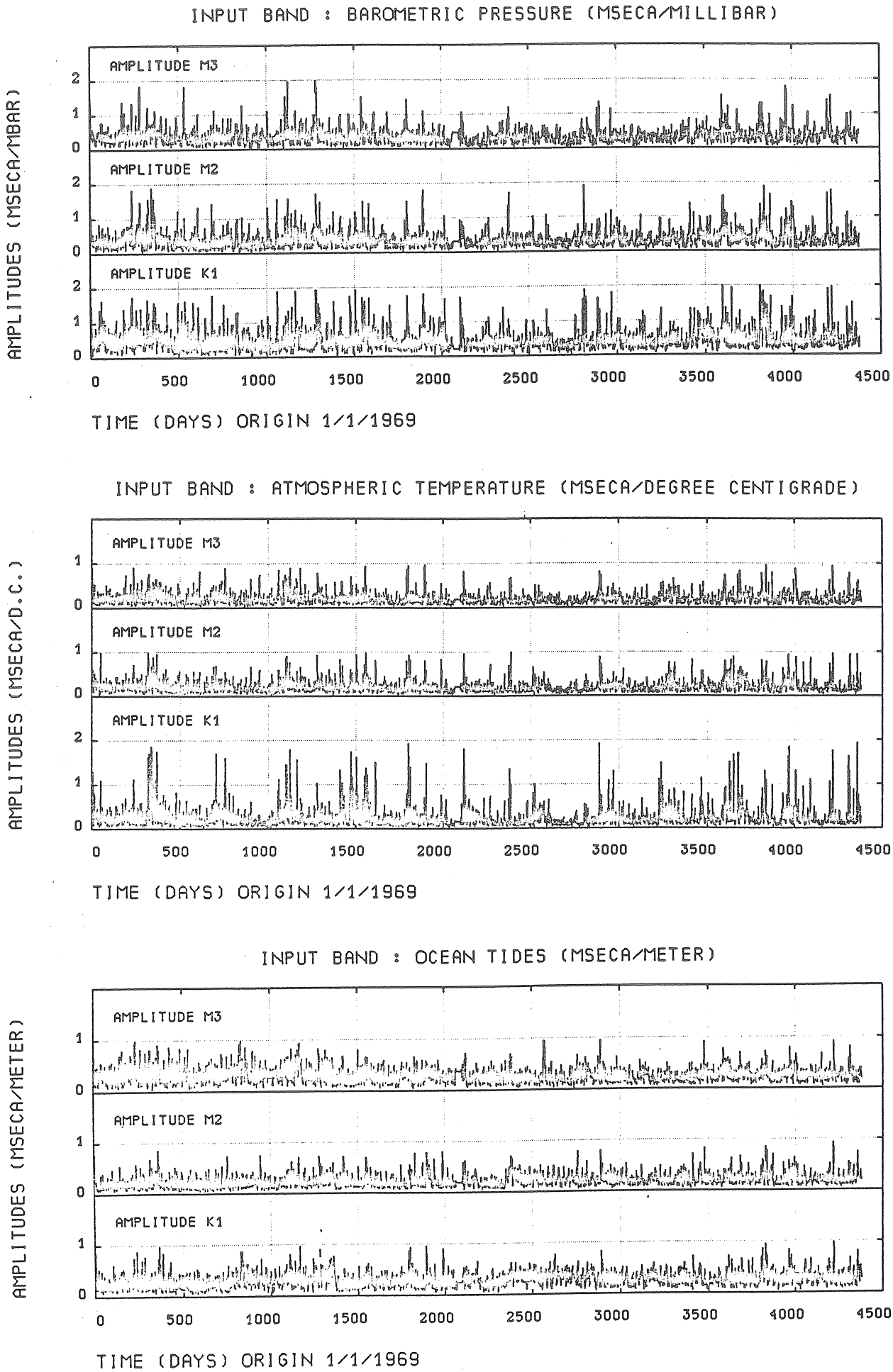

Fig.8. Time evolution of the amplitude responses of the perturbation inputs at the frequencies of the waves K_1, M_2 and M_3 (Kalman filtering); EW component.

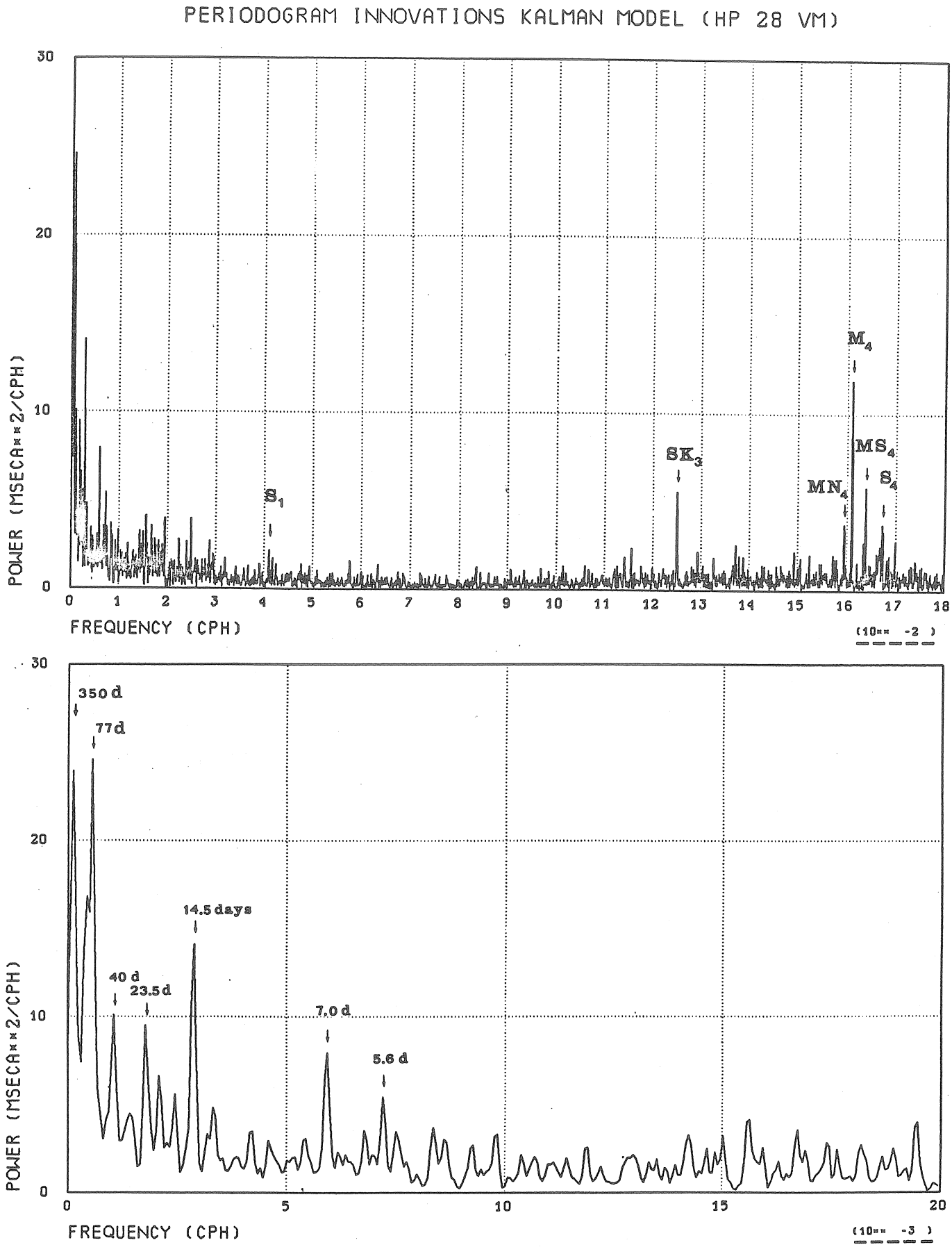

Fig.9. Residual power spectrum (Kalman filtering); EW component.

8. Kalman filtering of NS pendulum data

For the observing interval considered a Kalman filtering analysis was performed on the tilt observations, recorded with the NS Verbaandert-Melchior pendulum no° 7 at the station of Dourbes. The four tidal input functions are again computed hour by hour by the Cartwright-Tayler-Edden harmonic model in the true azimuth (-7.84° N-E) of the instrument. The three perturbation channels are taken to be the same as for the EW pendulum no° 28. The following sampling rates of the impulse responses are used: Δt_1=82 h, Δt_2=43 h, Δt_3=40 h, Δt_4=81 h, Δt_5= Δt_6= Δt_7=3 h; the truncation points of the impulse response weights are chosen as follows: $p_1=p_2=3$, $p_3=5$, $p_4=2$, $p_5=p_6=p_7=3$.

Table 7 shows the impulse response coefficients a_{kj}, $1 \leqslant k \leqslant 7$, together with their estimated standard errors Δa_{kj}, obtained with the least squares algorithm.

Table 7

Impulse response weights HP 7 VM (least squares estimation)

j	Tidal channels							
	a_{1j}	Δa_{1j}	a_{2j}	Δa_{2j}	a_{3j}	Δa_{3j}	a_{4j}	Δa_{4j}
0	0.5449	0.305	0.6536	0.018	0.5686	0.008	0.7935	0.197
1	-0.1600	0.305	0.1131	0.017	0.1241	0.009	0.0869	0.108
2	-0.0860	0.306	0.0280	0.017	0.0610	0.010	0.0458	0.197
3	-0.2933	0.305	0.2008	0.018	0.0410	0.010		
4					-0.0238	0.006		
5					-0.0056	0.007		

j	Non-tidal channels					
	a_{5j}	Δa_{5j}	Δa_{6j}	a_{6j}	a_{7j}	Δa_{7j}
0	-0.1394	0.010	-0.0213	0.007	-0.2059	0.022
1	-0.0917	0.011	-0.0236	0.007	0.0286	0.022
2	-0.0001	0.011	-0.0101	0.007	0.1300	0.022
3	0.0484	0.010	0.0103	0.007	0.0074	0.022

From the least squares estimation the following statistical information was obtained: TSS = 2.404 10^5 $mseca^2$, SSR = 2.262 10^5 $mseca^2$, RSS = 1.425 10^5 $mseca^2$ (estimated residual variance 0.14 $mseca^2$), R^2 = 0.9408, ESS = 94.08 %. The amplitude and phase response curves for the long-period tidal band are represented in Fig. 10 and the comparison between the tidal parameters, obtained with the MISO model and Venedikov's harmonic analysis, is compiled in Table 8 for the main tidal constituents.

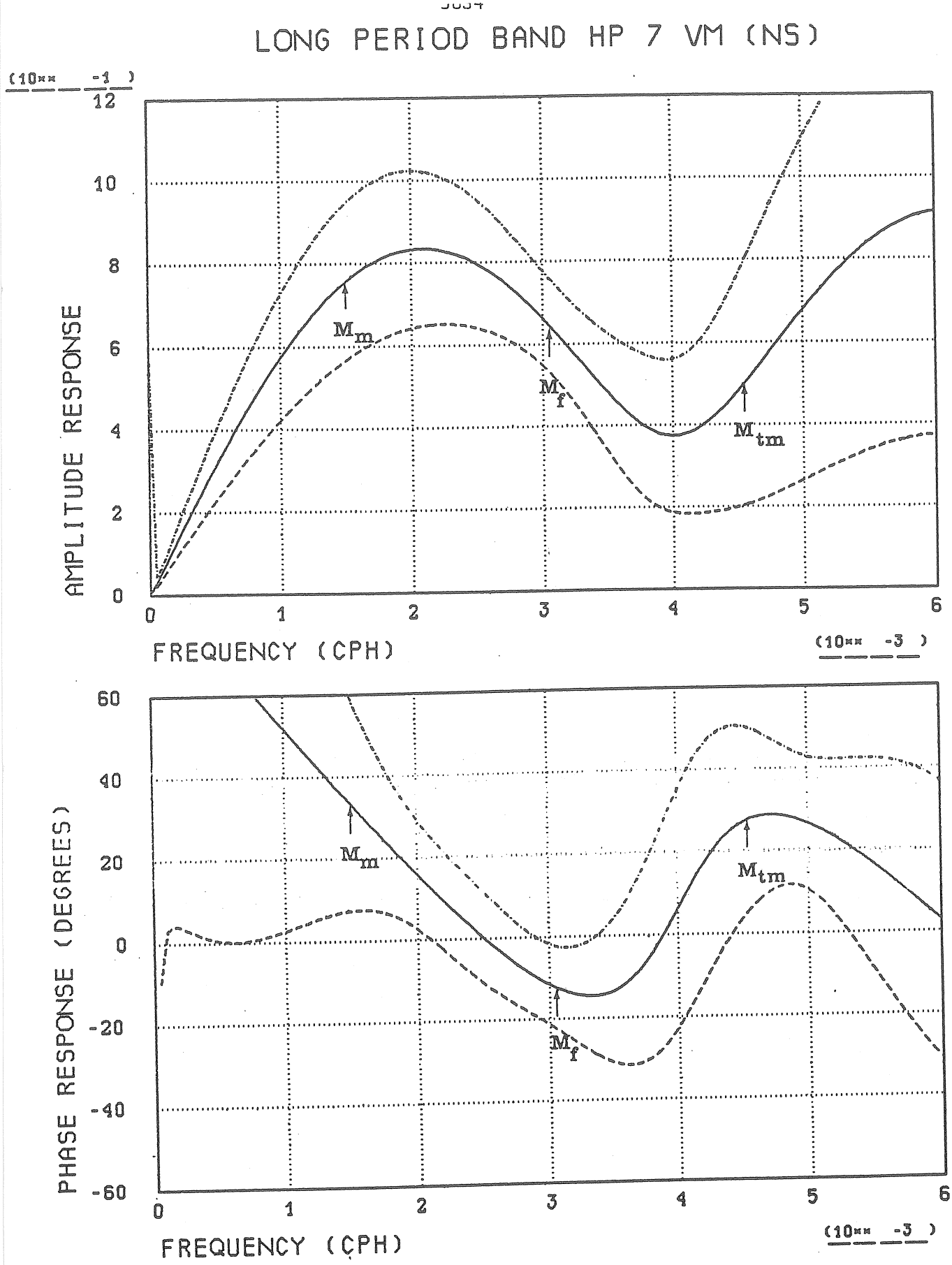

Fig.10. Transfer function in the long-period band corresponding to $H_1(f)$; NS component.

Table 8

Comparison MISO and harmonic analysis HP 7 VM (NS)

Tidal wave	MISO model				Venedikov method			
	γ	$\Delta\gamma$	κ	$\Delta\kappa$	γ	$\Delta\gamma$	κ	$\Delta\kappa$
M_{sm}	0.5178	0.0642	5.98°	12.25°				
M_m	0.5683	0.0680	7.35	9.13				
M_{sf}	0.5942	0.0466	-17.89	3.59				
Q_1	0.6749	0.0048	19.97	0.60	0.9070	0.0433	24.05	2.73
O_1	0.7873	0.0052	5.67	0.38	0.8123	0.0081	5.26	0.57
NO_1	0.6868	0.0037	-6.93	0.29	0.8144	0.0768	30.42	5.40
P_1	0.5272	0.0032	-3.47	0.36	0.4132	0.0167	3.39	2.32
K_1	0.5085	0.0034	-0.51	0.39	0.5126	0.0056	-1.08	0.63
J_1	0.5899	0.0051	21.48	0.36	0.6030	0.0932	10.86	8.86
OO_1	0.8571	0.0100	18.23	0.41	0.7332	0.1647	-20.66	12.87
$2N_2$	0.6979	0.0033	-13.51	0.28	1.2566	0.0186	5.96	0.85
N_2	0.6048	0.0025	-17.98	0.23	0.5319	0.0029	-19.20	0.31
$2M_2$	0.5885	0.0023	-18.12	0.21	0.3911	0.0151	-27.45	2.21
M_2	0.5010	0.0017	-13.97	0.20	0.4423	0.0005	-8.79	0.07
L_2	0.4947	0.0020	-5.11	0.24	0.4184	0.0170	49.56	2.33
S_2	0.5290	0.0015	-4.18	0.16	0.5301	0.0011	1.26	0.12
K_2	0.5318	0.0015	-4.59	0.16	0.5356	0.0042	-0.28	0.45
M_3	0.7144	0.0218	7.64	1.61	0.7920	0.0151	9.00	1.09

Figure 11 shows the residual periodogram in the frequency intervals $0 \leqslant f \leqslant 0.18$ cph and $0 \leqslant f \leqslant 0.03$ cph. In the diurnal band small peaks are observed at the frequencies of the waves O_1 and S_1, while in the SD-band peaks at μ_2 and M_2 stand out clearly. The residual power in the TD- and QD-bands for this NS inclinometer is very small. The low-frequency interval is dominated by an important long-period peak at nearly one year . Much of the residual power is concentrated in the semi-diurnal band and is interpreted as being induced by the ocean tides. In this respect it is concluded from Fig.2 and Fig.11 that ocean tides have a more pronounced effect in the NS-direction than in the EW-direction for the station concerned.

The results of this least squares computation are used as initial parameter estimates of a Kalman filtering analysis, adopting the same values for the constant variance r_t of the measurement noise and the diagonal elements q_{jj} of the error covariance matrix Q_t as in Section 7. For the input channel u_1 the values $q_{jj} = 10^{-6}$ are selected a priori. Since the sum of squares explained by the Kalman filter model is SSR = $2.292\ 10^5$ mseca^2, a residual sum of squares RSS = $1.117\ 10^4$ mseca^2 and an estimated variance of 0.11 mseca^2 of the

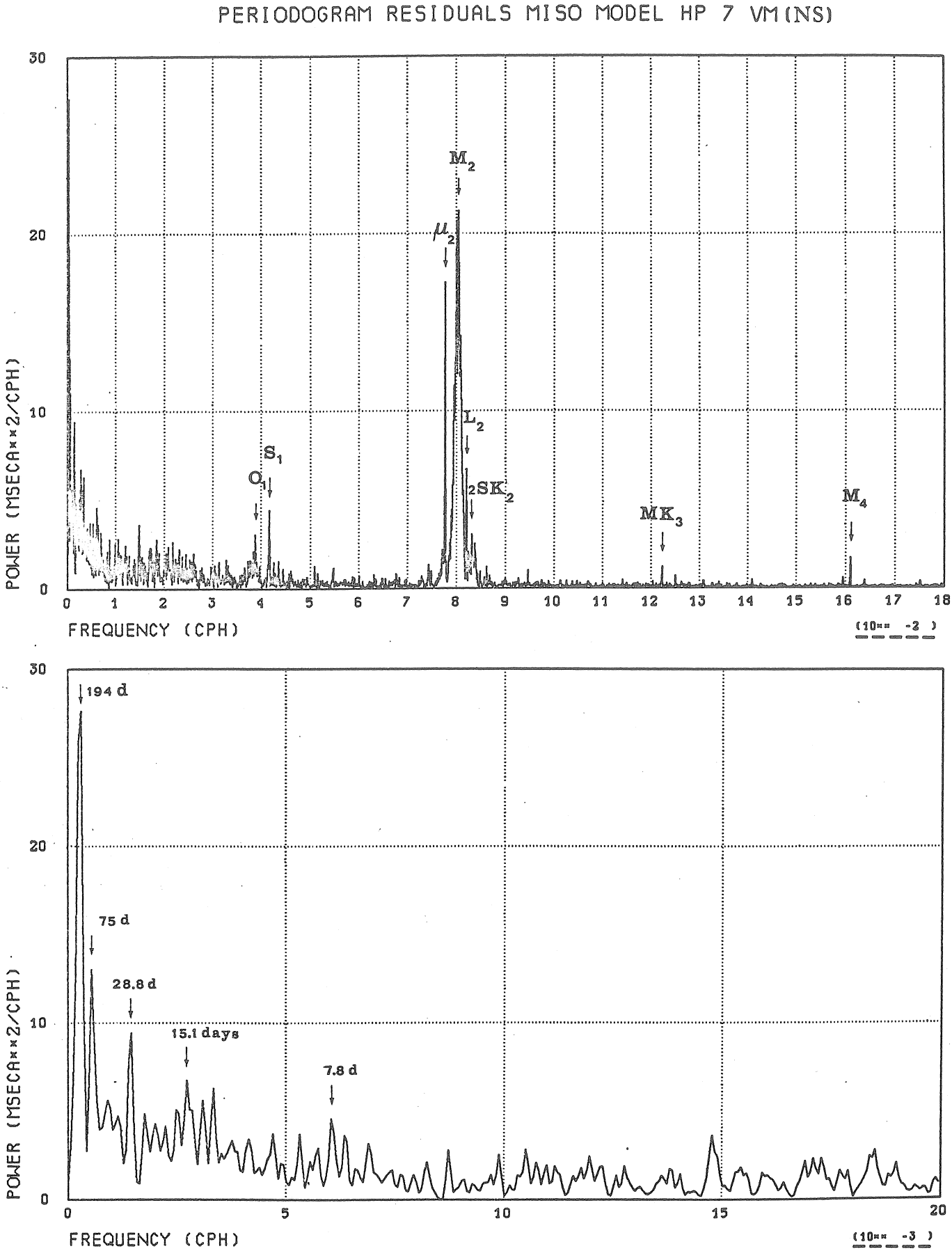

Fig.11. Residual power spectrum (least squares estimation); NS component.

innovations are obtained, which gives a percentage explained sum of squares of ESS = 95.35 %.

Figures 12 and 13 respectively show the time evolution of the amplitude and phase response at the main tidal constituents in the long-period wave band. It is difficult to conclude unambiguously whether or not these tidal parameters are constant. Table 9 gives the means and standard deviations of the amplitude ratios and the phase differences, viewed as functions of time.

Table 9

Means and standard deviations of γ and κ

	γ		κ	
	mean	st.dev.	mean	st.dev.
S_{sa}	0.4176	0.226	18.06°	33.51°
M_m	0.8953	0.146	15.02	12.44
M_f	0.6461	0.139	-21.63	18.24
M_{tm}	0.7147	0.119	37.96	20.71
Q_1	0.6702	0.030	20.89	4.71
O_1	0.7865	0.031	5.45	3.16
K_1	0.4797	0.040	0.72	3.30
M_2	0.4748	0.017	-10.48	2.34
S_2	0.5493	0.018	-0.74	1.90
K_2	0.5550	0.018	-1.53	1.93
M_3	0.7145	0.108	-7.18	5.62

Table 10 shows the means and standard deviations of the amplitude responses, considered as functions of time, of the three perturbation inputs at the frequencies of the principal tidal waves.

Table 10

Amplitude responses non-tidal inputs

	u_5 mseca/mbar		u_6 mseca/deg.cent.		u_7 mseca/meter	
	mean	st.dev.	mean	st.dev.	mean	st.dev.
M_f	0.44	0.50	0.27	0.36	0.15	0.17
K_1	0.49	0.38	0.25	0.28	0.21	0.17
M_2	0.38	0.29	0.19	0.20	0.26	0.18
M_3	0.28	0.23	0.17	0.18	0.24	0.16

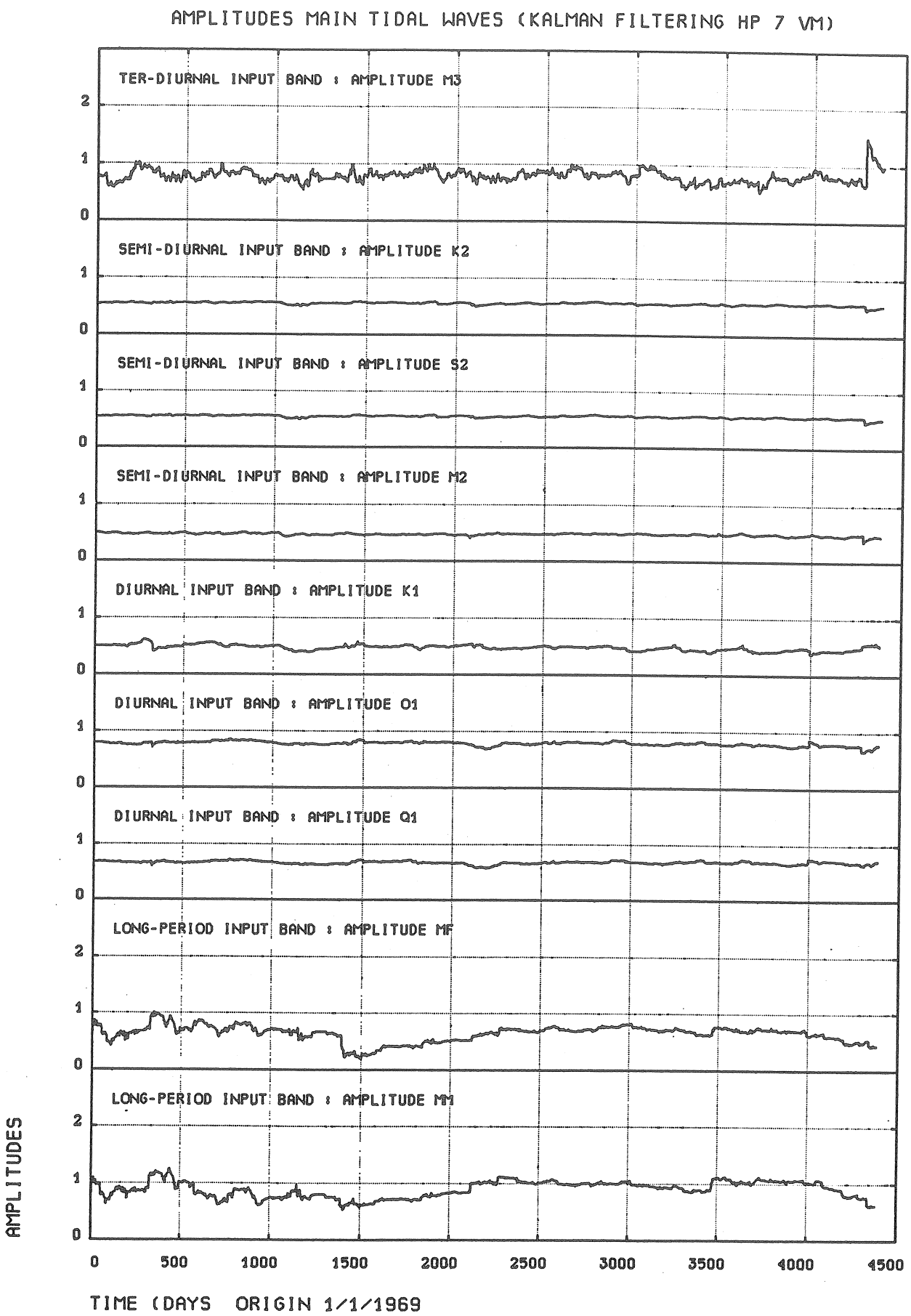

Fig.12. Time evolution of the γ-factors for the main tidal waves (Kalman filtering); NS component.

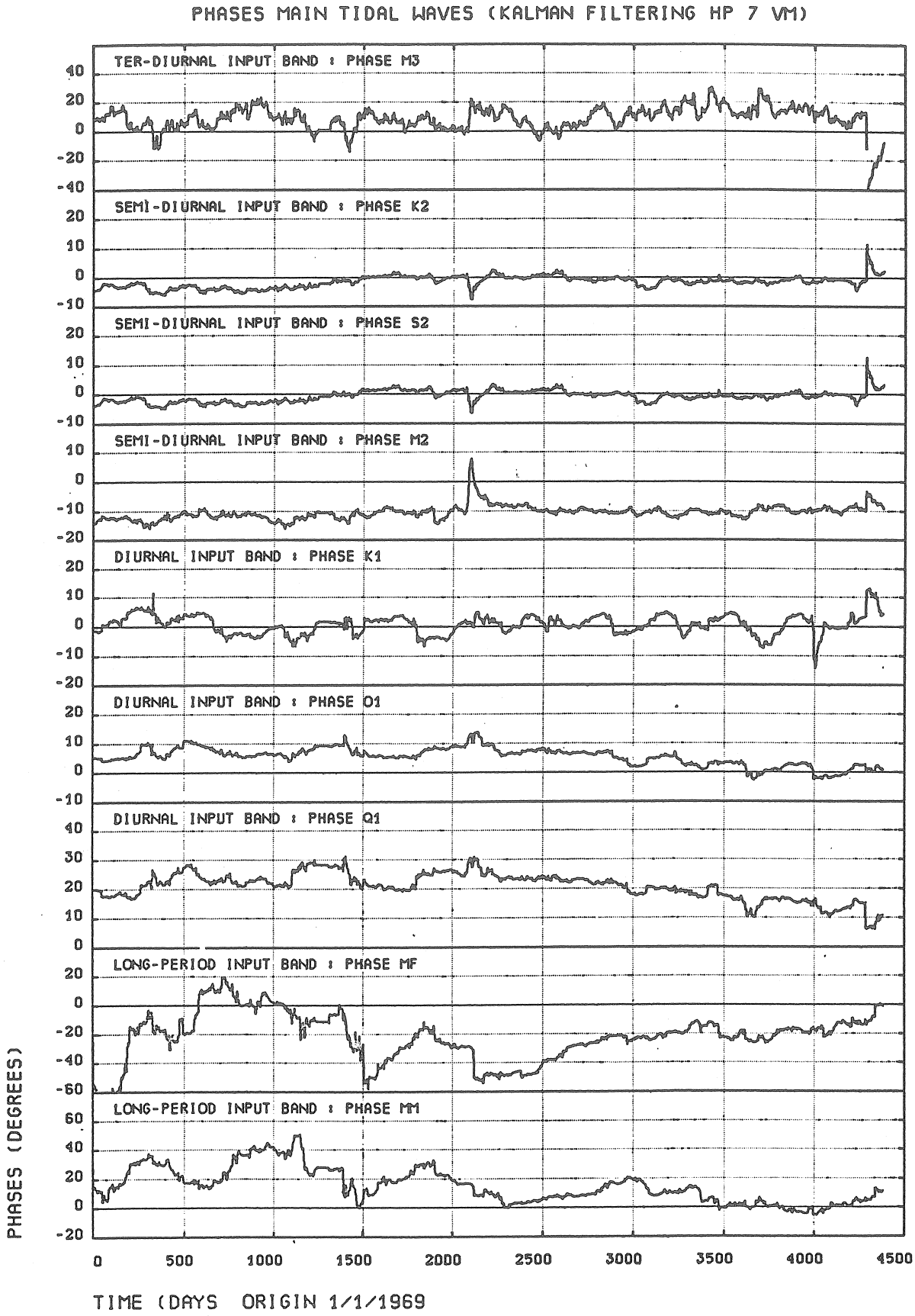

Fig.13. Time evolution of the phase differences κ for the main tidal waves (Kalman filtering); NS component.

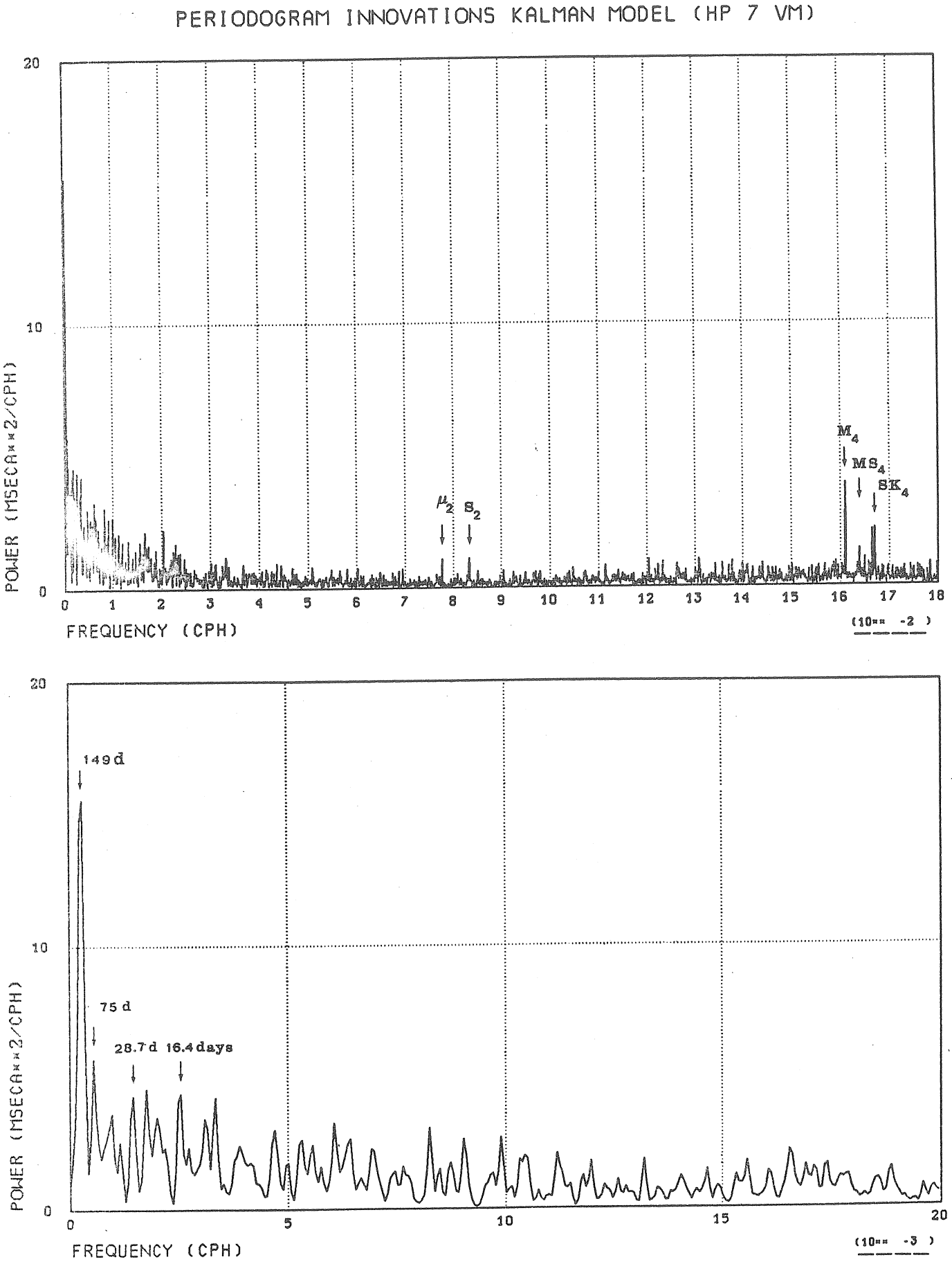

Fig.14. Residual power spectrum (Kalman filtering); NS component.

Figure 14 represents a power spectrum estimate of the innovations obtained by the Kalman filtering method. In comparison with Fig.11 it is noteworthy that the residual power in the diurnal and semi-diurnal bands is now absorbed by the recursive procedure and that the peaks in the low-frequency interval have smaller amplitude.

9. Conclusions

The harmonic analysis of Earth tide observations gives a point-wise estimation of the response function of the Earth at the frequencies of the principal tidal waves. The fact that the weaker lines are hopelessly contaminated by the extraneous noise and the nearby dominant constituents accounts for the inconsistensies in the associated γ- and κ-factors from different instruments and observing intervals. An advantage of the input-output model is that the tidal inputs can be included a priori in the analysis and that one can increase the number of subsystems for other influencing tidal and non-tidal phenomena. In an attempt to incorporate the geophysical environment of the instrument the relative importance of the MISO model increases with the complexity of the spectral inputs.

It is interesting to note that in this approach only direct computations or measurements of the input channels are used, that no elimination of the 'drift' is necessary and that no explicit filtering of the data is needed. The results are represented as smoothed transfer functions, associated with the individual inputs, which can be directly interpreted in terms of the usual tidal parameters.

The Kalman filter scheme can be used to study possible non-stationarity of the system model. A drawback of this approach is that subjective information about the variance of the measurement noise and the error covariance matrix of the time variations of the model parameters has to be adopted. For the observation interval concerned the tidal factors γ and κ are interpreted as being constant, but the amplitude responses of the disturbing input channels in the tidal wave bands are concluded to be time-variable.

A further development should be the combination of the harmonic model to describe the tidal contributions and an input-output model to include the influences of the perturbation phenomena.

Acknowledgment

The author expresses his indebtedness to Prof. Melchior for providing the ocean tide observations and his constant interest in

this controversial subject.

References

Bennet R.J.,1979, Spatial time series, Pion Ltd, London.

Box G.E., G.M. Jenkins,1970, Time series analysis, Holden-Day, San Francisco.

Cartwright D.E., R.J. Tayler,1971, New computations of the tide-generating potential, Geoph.J.R.astr.Soc.,23,45-74.

Cartwright D.E., A.C. Edden,1973, Corrected tables of tidal harmonics, Geoph.J.R.astr.Soc.,33,253-264.

De Meyer F.,1982, A multi input-single output model for Earth tide data, Bull.Inf.Mar.Terr.,88,5628-5674.

Jazwinsky A.H.,1970, Stochastic processes and filtering theory, Academic Press, London.

Jenkins G.M., D.G. Watts,1968, Spectral analysis and its applications, Holden-Day, San Francisco.

Johnstone J.,1972, Econometric methods, McGraw-Hill, New York.

Kalman R.E.,1960, A new approach to linear filtering and prediction problems, Journal of Basic Engineering, Transactions of the American Society of Mechanical Engineers,D82,35-45.

Kalman R.E.,1963, New methods in Wiener filtering theory, Proc.Symp. Eng.Appl.Random Functions, John Wiley, New York.

Kalman R.E., R.S. Bucy,1961, New results in linear filtering and prediction theory, J.Basic Eng.,83,95-108.

Lee R.C.K.,1964, Optimal estimation,identification and control, M.I.T. Press, Cambridge.

Munk W.H., D.E. Cartwright,1966, Tidal spectroscopy and prediction, Phil.Trans.Roy.Soc.London, Ser.A,259,533-581.

Robinson E.A.,1980, Physical applications of stationary time-series, Charles Griffin, London.

Young P.C.,1970, An instrumental variable method for the real-time identification of a noisy process, Automatica,6,271-297.

Erratum

The interpretation of Fig.3.b and Fig.6.b of the paper of De Meyer (1982) is in error. Since the frequency is expressed in cycles/hour,the periods (given in days), corresponding to the spectral peaks, should be divided by 24.

INFORMATION ON A PROGRAM FOR EARTH TIDE DATA PROCESSING

A.P. VENEDIKOV,
Geophysical Institute, Sofia.

This paper is an account of the possibilities of a computer's program developed by the author. The main object of the program is the analysis of Earth tide data, i.e. the derivation of the Earth tidal parameters : amplitude factor and phase shift.

As it can be seen from the "historical" review implemented in paragraph 1 the program is a product of a long time work at different places, using different computers as well as the help of a number of researchers. As a result the program has been provided by a series of additional facilities. Some of them are designed to make easier the practice of the analysis, while some others can be used for special purposes.

In the following most of the possibilities of the program and its general functions will be enumerated. We expect that such an exchange of our experience can be interesting not only for people intending to use this very program.

1. Development of the program.

It has started in 1965 and continued in 1966 and 1967 in ECET in the Royal Observatory of Belgium. This has been done under the direction and the initiative of P. Melchior, with the important help of P. Pâquet, B. Ducarme and other people from the Royal Observatory. The computers used were an IBM 1620 and an IBM 7040. A version of the program has been published (Venedikov & Pâquet, 1967).

The program at that time was designed for the application of a new method for analysis (Venedikov, 1966a, 1966b, Melchior & Venedikov, 1968, Melchior, 1978, pp. 176-182). Its principal properties are :

1.1. Construction of numerical filters by the leastsquares method.

1.2. Filtering of independant intervals of length 48 hours which eliminates the drift and separates the main tidal species.

1.3. Processing of the filtered numbers by the leastsquares method.

1.4. Introduction of specific unknowns with a grouping of the closed tidal waves.

1.5. Processing of tidal records with arbitrary lengths and interruptions.

1.6. Possibility to derive the ter-diurnal (TD) tides together with the diurnal (D) and semi-diurnal (SD) tides.

1.7. Severe estimation of the precision, specific for D, SD, and TD tidal species.

Later we have tried to improve the program as well as the method for analysis in Sofia. We have used several small computers (IBM 1460, FACOM 750, ZIT 150, ICL 1200).

A more important step has been undertaken in 1973 in the Department of Solid Earth Physics of the University in Uppsala with the help of A. Vogel, A. Anderson, B. Kulinger, K. Lund and others. The computer used was an IBM 370 belonging to the University.

This work has continued in Sofia first on the computer ICL 4/50 and then, till now, on IBM 370/145. We have been helped, in the framework of a cooperative project KAPG, by Z. Šimon, T. Chojnicki, P. Varga, S. Barsenkov, M. Kuznetzova, V. Volkov, H.-J. Dittfeld, W. Schwahn and others.

In 1978, with the participation of B. Ducarme, we have adjusted a new version of the program for ICET. We have it applied there on an UNIVAC computer.

In its second stage (after 1973) the program is designed for the application of a variant (Venedikov, 1977, 1978) of the method mentioned above. There are new elements concerning merely the items 1.2. and 1.3, and namely :

1.2. The filters to be used (including the length of the filtered intervals) are not fixed. They can be chosen in one or another way at each application of the analysis.

1.3. The filtered numbers are provided by some weights reflecting a variation of the quality of the data with time. They can be taken into account in the application of the method of the least squares.

The item 1.6. was enlarged with the determination of the long period waves (Venedikov & Ducarme, 1979).

The program in its present state is stored in the computer used under the name SVETLA. In the following we shall call it shortly SV.

2. General description.

SV consists of four principal elements whose interrelation is shown of Fig. 1. They are :

2.1. Data management D. It organizes a data bank which allows the manipulation of a multitude of Earth tide records. The bank may comprise some other kinds of records for special purposes. Here it is possible, at the time of a processing, to introduce a series of corrections of the data. D is an initial element of SV.

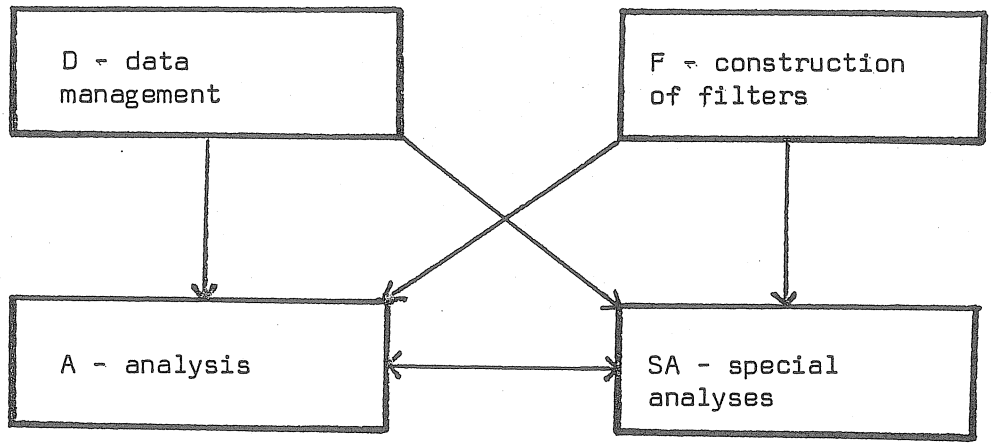

Fig. 1.

2.2. Construction of filters F. This is also an initial element of SV. Each processing begins with the computation of the coefficients and the characteristics of some filters. F can create many variants of filters for a variety of problems. In SV we do not use ready filters, though some fixed variants are presumed. The advantages of such a practice are : (i) we avoid the organization of an external storage for the filters, (ii) the analyses can be realized easily in different variants and (iii) it is possible to use SV for particular tasks.

2.3. Analysis A. It provides the tidal parameters according to the method mentioned in paragraph 1.

2.4. Special analysis and processings SA. We have in mind several features of SV which are usually related to A. However, in some cases, they may have their own output. The two way arrow between A and SA means that A may use a product of SA as well as that SA may use a product of A.

In the following paragraphs we shall consider the general way of work of D, F, A and SA and their products.

3. Data management D.

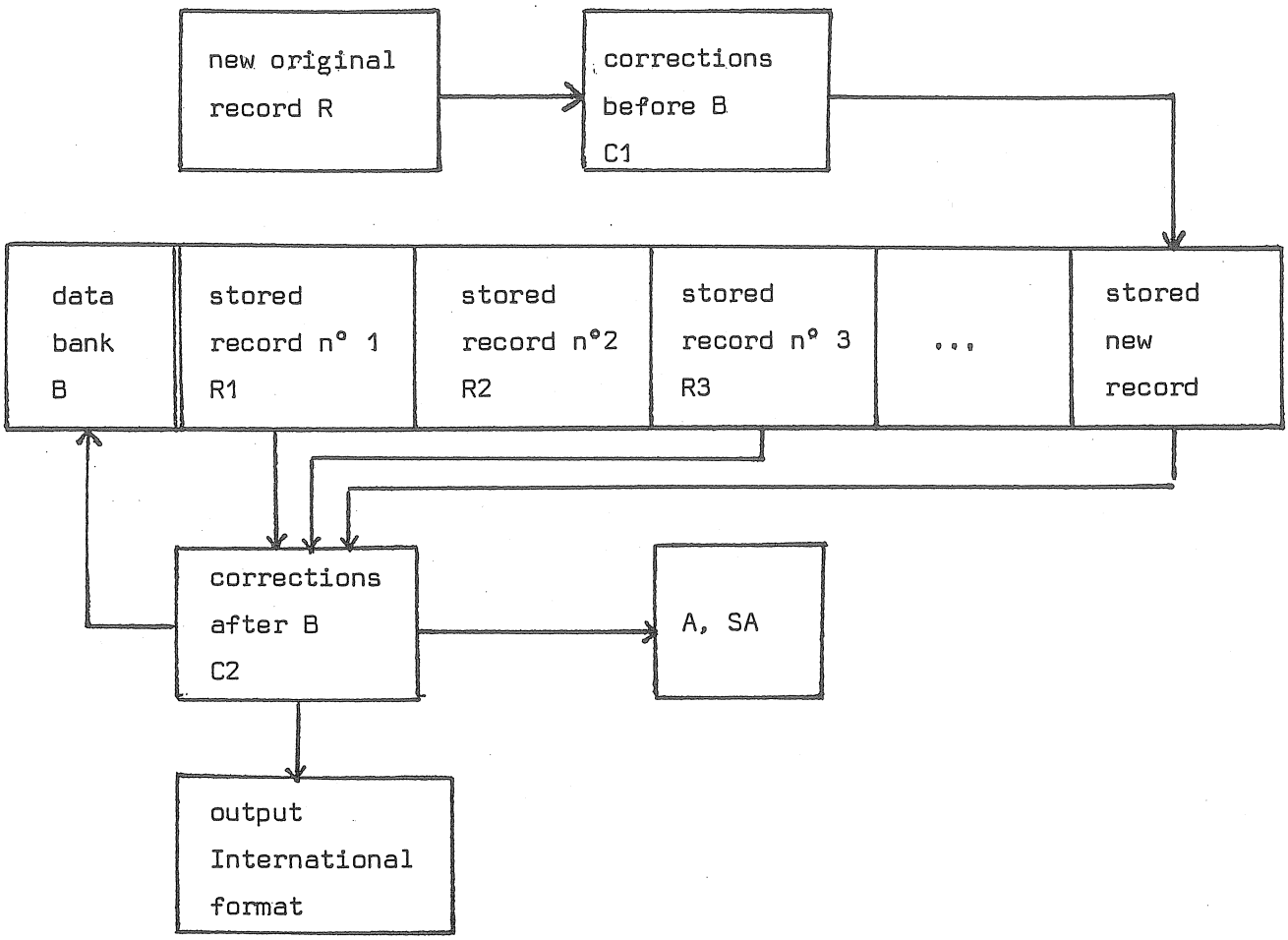

Fig. 2.

The general scheme of this part of SV is given on Fig. 2. Here we have three principal elements : R, B and C (in SV C1 and C2 are identical) which we shall consider in the following.

3.1. A record R is the original data (ordinates) taken from an Earth tide record. In some cases R can be a record of another kind of data (oceanographic, meteorological, hydrological). We have the following requirements and options :

3.1.1. R is a sequence of hourly ordinates in arbitrary units. It is divided in portions of 12 hours (for example 12 ordinates per punched card or per a record in a magnetic tape ; it is to be distinguished the word record used here and the same word used in the computer's slang) as in the International format (Ducarme, 1978). Each 12 h. are to be accompanied by the date in U.T. of the first ordinate.

3.1.2. The format of the data can be arbitrary, even it can vary within a R. However the International format is to be recommended.

3.1.3. R without a date at each 12 h. is also acceptable. In such a case the dates at the begining of R as well as after each interruption in R should be indicated. Such a practice is not recommended.

3.1.4. Fictive 12 h., in which the date is replaced by some indicators, indicate the interruptions and the end of R as well as corrections to be introduced through C1.

3.1.5. Usually R includes the title of the station, its coordinates and, if the unit of the ordinates is not a tidal one, a calibration table. However, each of these informations, can be introduced later, through C2.

3.2. Data band B in which a sequence of records R is collected. It has the following general properties.

3.2.1. The data are written in B in a highly compressed format, nearly three times more economical than the International format.

3.2.2. For the exchange of data the International format is accepted as a convenient one and there is an output from B (through C2) in this format.

3.2.3. Usually (see 3.1.5) each R in B is accompanied by the whole information necessary for the analysis.

3.2.4. Each R enters B when it appears. Later on it can be processed as many times as we want calling it simply through its sequential number in B. A repeated processing we way have when we want to apply some new corrections, a new kind of analysis or when we want to joint a given

R with a new configuration of other records (see 3.2.5)

3.2.5. B allows a joint processing of several records without importance of their disposition in B. They can be called, besides through the sequential numbers, by the indication of some characteristics such as geographic coordinates, name of station, number of instrument. In the example on Fig. 2 the records R1 and R3 written on B earlier plus the new record will be processed jointly. Using this possibility the observations by one instrument at one stations can be collected in B in small portions. At the end of the observation or at a given stage all portions can form one single record without particular cares. Other uses of this possibility will be given in paragraph 6.

3.3. Corrections C. Between R and B C (as C1) introduces corrections in the original data and the corrected data enter B. After B (as C2) it corrects the data for the analysis or for an output, the data in B remaining untuched. C2 can also correct the data and rewrite them in B. In addition C2 may provide an information concerning the processing only (A, SA).

The corrections can be :

3.3.1. Some ordinates can be replaced by new values.

3.3.2. The dates of some portions of 12 h. can be changed.

3.3.3. Some omitted portions of 12 h. can be included.

3.3.4. Some data can be rejected.

3.3.5. New interruptions in R can be declared.

3.3.6. Known shift corrections can be introduced.

3.3.7. A scale factor which can vary in a stepwise way can ne applied.

3.3.8. Calibration through linear or not linear interpolation.

The following points concern C2 only.

3.3.9. When the place of a shift (displacement in the recorded curve) in R is known but its value is not known, it can be determined and introduced. The precision of this operation is estimated and its effect on the following processing is taken into account.

3.3.10. A correction in seconds to the dates can be introduced. It may vary within R.

3.3.11. When the response of the instrument is not the same for all tides corresponding phase and amplitude corrections can be introduced.

3.3.12. Ocean tidal corrections can be introduced when they are expressed in amplitude factors and phase shifts as well as through the residual vectors.

3.3.13. The titles an the coordinates can be replaced.

The input to SV that concerns C is organized in a rather flexible way. Each kind of information has an input number. When a given number appears at the input, the following input is related to the corresponding information. In such a way it is not necessary to observe any sequence in the input. It is possible to enter at once as well as at different stages of the processing the information about different R.

4. Construction of filters F.

A set of filters in SV is a linear operator which solves a system of equations according to the method of the least squares. The equations approximate an arbitrary interval of an arbitrary record through a few components. A component is a function of the time t measured from the centre of the arbitrary interval.

For example in a variant used for the analysis there are tidal components : S1, O1, S2, N2, M3 (cosine and sine terms) and non tidal components (included for the drift) : t^k (k = 0, 1, 2, 3). The lenght of the interval is 36 hours.

Each component is transformed in F into a filter which amplifies this very component. Its effect upon the other components depends on the way of their inclusion in the equations. Usually a filter eliminates totally some of the components and only an orthogonal constituent of the remaining components. More details are given in (Venedikov, 1977, 1978).

When the equations include only tidal components and components representing the drift the filters are usually designed for the tidal analysis. When some special functions are considered we get some special filters. For example if a component is the function d(t) defined as : d(t)= 0 for $t < t_d$ and d(t) = 1 for $t \geq t_d$ we get a filter for the determination of a shift (displacement) in a record at time $t = t_d$ within any arbitrary interval.

The general scheme of F is given on Fig. 3. The functions and the possibilities of its elements are the following :

4.1. List of components BLD. This is a block data program which provides the information necessary for the constitution of 520 components :

4.1.1. 504 waves of the tidal potential development of Cartwright, Tayler, Edden (1971, 1973).

4.1.2. Two non-Earth tidal waves with periods 6 and 4 hours. They can be used for the study of an ocean tidal effect.

4.1.3. Six aperiodic components. When the k^{th} (k = 1, 2, ...6) of them is addressed the function $t^{(k-1)}$ is computed.

4.1.4. Eight particular waves with periods longer than 24 hours. They are used to characterize the effect of a filter on a periodic drift. They can also be used for the approximation of the drift by a combination of a polynomial with long period functions. When particular waves are to be studied they replace some of these eight waves.

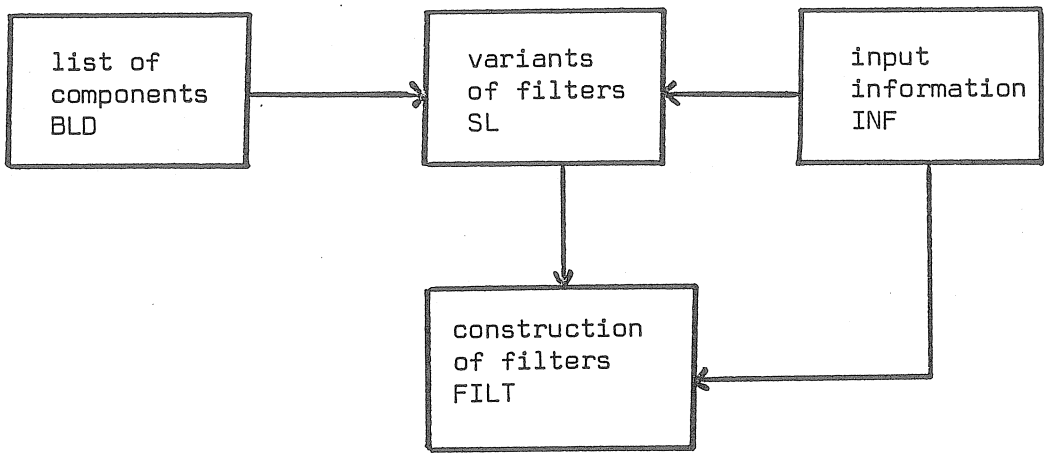

Fig.3.

4.2. Variants of filters SL. It provides the indices of the components existing in BLD which participate in different variants of filters. There are several variants of configurations of tides as well as several variants of representation of the drift. SL is applied in two principal ways :

4.2.1. SHORT - for the determination of D, SD and TD tides. There are 40 variants of configuration of the tides.

4.2.2. LONG - for the determination of long period tides (Mf). There are 24 variants of configuration of the tides.

4.3. Input information INF. It provides the information about what kind of filters is to be constructed and which variant of components is to be chosen. The information is an input to SV physically obtained through the block C (3.3). It can comprise :

4.3.1. No-information - then a fixed standard variant for the analysis is chosen among all variants existing in SL.

4.3.2. The index of a variant of tidal configuration in SL.

4.3.3. The variant of the representation of the drift.

4.3.4. New variants which are not presumed in SL.

4.3.5. The length of the filters. It may vary from 12 to 72 hours for SHORT and from 336 to 720 hours for LONG.

4.3.6. Particular waves which are not prescribed by BLD and which we want to amplify or to eliminate for special purposes.

4.3.7. Indications for the construction of special filters.

4.4. Construction of the filters FILT. Here the coefficients of the filters as well as their response to the components provided by BLD are computed. It works depending on BLD, SL and INF. The principal possibilities are :

4.4.1. Filters for the analysis.

4.4.2. Filters for interpolation and extrapolation.

4.4.3. Filters for the determination of a shift.

4.4.4. Filters for the determination of particular periods.

4.4.5. Filters for the determination of the drift and its derivatives.

4.4.6. Filters for the estimation of the precision within the filtered intervals.

4.4.7. FILT can be called from any program for any processing of data (not only tidal data) which needs a filtering.

5. Analysis A.

The method for analysis was described in paragraph 1.

The general scheme of its realization is shown on Fig. 4.

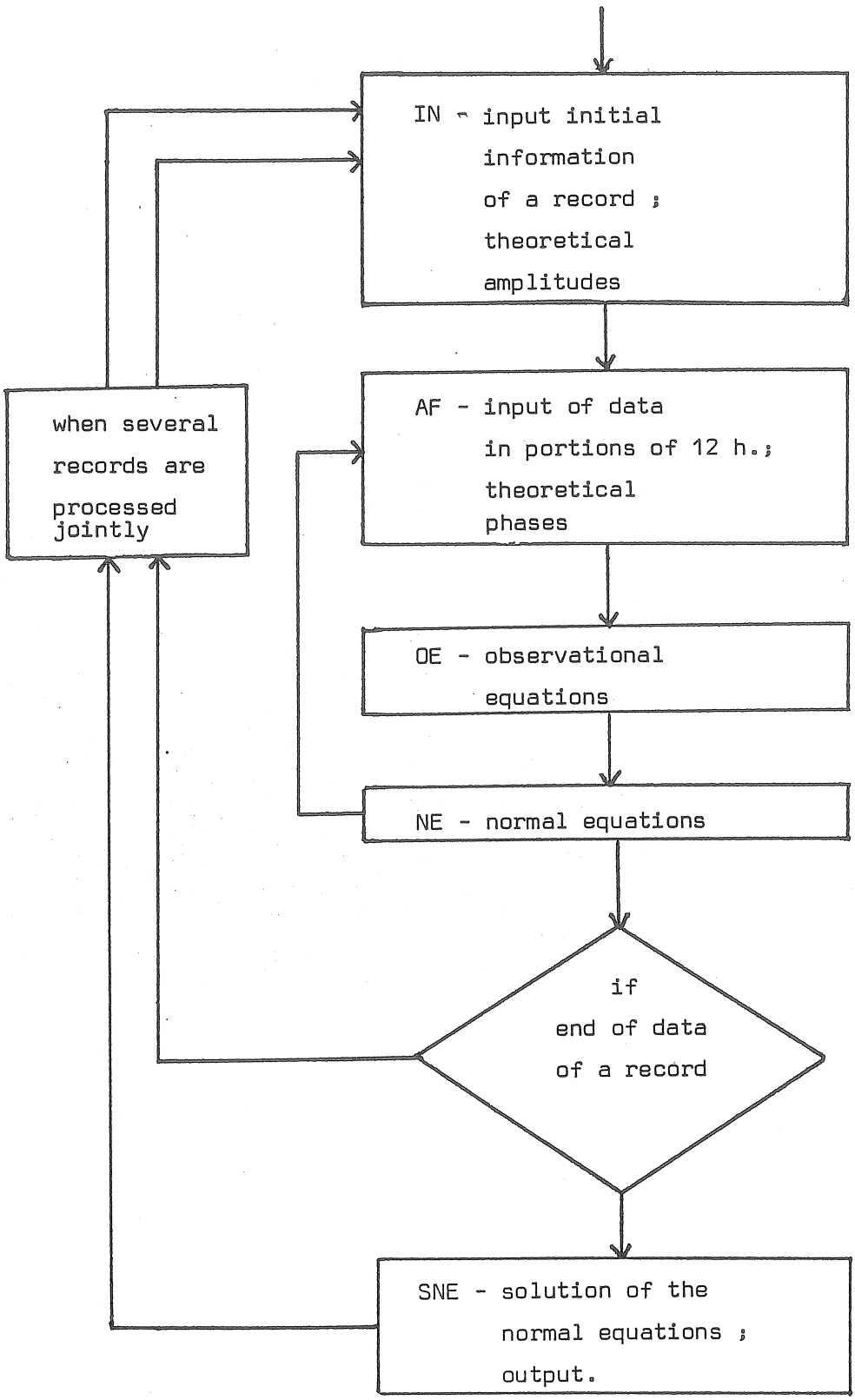

Fig. 4.

The meaning of its elements is the following :

5.1. IN - the title of the record to be processed and its geographic coordinates enter SV. Here the theoretical amplitudes are calculated.

5.1.1. For gravimetric and clinometric observations the formulae given by Picha, Skalski and Šimon (1973) are used. They orientate the theoretical components of the tide towards the normal to the Earth ellipsoid. The horizontal components are orientated in the azimuth of the observations.

5.1.2. For extensometric observations a program provided by ICET is used. Initially this program was designed for the determination of the residuals relative to a Molodenski's model.

5.1.3. When some particular (non-tidal) waves are to be considered, theoretical amplitudes equal to 10^k are accepted. Here k is to be chosen according to the possible magnitude of the observed amplitude.

5.1.4. When non-tidal series are processed it is possible to choose only one single wave from each group of waves. This can be used when one does not expect all details of the tidal process to be reflected in such series.

5.2. AF - application of the filters. The filtered numbers with their mean square errors for a given interval of the record are determined. According to Fig. 4. after a processing of the filtered numbers the control of SV passes back from NE to AF. Then a subsequent interval is processed and so on.

5.2.1. SV can apply at once several sets of filters which differ in the power of the polynominals used for the representation of the drift (eliminated power). The powers for the even filters can be : k_1 = 1, 3, 5 and for the odd filters : k_2 = 0, 2, 4. Next SV processes simultaneously the couples k_1, k_2 = (1,0), (1,2), (3,2), (3,4), (5,4).

5.2.2. The mean square errors are computed basing on that the filtering procedure is equivalent to an approximation of the data within the filtered interval. This is done in two variants : (i) the series (L_{T+t} + L_{T-t}) and (L_{T+t} - L_{T-t}) are approximated separately through the even and the odd filters and separate mean square errors are determined and (ii) the ordinate L_{T+t} is directly approximated. Here L_{T+t} is an ordinate at time T+t, T is the central epoch of the filtered interval and t is the time within the interval measured from T. In (i) t takes only values t > 0, while in (ii) t takes all values.

In SV there are several possibilities that facilitate automatically the manipulation of the data at AF :

5.2.3. The data enter SV in portions of 12 hours until there are at disposition N' ordinates, N' $\geq$ N. The first N of them are processed and the remaining N' - N await a next application of filters. Thus N can be any number, not necessarily a multiple of 12.

5.2.4. Usually the shift of the filters at their application should be $\Delta N = N$. Thus we deal with intervals without overlappings as well as without omissions of the data. However SV allows $\Delta N < N$. This is of no use for the analysis but it can be of an experimental interest, for example for checking the data.

5.2.5. It is also possible to shift the filters at $\Delta N > N$, i.e. with an omission of $\Delta N - N$ ordinates between each couple of neighbouring intervals. This option may improve the independance of the intervals from each other and thus it may make the estimation of the precision more severe.

5.2.6. When there is an interruption in the record we may have in our disposition only N' ordinates, N' $<$ N. Usually these data are ignored and omitted. However we can give an information to SV that in such cases, when the lacking data do not exceed a given number N", i.e. when N' - N $<$ N", then a shift $\Delta N = N'$ is allowed. This can be usefull when LONG is applied and N' covers nerar 14 days.

5.2.7. The sequence of the data is checked-up and when it is broken an interruption in the record is declared.

5.3. Observational equations OE for the detailed numbers. They are composed relatively to the most detailed grouping (separation) relative to a record of length one year or more, whatever the real length of the record is.

5.4. Normal equations NE. Here the crossproducts of the coefficients calculated in OE are accumulated for each AF. At the end of a record a system of normal equations is obtained. According to 5.3. it is relative to the most detailed grouping, i.e. it contains the greatest possible number of unknowns. When one single record is processed the control of SV after NE passes to SNE. When more than on record are processed jointly there are two cases : (i) the coefficients of the NE are kept at their places in the storage, the control goes back from NE to IN and a next record is accepted and processed, and (ii) the coefficients of the NE are kept in another place of the storage, the control passes to SNE when the results

(tidal parameters) for the record are outputed ; then the control goes to IN when another record is accepted ; its coefficients obtained in NE are manipulated in the same way.

5.5. Solution of the normal equations SNE. It is realized through the inversion of a matrix using the method of the squared root. The tidal parameters with their estimates of the precision are outputed. The following possibilities are available.

5.5.1. Initially the NE, according to 5.3. and 5.4., are obtained relatively to the most detailed grouping. In SNE, if necessary, the elements of the equations are further grouped, corresponding to the lenght of the record as well as to the wishes of the user. In principal the grouping (the separation power) is defined by the length. However, there are cases when the length does not provide a priori a unique solution. For example we may have three variants for a record of 6 months : (i) S1 joints K1, (ii) S1 joints P1 and (iii) S1 is ignored. Still, there may be a room for experiments when there is a minor deviation of a length from a theoretical condition - while these conditions are absolute for a Fourier analysis, they are somewhat softer for the method of the least squares which takes into account the interractions between the tides. In SV there are fixed 14 variants of grouping and upto 5 of them can be applied at once. The results can be compared using the method Analysis of variance (Venedikov, 1979 a).

5.5.2. It is possible to get at once up to 5 variants of weighing of the filtered numbers : (i) separate weights for the even and for the odd filters - the mean square errors 5.2.2. (i) are used, (ii) common weights for the both kinds of filters - 5.2.2. (ii) is used, (iii) no weights, (iv) among the variants 5.2.1. this one who gives the lowest mean square error for a given filtered interval is chosen ; the comparison is made separately for the even and the odd filters, (v) same as (iv) but the choice is made among the couples of filters k_1, k_2.

5.5.3. In the usual option SHORT, SV furnishes in parallel D, SD and TD. It is possible, for example when some very short filters are used, to get merely SD with TD as well as only TD. One can expect that a shortening of the filters may improve the separation of the shorter waves from the drift and, generally, from the noise.

5.5.4. In principal the method for analysis applied by SV can determine separately all long period waves. Now the length of the filters is limited to 720 hours. This is related to a realistic supposition that no longer waves than Mf can practically be derived. There are no problems this limitation to be canceled.

5.5.5. The results can be accompanied by the residual vectors relative to a Molodenski's model. A program of ICET is implied.

6. Special analyses and processings SA.

6.1. Time variations of the Earth tidal parameters

δ (amplitude factor) and α (phase shift). They are interesting in at least four aspects : (i) checking-up the quality of the data, (ii) study of the instrumental response (sensibility), (iii) study of the relations between the Earth tides (or the observed Earth tides) and other phenomena, and, which seems to be a most actual problem, (iv) search of earthquake predictors.

6.1.1. Corrections for a theoretical variation. When the variations are studied through a subdivision of a record into some shorter intervals without overlapping (and we would never recommend overlapping intervals), the analysis of these intervals may have a limited separating power. Fer example in the case of intervals of a few days we can separate only the principal species D, SD and TD. As a consequence we may observe a variation which is simply due to the interraction of tides with different δ as well as α. For that reason there is an option of SV to enter corrections through the parameters derived from the global analysis of the whole record. Its effect is that the expected values, when there are not real variations, they become $\delta = 1$ and $\alpha = 0$.

6.1.2. Short time variations. For each filtered interval the numbers $\xi_T = \delta_T \cos \alpha_T$, $\eta_T = -\delta_T \sin \alpha_T$, δ_T and α_T are determined (Venedikov, 1981). Here T is the central epoch of an interval. In the case of SHORT only the groups D, SD and TD are separated. In the case of LONG there is a single group Mf. In principal the operation is similar to this one used by Ducarme (1979) and Nakai (1977) but the way of its realization is another one. We use the coefficients obtained in OE (Fig. 4.) and the computation is in parallel to this element of SV.

6.1.3. Detection of anomalies using ξ_T and η_T. The mean values $\overline{\xi}$ and $\overline{\eta}$ of ξ_T and η_T with their standard deviations (mean square errors) σ_ξ and σ_η can be determined by SV. The comparison of each ξ_T and η_T with $\overline{\xi} \pm s.\sigma_\xi$ and $\eta \pm \sigma_\eta$, where s is the Student's coefficient for a fiducial probability, may detect an anomaly (or anomalies) in the data near the epoch T. Here as well as in other statistical analyses ξ_T and η_T are to be prefered than δ_T and χ_T because ξ_T and η_T have at least theoretically a normal distribution.

6.1.4. Relation between the short time variation of parallel Earth tide records. Several records covering one and the same time interval are processed consecutively. For each one of them the numbers ξ_T and η_T are determined and stored by SV. After the last record the serie ξ_T and η_T for all records are considered in parallel and they are submitted to a correlation-regression analysis. A practical problem raises from that the records may cover somewhat different time intervals as well as they may have interruptions at different moments. A special feature of SV adjusts the records and it chooses from them only the data that coincide in time.

6.1.5. Study of the influence of non-Earth tidal phenomena (a kind of a multi-channel analysis). When some of the records are, say, ocean tides, meteorological or hydrological series, the scheme 6.1.4. can estimate their influence on, or their relation with, the Earth tidal series. In the application of the regression analysis a given Earth tidal record is to be conceived as a dependent variable, while the other records - as independent variables. The last ones can be completed by a polynomial of T as well as by a series ξ_T and η_T for a theoretical model of a record. For the search of sophisticated relations a non-linear regression analysis, combined with a partial correlation analysis, is available.

6.1.6. Slower time variations can be studied in the following way. The whole record is subdivided in intervals (without overlapping ; the overlapping would provide smoothed variations with unclear stochastic properties). This can be done by SV in two ways : (i) the length of the intervals (one and the same for all intervals) is given by the user, or, which is less comfortable, (ii) the dates that separate the intervals are given. Each interval is analysed as usually with a separation of tidal groups corresponding to the length. The last one must cover at least three filtered intervals.

6.1.7. Study of the slow time variations through the analysis. The unknown tidal parameters in OE (5.3) are considered as polynomials of the time of a low order. The zero power term are associated with the constant part of the parameters. The remaining terms reflect eventual changes. It is possible to implement two different polynominals before and after a given event, for instance an earthquake. In such a case this way of work can be of some use for the earthquake prediction problem.

6.1.8. Another kind of a multi-channel analysis. The time in the scheme 6.1.7. can be replaced by one or a few non-Earth tidal series, to be more precise, by the filtered numbers of such series. Then the terms that are related in 6.1.7. to the changes with the time will now reflect the

influence of the additional series on the eventual variations of the parameters. However in this way of work there are serious problems. For instance the presence of tidal periodicities in the series may make the equations unstable.

6.2. Simultaneous analysis of several Earth tidal records (Venedikov, 1979 b). This option of SV was already concerned in 3.2.5. as well as in 5.4.

6.2.1. In a simplest variant several records can form one single record. Usually this is to be applied when we store in the bank B short parts of a recording of one instrument in one station. In principal there are not such limitations - the records can be obtained from different instruments working at any time, even in different stations. In this case 5.4.(i) is used.

6.2.2. Comparison of different records. In this case 5.4. (ii) is used. In addition to a global result relative to the integrating record we get the results from the analysis of the individual records. All results are compared through the method Analysis of variance. When records from different stations are processed this can have a sense if ocean tidal corrections are implied.

6.2.3. Comparison of different parts of one record. The technics 6.2.2. is applied in combination with 6.1.6. As individual records we conceive the intervals into which a record is subdivided.

6.3. Residuals.

6.3.1. Gross drift (drift & noise). Immediately after an analysis, with the obtained tidal parameters, SV can compute a theoretical curve corresponding to the recored analysed. Then it determines, hour by hour, the differences between the observed and the theoretical ordinates. Such residuals represent the drift plus the errors (noise) of the ordinates with the lowest possible smoothing due to the theoretical curve only. We would dare to say that any other kind of determination of the drift, hour by hour, provides a highly smoothed drift.

6.3.2. Hourly residuals free from the drift. In our way of analysis the drift is eliminated through a filtering of short intervals. Within each interval SV can restore the drift which is eliminated using the filtered numbers. The residuals are then obtained after a subtraction of the drift so obtained, plus a theoretical curve, from the observed record. In our opinion these residuals, as well as all other kinds of hourly

residuals, which pretend to be free from the drift, can offer but a very poor information of the coloured noise which actally influences our results.

6.3.3. Residuals in the filtered numbers. Using the values of the tidal parameters as well as the responses of the filters used, SV can compute theoretical values of the filtered numbers. The last ones, subtracted from the filtered numbers obtained from the record, give this kind of residuals. They are directly related to the real noise which actually influences the results. They are namely used in our way of analysis for the estimation of the precision.

6.4. Plotting facilities. SV uses a plotter Benson through several subroutines offered by the computing centre. They cannot be applied directly in another place but they can be easily replaced by other appropriate subroutines. SV can plot the following curves :

6.4.1. The original record.

6.4.2. A theoretical model, corresponding to a record.

6.4.3. The time variations of the tidal parameters 6.1.2. and 6.1.6.

6.4.4. All kinds of residuals 6.4.

As a conclusion we want to appreciate once again the important help of all institutions as well as of all persons mentioned at the begining of the paper.

REFERENCES

Cartwright, D.E., Tayler, R.J., 1971 : New computations of the tide-generating potential. - Geoph. J.R. Astr. Soc. 23.

Cartwright, D.E. Edden, A.C., 1973 : Corrected tables of tidal harmonics. - Geoph. J.R. Astr. Soc. 33.

Ducarme, B. 1978 : Data standardisation in tidal research. - B.I.M. 78.

Melchior, P., Venedikov, A., 1968 : Derivation of the wave M_3 ($8^h.279$) from the periodic tidal deformation of the earth. - Obs. Roy. Belg. Comm. S.A. 7, S. Geoph. 89, Ph. Earth Pl. Int. Vol. 1.

Melchior, P., 1978 : The tides of the planet Earth. - Pergamon Press. 2nd edition 1983.

Picha, J., Skalski, L., Šimon, Z., 1973 : The problem of the tidal corrections to the high precision observations of the gravity force (in russian). - Geofys. Sbornik vol. XXI, Prague.

Venedikov, A.P. 1966 a : Sur la constitution de filtres numériques pour le traitement des enregistrements des marées terrestres.- Acad. Roy. Belg. Bull. Cl. Sc. 6, LII.

Venedikov, A.P., 1966 b : Une méthode pour l'analyse des marées terrestres à partir d'enregistrements de longueurs arbitraires. Acad. Roy. Belg. Bull. Cl. Sc. 3, LII.

Venedikov, A.P., Pâquet, P., 1967 : Sur l'application d'une méthode pour l'analyse des marées terrestres à partir d'enregistrements de longueur arbitraire. - B.I.M. 48.

Venedikov, A.P., 1977 : Analysis of Earth tidal data. - Proc. 8 Int. Symp. Earth tides, Bonn, 19-24 sept. 1977, Inst. Theor. Geod. Univ. Bonn, published M. Bonatz and P. Melchior.

Venedikov, A.P., 1978 : Analysis of Earth tidal records (in russian). - W.Gr. 3.3. Study Earth Tides, Budapest, Ed. Varga, 1.

Venedikov, A.P., Ducarme, B., 1979 : Determination of long period tidal waves. - B.I.M. 81.

Venedikov, A.P., 1979 a : Testing of the grouping of the waves in the analysis of the Earth tidal data. - B.I.M. 81.

Venedikov, A.P., 1979 b : Simultaneous analysis of different Earth tidal records, B.I.M. 81.

Venedikov, A.P., 1981 : Determination of the tidal parameters from short intervals in the analysis of Earth tidal records.- B.I.M. 85.

Traduction

DETERMINATION DES PARAMETRES DES ONDES DE MAREES PAR LES OBSERVATIONS GRAVIMETRIQUES A YALTA D'APRES DES SERIES MENSUELLES ANALYSEES PAR LA METHODE DE VENEDIKOV

V.P. SCHLIAKHOVII, P.S. KORBA

Rotation et déformations de marées de la Terre N. 14, pp. 31-38, 1982

L'attention s'est accrue ces derniers temps sur l'amélioration en précision de la détermination des paramètres des petites ondes de marées terrestres, en particulier dans la gamme du tiers de jour.

L'amplitude de la plus grande onde M_3 est plus petite de presque deux ordres que l'amplitude de l'onde semi-diurne principale M_2. On a élaboré des méthodes de séparation de cette onde principale d'un tiers de jour {1, 2, 7} mais la précision de détermination de cette onde n'est pas élevée. Même dans les observations de marées gravimétriques qui, comparativement aux enregistrements clinométriques et extensométriques sont sensiblement moins perturbées, elle est environ de 10 à 20 % pour une série annuelle d'observations. En étudiant la composition spectrale des variations de la pesanteur à Yalta, parmi les autres ondes de la gamme ter-diurne, on a réussi à séparer nettement l'onde principale M_3 {3}. D'après ces données $\delta_{M_3} = 1{,}165 \pm 0{,}105$. D'autre part l'analyse harmonique de ces mêmes observations par la méthode de Venedikov a donné $\delta_{M_3} = 1{,}105 \pm 0{,}301$ {4}. Ce désaccord a conduit à réduire les données par une autre méthode. Nous avons utilisé la méthode de Venedikov, appliquée à des séries mensuelles indépendantes {7} portant sur 15 mois d'observations {3}. On y a ajouté cinq autres séries mensuelles qu'on n'avait pas utilisées lors de l'analyse spectrale par suite d'interruptions dans l'enregistrement. Tous les calculs ont été faits sur IBM EC-1020 avec un programme de P.S. Doubik.

La table 1 donne les valeurs des paramètres de marées terrestres δ et $\Delta\phi$ pour l'onde principale M_3 (43,476 degrés/heure) et pour deux autres ondes plus faibles de vitesses angulaires de 42,933 et 44,574 degrés/heure. Les valeurs δ et $\Delta\phi$ sont relativement stables d'une série à l'autre mais les autres ondes donnent des résultats moins sûrs.

TABLE 1 Valeurs δ et $\Delta\phi$ pour les ondes ter-diurnes

N° des séries	Début de la série	M_{3101} 42°933/h		M_3 43°476/h		M_{3200} 44°574/h	
		δ	$\Delta\varphi$	δ	$\Delta\varphi$	δ	$\Delta\varphi$
I	30.VI 1966 r.	2,157 ±1,836	−100,1° ± 49,3	0,608 ±0,473	+23,5° ± 44,7	6,757 ±2,557	− 0,7° ± 21,6
2	30.VII	1,120 ±1,540	−138,7 ± 78,8	2,562 ±0,457	+12,5 ± 10,2	3,243 ±2,438	−98,7 ± 43,3
3	29.VIII	1,858 ±2,264	−165,0 ± 70,4	0,798 ±0,702	−10,2 ± 50,5	6,106 ±3,719	−40,2 ± 34,9
4	17.XI	2,360 ±3,094	−0,4 ± 75,5	1,583 ±0,661	−31,8 ± 23,9	8,959 ±3,404	−87,5 ± 21,8
5	17.XII	3,420 ±3,358	+156,6 ± 56,3	0,962 ±0,680	+29,5 ± 40,5	1,192 ±3,475	+34,5 ±166,8
6	3.III 1967 r.	2,643 ±2,590	+31,0 ± 56,0	2,025 ±0,788	−3,0 ± 22,4	4,360 ±4,033	+40,3 ± 53,0
7	2.IV	5,337 ±1,652	−36,1 ± 17,7	0,868 ±0,504	−48,3 ± 33,2	2,124 ±2,553	−64,8 ± 69,0
8	2.V	2,660 ±1,692	−162,7 ± 36,6	0,965 ±0,462	−11,4 ± 27,4	2,832 ±2,340	−80,5 ± 47,1
9	1.VI	1,191 ±1,304	+78,9 ± 62,4	1,473 ±0,294	−29,4 ± 11,4	1,860 ±1,474	−76,0 ± 45,3
10	1.VII	4,311 ±3,212	+7,7 ± 43,9	1,045 ±0,582	+75,5 ± 31,8	4,838 ±2,824	−22,3 ± 33,2
11	31.VII	0,968 ±2,278	−144,3 ±134,7	1,647 ±0,528	−18,3 ± 18,3	1,130 ±2,593	+11,4 ±132,0
12	30.VIII	1,647 ±2,956	−4,8 ±104,0	0,740 ±0,828	+29,1 ± 63,9	3,072 ±4,075	+178,6 ± 76,2
13	29.IX	1,844 ±2,673	+147,1 ± 83,1	2,234 ±0,824	−6,5 ± 21,1	2,581 ±4,042	+37,7 ± 89,6
14	29.X	4,350 ±3,428	+0,3 ± 44,7	1,841 ±1,034	+8,1 ± 32,1	6,294 ±5,056	−23,9 ± 46,0
15	28.XI	8,624 ±4,921	+141,9 ± 32,7	3,803 ±1,313	+40,8 ± 19,8	1,912 ±6,408	−141,6 ±192,3
16	28.XII	4,900 ±3,194	−124,0 ± 37,2	0,862 ±0,701	−22,4 ± 46,6	8,568 ±3,412	−5,9 ± 22,8
17	27. I 1968 r.	1,208 ±4,177	−12,1 ±196,4	2,860 ±0,826	−5,4 ± 16,6	1,130 ±3,978	−166,4 ±200,9
18	26. II	6,285 ±2,756	−36,3 ± 25,0	0,776 ±0,652	−10,0 ± 48,3	1,629 ±3,141	−124,2 ±110,3
19	27.III	4,509 ±3,275	−54,4 ± 41,5	1,490 ±0,926	−7,4 ± 35,7	7,806 ±4,448	+37,3 ± 32,6
20	26.IV	1,544 ±2,077	+91,2 ± 76,7	0,742 ±0,641	−5,5 ± 49,4	4,623 ±3,060	−120,5 ± 38,0

La table 2 donne les valeurs δ_{M_3} et $\Delta\phi$ obtenues par différentes méthodes. Les valeurs moyennes de δ et $\Delta\phi$ déterminées par la méthode de Venedikov sont calculées pour différentes variantes : la première par simple moyenne vectorielle pour toutes les séries; la seconde par moyenne vectorielle simple, mais sans tenir compte des quatre valeurs anormales, la troisième par moyenne vectorielle pondérée inversément proportionnelle au carré de l'erreur quadratique moyenne. Dans cette même table nous donnons les paramètres δ_{M_3} et $\Delta\phi$ obtenus dans les travaux précédents {3} et {4}. On constate que la plus petite erreur est obtenue par l'analyse spectrale, et la plus grande par l'analyse harmonique globale des données. Or le résultat obtenu par analyse globale est le plus proche de la valeur théorique δ_{M_3} = 1,069, bien que l'erreur de sa détermination soit la plus grande (environ 30 %). Cependant on ne peut pas

faire confiance totale à ce résultat car dès la préparation des ordonnées on a découvert par un filtre d'erreurs quelques petites erreurs de calcul.

TABLE 2 Valeurs moyennes des paramètres de l'onde M_3 obtenues par différentes méthodes.

Paramètre	Méthode Venedikov en séries mensuelles			Méthode Venedikov globale	Analyse spectrale
	Poids égaux (toutes les séries	Poids égaux (16 séries)	Poids $p = 1/m^2$ (toutes les séries)		
δ	I,344	I,I37	I,223	I,I05	I,I65
	±0,I87	±0,I40	±0,I55	±0,30I	±0,I05
$\Delta\varphi$	-7,0°	-6,I°	-5,9°	+2,3°	-
	±II,0	±6,7	±6,I	±II,0	-

Les valeurs moyennées des séries mensuelles, correspondent avec la théorie dans les limites de l'erreur quadratique moyenne. Ainsi l'onde M_3, malgré sa petite amplitude, peut s'extraire par n'importe quel procédé mais la précision de sa détermination provenant d'une courte série d'observations n'est pas élevée.

Toutes les séries mensuelles ont également été soumises à l'analyse harmonique pour déterminer les paramètres des ondes diurnes et semidiurnes en utilisant la méthode Venedikov sur séries mensuelles {7}. Ceci permet d'obtenir les erreurs pour chaque série mensuelle, ce qui permet en fin de compte de faire une moyenne pondérée vectorielle.

Les résultats obtenus sont donnés dans les tables qui donnent la possibilité de suivre la dynamique de comportement des valeurs δ et $\Delta\phi$ et aussi de leurs erreurs dans le temps, pour chaque onde séparément (ondes diurnes dans la table 3 et ondes semidiurnes dans la table 4). Les valeurs moyennes sont données dans la table 5 : moyennes vectorielles simples et vectorielles pondérées.

A l'inverse des données des tables 3 et 4 ces résultats sont corrigés du retard instrumental. La table 5 permet de comparer les valeurs de δ et $\Delta\phi$ obtenues précédemment par la méthode Venedikov appliquée aux données globales.

TABLE 3 Résultats de l'analyse harmonique : ondes diurnes

N° de la série	Q_1		q_1		M_1		K_1		J_1		OO_1	
	δ	$\Delta\varphi$	δ	$\Delta\varphi$	δ	$\Delta\varphi$	δ	$\Delta\varphi$	δ	$\Delta\varphi$	δ	$\Delta\varphi$
I	I,II46 ±I074	− 5,39° ± 5,5I	I,I438 ± 207	−0,73° ±I,04	I,3456 ±2385	− I,59° ±I0,I3	I,I596 ± I24	−3,78° ±0,62	I,0957 ±2554	−I6,83° ±I3,37	I,7760 ±4082	+3I,68° ±I3,I7
2	I,235I ± 866	− 6,85 ± 4,02	I,I950 ± I94	+I,I5 ±0,93	I,4037 ±I748	−II,54 ± 7,I2	I,I424 ± I38	−I,73 ±0,69	I,2536 ±2067	+30,89 ± 9,45	I,4898 ±3I29	+ 5,53 ±I2,03
3	I,0938 ±I028	− 7,72 ± 5,38	I,I555 ± 239	+0,I0 ±I,I8	0,9702 ±I90I	− 5,3I ±II,2I	I,I088 ± 227	+I,I4 ±I,I5	I,2902 ±2458	−4,92 ±I0,89	0,9496 ±33I0	− I,I4 ±I9,99
4	I,I577 ±I487	+ 0,40 ± 7,33	I,I277 ± 23I	−0,82 ±I,I7	I,8980 ±2488	−20,73 ± 7,52	I,0697 ± I36	+2,88 ±0,75	0,8373 ±346I	+ 2,03 ±23,66	0,5836 ±392I	−I9,80 ±38,5I
5	I,3663 ±I890	−I6,35 ± 7,94	I,I327 ± 286	+0,I0 ±I,45	I,I328 ±3253	−49,89 ±I6,45	I,0986 ± I62	+I,26 -0,85	I,6506 ±4379	−I0,29 ±I5,22	I,5630 ±5344	−I2,73 ±I9,60
6	I,2373 ± 89I	− 3,95 ± 4,I3	I,I30I ± 204	−0,88 ±I,04	I,4524 ±I558	+ 0,59 ± 6,I5	I,I5I2 ± 202	+I,26 ±0,99	I,48I6 ±2I6I	+I2,95 ± 8,38	I,2763 ±2635	−2I,I9 ±II,8I
7	I,I507 ± 580	− 7,7I ± 2,88	I,I679 ± I30	−0,43 ±0,64	I,2I5I ± 999	− 3,0I ± 4,7I	I,I479 ± II2	−0,II ±0,56	I,I648 ±I405	+ I,20 ± 6,9I	I,0965 ±I705	− 3,I6 ± 8,92
8	I,I988 ± 767	− I,I2 ± 3,68	I,I423 ± I52	−0,32 ±0,76	I,3090 ±I330	− 3,84 ± 5,8I	I,I650 ± I00	+0,30 ±0,50	I,3408 ±I858	− 7,90 ± 7,93	I,44I5 ±2267	−2I,24 ± 9,0I
9	I,0950 ± 949	+ 8,69 ± 4,96	I,I530 ± I54	−I,29 ±0,76	I,3306 ±I6I5	− 3,I4 ± 6,95	I,I460 ± 92	−I,00 ±0,46	I,2658 ±2270	−II,I4 ±I0,29	0,9289 ±2696	− 2,29 ±I6,64
I0	0,9538 ±I347	− 5,53 ± 8,09	I,I382 ± I97	−0,I8 ±0,99	I,0672 ±2207	−I4,22 ±II,84	I,I677 ± I22	−4,2I ±0,60	I,2967 ±3I73	+ I,34 ±I4,00	0,5I03 ±3468	+26,90 ±38,93
II	I,3296 ±II33	+ 0,64 ± 4,90	I,I5I5 ± I89	−I,57 ±0,94	I,I44I ±I866	− I,50 ± 9,33	I,II23 ± I40	−I,9I ±0,72	I,4786 ±267I	−I2,79 ±I0,35	I,0972 ±2834	+ 7,96 ±I4,8I
I2	I,3939 ±I298	+ 0,73 ± 5,3I	I,I244 ± 262	+I,57 ±I,34	I,4649 ±220I	−I6,39 ± 8,60	0,986I ± 254	−7,75 ±I,45	I,3530 ±3097	+I4,08 ±I3,I4	I,54I9 ±343I	− I,49 ±I2,75
I3	I,I642 ±I327	− 6,94 ± 6,55	I,0664 ± 300	+0,82 ±I,6I	0,8225 ±2384	−26,50 ±I6,59	0,9620 ± 27I	I0,75 ±I,63	+ I,I2I9 ±3259	−I2,93 ±I6,6I	I,2I03 ±3879	− 3,48 ±I8,37
I4	I,025I ±I975	+ I,06 +II,04	I,0684 ± 440	−0,74 ±2,35	I,5634 ±38I2	+3I,07 ±I3,95	I,0095 ± 295	+I,30 ±I,7I	I,2I26 ±4938	−I7,06 ±23,32	0,78I3 ±6438	− 8,27 ±47,2I
I5	I,0670 +I897	−I0,40 +I0,I6	I,II7I ± 370	−0,I8 ±I,90	0,9798 ±3868	−49,25 ±22,63	I,0247 ± 2II	+5,34 ±I,2I	0,943I ±4783	+25,80 ±29,I0	0,9220 ±6495	+22,I2 ±40,35
I6	0,9994 ±I827	+ 7,I9 ±I0,5I	I,2046 ± 297	+I,78 ±I,42	I,2I62 ±3659	+36,96 ±I7,22	I,0808 ± I76	+I,06 ±0,94	0,9537 ±4609	+I8,83 ±27,67	I,II62 ±5333	+4I,37 ±27,38
I7	I,II52 ±I629	+ 4,52 ± 8,35	I,I576 ± 248	+0,79 ±I,23	I,29I6 ±305I	− 8,02 ±I3,49	I,I005 ± I83	+2,24 ±0,94	I,2II3 ±4058	+22,3I ±I9,20	I,654I ±3808	− 0,85 ±I3,I7
I8	I,2264 ±II26	− 4,34 ± 5,27	I,I20I ± 200	−I,66 ±I,02	I,II0I ±2I05	− 8,54 ±I0,84	I,I865 ± I97	+0,33 ±0,93	I,2950 ±2800	−I2,44 ±I2,40	0,9774 ±2698	+ 7,83 ±I5,83
I9	I,2I28 ± 959	+ 4,I4 ± 4,52	2,I639 ± I99	−I,80 ±0,98	0,9828 ±I877	+ 4,70 ±I0,92	I,I669 ± I79	+0,42 ±0,89	I,0555 ±2388	+ 2,I8 ±I2,93	I,4495 ±2726	+II,27 ±I0,77
20	I,4864 ±I565	− 3,I2 ± 6,04	I,I468 ± 349	−0,54 ±I,75	0,6071 ±3362	+ 8,I2 ±3I,68	I,I453 ± 240	+0,93 ±I,22	I,333I ±3904	−I5,52 ±I6,79	I,4658 ±5460	−I6,55 ±2I,36

TABLE 4 Résultats de l'analyse harmonique : ondes semidiurnes

N° de la série	$2N_2$		N_2		M_2		L_2		S_2	
	δ	$\Delta\varphi$	δ	$\Delta\varphi$	δ	$\Delta\varphi$	δ	$\Delta\varphi$	δ	$\Delta\varphi$
I	0,8090	- 3,67°	I,2015	- 2,67°	I,1545	- 0,59°	0,7040	-54,13°	I,1918	+ 1,38°
	±1980	±14,00	± 415	± 1,99	± 81	± 0,40	±4751	±38,71	± 236	± 1,14
2	I,0011	+ 4,76	I,1277	+ 1,06	I,1886	- 0,56	I,8551	- 6,36	I,2660	- 5,39
	±1569	± 9,02	± 378	± 1,93	± 83	± 0,40	±3531	±10,89	± 169	± 0,77
3	0,9615	- 1,49	I,1706	- 5,02	I,1721	- 1,87	0,9658	+ 5,70	I,2855	- 5,11
	±2084	±12,42	± 506	± 2,47	± 114	± 0,56	±4071	±24,14	± 186	± 0,82
4	2,0282	-19,56	I,1658	- 2,22	I,1618	- 1,62	2,8271	+ 0,17	I,1848	+12,47
	±9999	±29,85	± 879	± 4,34	± 132	± 0,65	±6164	±12,47	± 310	± 1,48
5	I,5376	+ 3,26	I,2242	+ 0,13	I,1594	- 1,90	I,8662	-80,63	I,1168	+ 8,01
	±8164	±30,15	± 826	± 3,88	± 126	± 0,62	±7306	±22,38	± 351	± 1,80
6	I,1703	+ 7,35	I,1716	- 6,65	I,1891	- 0,89	I,1172	-72,54	I,1626	+ 2,38
	±2156	±10,49	± 531	± 2,60	± 117	± 0,56	±3656	±18,71	± 178	± 0,88
7	0,6648	-12,52	I,1548	- 4,37	I,1661	- 1,41	I,2816	-22,35	I,1635	- 0,83
	±2157	±18,65	± 517	± 2,56	± 112	± 0,55	±3008	±13,46	± 182	± 0,89
8	I,0113	- 4,91	I,1817	- 1,00	I,1830	- 1,81	0,9578	- 4,89	I,1645	- 3,04
	±1292	± 7,35	± 266	± 1,28	± 50	± 0,24	±1346	± 8,05	± 108	± 0,52
9	0,8028	+ 1,42	I,2255	- 1,25	I,1686	- 1,27	I,0859	-11,13	I,2076	+ 0,05
	±3136	±22,25	± 391	± 1,83	± 61	± 0,30	±1831	± 9,65	± 190	± 0,89
10	2,0455	-49,64	I,3185	-11,59	I,1858	- 1,09	2,0408	- 7,87	I,2518	+ 7,55
	±9456	±26,57	± 656	± 2,85	± 89	± 0,43	±3104	± 8,67	± 252	± 1,16
11	0,8871	-57,57°	I,1807	+ 3,85°	I,1827	- 1,35°	I,4204	+26,69°	I,2419	- 0,72°
	±3028	±19,57	± 526	± 2,55	± 87	± 0,42	±2968	±11,94	± 167	± 0,78
12	0,7898	- 6,98	I,2388	+ 0,86	I,1822	- 1,04	0,7632	+37,57	I,1560	+ 5,58
	±3259	±23,78	± 751	± 3,46	± 146	± 0,71	±4044	±30,36	± 231	± 1,14
13	I,1386	+14,10	I,1793	- 6,40	I,1283	- 0,41	0,6471	-15,68	I,1669	+ 8,94
	±1290	± 6,47	± 318	± 1,54	± 68	± 0,34	±1524	±13,51	± 105	± 0,51
14	I,4386	- 8,46	I,0354	- 6,59	I,1817	- 0,55	0,7577	-61,54	I,1283	+11,59
	±3783	±14,98	± 911	± 5,06	± 189	± 0,92	±3865	±29,19	± 360	± 1,80
15	0,5211	+ 3,08	I,2318	- 6,90	I,1326	- 0,24	I,5223	+ 1,46	I,1339	+30,31
	±4749	±52,63	± 995	± 4,64	± 179	± 0,91	± 3759	±14,18	± 484	± 2,43
16	2,6088	+ 8,99	0,9979	+ 9,39	I,1492	+ 0,83	I,1973	+46,06	I,1026	+ 9,91
	±8161	±18,03	±1082	± 6,18	± 158	± 0,79	±3682	±17,62	± 400	± 2,08
17	0,9288	-27,76	I,1567	- 0,95	I,1466	- 2,06	0,9204	-23,57	I,0753	+ 7,44
	±9816	±60,24	±1026	± 5,06	± 138	± 0,69	±3533	±21,95	± 245	± 1,32
18	I,4400	-15,11	I,2394	+ 6,54	I,1387	- 0,72	0,6364	- 3,56	I,1637	+ 3,37
	±4068	±16,24	± 791	± 3,67	± 129	± 0,64	±3085	±27,65	± 193	± 0,95
19	I,3819	+ 0,36	I,1502	- 0,87	I,1544	- 1,97	0,5684	-41,07	I,1618	- 1,92
	±3011	±12,52	± 712	± 3,55	± 138	± 0,68	±2775	±27,96	± 217	± 1,06
20	I,3881	+16,22	I,1658	- 1,61	I,1645	- 1,36	I,1739	-15,49	I,2079	- 2,15
	±2024	± 8,34	± 497	± 2,44	± 104	± 0,51	±1830	± 8,93	± 212	± 0,99

TABLE 5 Valeurs moyennes des paramètres δ et $\Delta\phi$ des ondes diurnes et semidiurnes obtenues par la méthode de Venedikov.

Onde	Vitesse angulaire de l'onde (degré/h)	Amplitude théorique de l'onde µgal	Pour les séries mensuelles					
			Poids égaux		Poids p = $1/m^2$			
			δ	$\Delta\varphi$	δ	$\Delta\varphi$	δ	$\Delta\varphi$
Q_1	I3,3980	5,95	I,I745 ± 302	− I,42° ± I,4I	I,I794 ± 239	−I,I2° ±I,27	I,I790 ± 400	±I,00° ±I,40
O_1	I3,9425	3I,06	I,I402 ± 75	+ 0,62 ± 0,23	I,I485 ± 63	+0,48 ±0,23	I,I430 ± 78	+0,48 ±0,26
M_1	I4.4960	2,44	I,I434 ± 685	− 5,66 ± 4,55	I,2I82 ± 592	−6,I4 ±3,4I	I,2030 ± 720	−6,40 ±2,50
K_1	I5,0405	43,69	I,I053 ± I49	+ 0,85 ± 0,60	I,I270 ± I26	+0,56 ±0,60	I,I050 ± 57	+0,74 ±0,20
J_1	I5,5850	2,44	I,I9I4 ± 453	+ 0,70 ± 3,4I	I,2II5 ± 390	+0,I9 ±3,08	I,I350 ± 970	+0,80 ±3,70
OO_1	I6,I385	I,34	I,I395 ± 773	+ 2,66 ± 4,I2	I,I724 ± 637	+0,47 ±3,85	I,I220 ±II70	+0,50 ±4,20
$2N_2$	27,89I0	I,I7	I,I575 ±II08	− 5,63 ± 5,00	I,0I99 ± 570	+3,05 ±3,I8	0,9646 ±I280	+2,70 ±5,40
N_2	28,4400	7,34	I,I7I9 ± I54	− 0,I5 ± I,I0	I,I786 ± I00	−0,53 ±0,86	I,I726 ± 267	−0,I2 ±0,9I
M_2	28,9845	38,35	I,I645 ± 42	+ 0,6I ± 0,I3	I,I674 ± 43	+0,57 ±0,I2	I,I674 ± 53	+0,46 ±0,I8
L_2	29,5290	I,08	I,0327 ±I445	−I0,98 ± 7,27	I,9735 ± 973	−8,09 ±4,85	I,0030 ±I390	−4,50 ±5,80
S_2	30,0000	I7,84	I,I654 ± I6I	+ 6,II ± I,76	I,I793 ± II8	+3,73 ±I,32	I,I8I0 ± I05	+4,I4 ±0,36

La moyenne simple donne des valeurs plus régulières pour δ et la moyenne pondérée pour $\Delta\phi$. Cependant les erreurs sur les moyennes pondérées sont plus petites en δ et $\Delta\phi$ pour toutes les ondes.

On sait que les valeurs δ pour toutes les ondes de marées sont à peu près les mêmes à l'exception des ondes diurnes perturbées par l'effet de résonance du noyau liquide de la Terre. C'est pourquoi nous avons des raisons de considérer comme plus sûrs les résultats donnés par la moyenne simple qui donnent des valeurs plus proches des facteurs d'amplitude bien que leurs erreurs soient un peu plus grandes.

Les erreurs sont en bonne concordance sauf pour l'onde K_1. Cela s'explique par le fait que lors de la réduction globale cette onde a été purifiée de l'onde perturbatrice S_1. Toutes les données de Yalta ont été réduites par la méthode de Matveyev {6} dont les résultats correspondent dans les limites de la précision avec celles qui sont présentées ici.

On émet parfois l'hypothèse du caractère accidentel des perturbations dans les ondes de marées principales. Pour vérifier la véracité de ce point de vue on a calculé pour chacune des 20 séries analysées les valeurs moyennes des paramètres de marées terrestres δ pour le groupe Q_1, O_1, K_1, N_2, M_2, S_2, pour le groupe Q_1, O_1, N_2, M_2 et pour le groupe K_1, S_2 affectés de poids proportionnels aux amplitudes théoriques. Les variations temporelles de ces paramètres sont données sur la figure où on donne en outre les courbes de variations de δ pour les ondes O_1, K_1, S_2 et M_2.

On peut noter une certaine périodicité dans toutes les courbes. Elle apparaît le plus clairement dans $\delta_{(K_1)}$, $\delta_{(S_2)}$ et $\delta_{(K_1S_2)}$. Cette périodicité a un caractère annuel et peut être expliquée par la présence d'une onde perturbatrice d'origine solaire dans les observations de Yalta.

Les variations de l'échelle de l'enregistrement amèneraient sans aucun doute au même synchronisme dans les variations du paramètre δ. Cependant l'effet de ces variations resterait constant pour toutes les ondes, ce qui ne s'observe pas dans la réalité : pour l'onde lunaire M_2 cette périodicité est pratiquement peu sensible. L'hypothèse d'un caractère accidentel des perturbations de marées n'est pas correcte.

D'après les données obtenues on peut calculer la différence $(\delta_{O_1} - \delta_{K_1})$ caractérisant l'effet de résonance du noyau liquide de la Terre. Pour une moyenne vectorielle simple la différence $\delta_{O_1} - \delta_{K_1} = 0{,}035 \pm 0{,}016$ et pour la moyenne pondérée $\delta_{O_1} - \delta_{K_1} = 0{,}021 \pm 0{,}014$. Les erreurs moyennes sur cette différence atteignent 50 %, ce qui ne nous permet pas d'interpréter ces données à mieux qu'une décimale.

CONCLUSIONS

(1) L'onde M_3 s'extrait nettement dans les observations de Yalta. La précision de la détermination de cette onde par les méthodes d'analyse harmonique dépasse la précision de la détermination par analyse spectrale.

(2) Les valeurs moyennes des paramètres δ et $\Delta\phi$ des ondes principales, obtenues par la réduction de séries mensuelles et globalement coïncident.

(3) La synchronisation des variations des paramètres témoigne de l'influence non accidentelle des perturbations sur les différentes composantes de la marée terrestre.

(4) La présence des petites erreurs sur les ordonnées mesurées agit faiblement sur les constantes harmoniques δ et $\Delta\phi$ pour les ondes principales diurnes et semidiurnes.

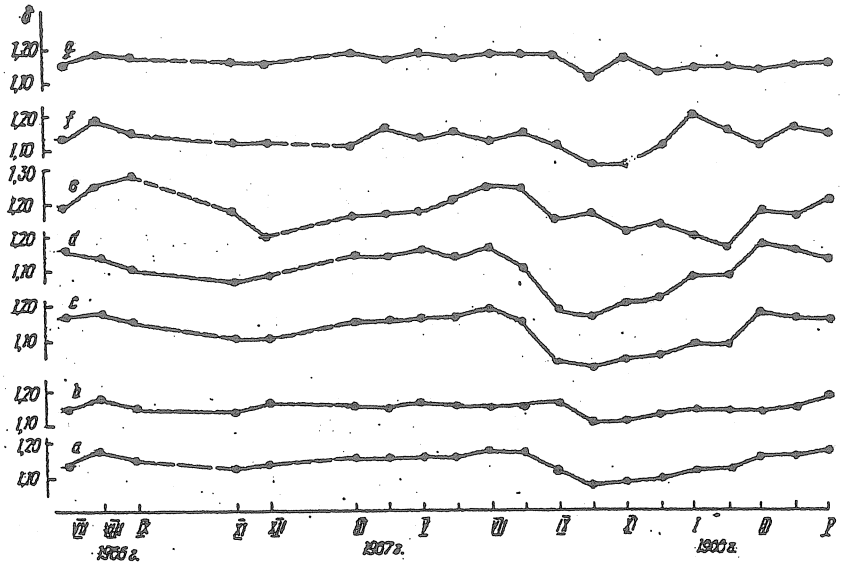

BIBLIOGRAPHIE

BARSENKOV, S.N., Calcul des marées du troisième ordre par les observations gravimétriques. Izv. Ac. des Sc. URSS. Physique de la Terre 1967, N° 5, pp. 28 à 32.

DOUBIK, B.S., Quelques problèmes d'analyse des observations de marées terrestres. Rotation et déformations de marées de la Terre 1980, publ. 12, pp. 33 à 47.

SCHLIAKHOVI, V.P., KORBA, P.S., Sur la composition spectrale de la force de pesanteur d'après les observations à Yalta. Rotation et déformations de marées de la Terre 1981, publ. 13, pp. 45 à 48.

KORBA, P.S., KORBA, S.N., L'onde ter diurne M_3 dans les variations de marées de la pesanteur en Crimée de 1964 à 1971. Rotation et déformations de marées de la Terre 1974, publ. 6, pp. 58 à 61.

KORBA, S.N., KORBA, P.S., Résultats de la réduction des observations de variations de marées de la pesanteur à Simféropol et Yalta par la méthode de Venedikov. Rotation et déformations de marées de la Terre, 1972, publ. 4, pp. 54 à 65.

KORBA, P.S., KORBA, S.N., Variations de marées de la pesanteur à Yalta en 1966-1968. Rotation et déformations de marées de la Terre, 1970, publ. 2, pp. 18 à 34.

VENEDIKOV, A.P., Une méthode pour l'analyse des marées terrestres à partir d'enregistrements de longueur arbitraire. Com. Obs. Roy. Belg. Ser. Geoph. , 71, 1966, N. 250, pp. 463-485.

SUR LES ERREURS DES PARAMETRES DETERMINES A PARTIR DES OBSERVATIONS DE MAREES TERRESTRES

B.S. Doubik, A.N. Novikova

Rotation et déformations de marées de la Terre - 14, pp. 39-40 - 1982.

Pour cette recherche nous avons choisi 270 jours d'enregistrements clinométriques dans la direction EW à la station Berezovaïa Roudka {1} que nous avons répartis en 9 séries mensuelles indépendantes et que nous avons réduites par les méthodes de Matveyev {2} et de Venedikov {3} avec moyenne successive des résultats mois par mois. Ensuite nous avons réduit par la méthode de Venedikov appliquée à l'ensemble, avec partage des ondes en groupes, pris pour la durée d'un mois. Nous donnons dans la table les résultats de la réduction. La variante M correspond à la méthode de Matveyev avec moyenne successive, la variante V correspond à la méthode de Venedikov en séries mensuelles avec moyenne successive et la variante $V_{O.M.}$ à la réduction par la méthode de Venedikov appliquée directement à tout l'ensemble de 270 jours.

Nous constatons que pour les ondes K_1 et S_2, les erreurs quadratiques moyennes obtenues par la méthode de Venedikov appliquée à tout l'ensemble donne des erreurs plus petites que la réduction par séries mensuelles indépendantes avec moyenne des résultats. Pour les autres ondes Q_1, O_1, M_1, N_2 et M_2 on a obtenu par contre de plus grandes erreurs dans la variante $V_{O.M.}$

Les observations utilisées sont sensiblement affectées par des influences d'origine thermique. Cependant des rapports analogues des erreurs des variantes de calcul proposées s'observent aussi lors de la réduction des observations gravimétriques qui sont à un moindre degré affectées par ces perturbations.

Nous avons utilisé la méthode de Matveyev uniquement dans un but de contrôle.

Le travail proposé n'a qu'un caractère d'illustration et nous nous abstenons à présent de toutes conclusions formelles. On peut seulement noter que lors de la construction de nouveaux schémas d'analyse il est souhaitable d'obtenir pour chaque composante un système d'équations surabondant, indépen-

dant des autres composantes. Cela sera justifié dans la mesure où se justifie la séparation des parties diurne et semi-diurne de la marée. Ensuite, plus la composante en vitesse angulaire s'éloigne de S_1 dans la partie diurne de la marée et de S_2 dans la partie semi-diurne de la marée, plus précisément doivent se déterminer ses paramètres puisque les perturbations principales des observations de marées terrestres sont d'origine thermique. Cependant quand les observations ne sont perturbées que par des erreurs accidentelles indépendantes on peut envisager aussi un seul système général d'équations pour toutes les composantes. Dans ce cas les composantes se détermineront avec la même précision et les erreurs sur l'amplitude et le déphasage dépendront finalement de la valeur de l'amplitude théorique correspondante.

En conclusion nous noterons qu'il faut toujours se rapporter critiquement aux résultats obtenus par la méthode de Venedikov et aux erreurs caractérisant leur précision et tirer des conclusions avec beaucoup de prudence.

Lors de la réduction des données par la méthode de Venedikov comme lors de la réduction par une autre méthode quelconque on peut obtenir des résultats perturbés à la suite des erreurs admises dans les ordonnées de départ. Dans une série de cas, pour mettre à jour les erreurs toujours possibles on utilise des combinaisons courtes ou la méthode des moindres carrés.

Pour déceler les erreurs admises lors de l'utilisation de la méthode de Venedikov et également d'autres méthodes, on peut utiliser les nombres M_i ou N_i ($i = 1, 2, \ldots$) obtenus pour chacun des intervalles lors de l'application de filtres pairs ou impairs de Venedikov. Ces nombres représentent la marée transformée avec une différence telle que la partie à longue période et la dérive sont quasi éliminées tandis que les autres ondes entrent avec des amplitudes variables et avec des vitesses angulaires multipliées par 48. Si on construit un graphique des M_i ($i = 1, 2, \ldots$) pour une partie d'enregistrement sans interruptions, on doit obtenir une courbe régulière. S'il y a des erreurs alors l'harmonie du graphique sera perturbée et dans ce cas il faut chercher quelles sont les ordonnées de l'intervalle correspondant qui sont erronnées, les corriger et répéter le calcul.

Il est préférable de construire deux graphiques : l'un pour les nombres M_i et l'autre pour les nombres N_i puisque les coefficients des filtres sont différents et le mieux est d'utiliser les nombres M_i et N_i obtenus par l'analyse de la marée semi-diurne.

Résultats de l'analyse harmonique

Variante	Ondes diurnes								Ondes semi-diurnes					
	Q_1		Q_1		M_1		K_1		N_2		M_2		S_2	
	γ	$\Delta\varphi$	γ	$\Delta\varphi$	γ	$\Delta\varphi$	γ	$\Delta\varphi$	γ	$\Delta\varphi$	γ	$\Delta\varphi$	γ	$\Delta\varphi$
M	0,853 ±680	57,36° ±40,68	0,652 ±173	4,06° ±10,98	4,764 ±2,677	124,74° ±33,32	2,901 ±1,001	−6,82° ±18,57	0,920 ±96	−6,17° ±9,56	0,697 ±23	−5,85° ±1,16	1,374 ±141	32,27° ±7,15
B	0,777 ±682	45,35 ±49,39	0,756 ±148	1,89 ± 6,71	5,387 ±2,584	110,78 ±28,71	2,900 ±963	−7,00 ±17,92	0,946 ±110	−6,28 ±9,94	0,694 ±26	−6,52 ±1,14	1,416 ±146	32,71 ±7,34
B_{aM}	0,653 ±1,938	53,52 ±170,20	0,971 ±368	3,86 ±21,72	2,276 ±3,418	138,54 ±86,08	2,725 ±228	6,26 ± 4,74	0,906 ±148	−4,46 ±9,36	0,694 ±28	−6,80 ±2,29	1,398 ±60	30,40 ±2,48

BIBLIOGRAPHIE

BALENKO, V.G., NOVIKOVA, A.N., DOUBIK, B.S., KAUTNII, A.M., Onde diurne non due aux marées dans les observations clinométriques à la station de Berezovaïa Roudka. Rotation et déformations de marées de la Terre, 1979. Publ. II, pp. 29-43.

MATVEYEV, P.S., Analyse harmonique d'une série mensuelle de marées terrestres. Dans le livre : Marées terrestres. Kiev : Naouk. Doumka, 1966, pp. 51 à 79.

VENEDIKOV, A.P., Une méthode pour l'analyse des marées terrestres à partir d'enregistrement de longueur arbitraire. Com. Obs. Roy. Belg. Ser. Geoph. , 1966, 71, N. 250, pp. 463-485.

RESULTATS DES OBSERVATIONS CLINOMETRIQUES DANS LA MINE N° 1 A KARLO-LIBKNECHTOVSKA

A.M. Koutnii, V.G. Balenko, V.Y. Tokar

Rotation et Déformations de la Terre 14, pp. 19-23, 1982

Dans le cadre d'un programme de recherches dans la zone Karlo-Libknechtovska on a réalisé des observations clinométriques dans quatre mines situées au nord-est et au sud-ouest de la zone. Le schéma de situation des stations clinométriques est donné à la Figure 1. Le but est d'obtenir des indications continues sur l'évolution de l'inclinaison de la surface terrestre pour contrôler la zone d'effondrement et en étudier les signes précurseurs en vue d'une prévision de ce genre de désastres spontanés. De 1976 à 1979 des observations ont été faites dans les puits N° 2 et N° 4. Les données obtenues sont publiées en {1}. Dans cet article-ci nous proposons les résultats et une courte analyse des recherches clinométriques dans la mine N° 1 située au nord-est, au bord de la zone, à 40 m du nord de la mine N° 2.

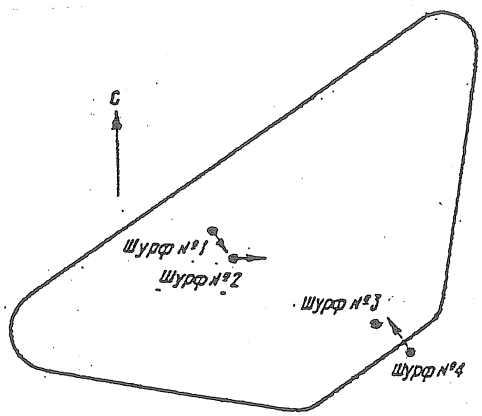

Fig. 1. Schéma de situation des stations clinométriques dans la zone d'effondrement.

Le puits N° 1, équipé en 1975, a une profondeur de 6 m et un diamètre de 1,1 m. Pour diminuer la convection de l'air il est divisé en trois sections identiques par des revêtements en béton armé. La plus haute d'elles a un diamètre un peu plus grand et est reliée avec les autres, ce qui probablement favorise un amortissement plus rapide des déformations thermo-élastiques de la surface de la Terre suivant la profondeur. Sur le fond du puits on a placé un socle de forme cylindrique massive, de diamètre de 0,9 m, de hauteur de 1,2 m

et qui émerge de 10 cm par rapport à la surface du sol. La coupe verticale du puits est indiqué à la figure 2 et des indications plus détaillées sur sa construction sont données dans le travail {2}.

Des observations régulières y ont commencé en juillet 1979 à l'aide d'une paire de clinomètres photoélectriques Ostrovskii {3} qui avant cela enregistraient les inclinaisons dans le puits N° 2. L'appareil HΦ-06 est placé dans la direction NS et l'appareil HΦ-07 dans la direction EW avec une précision d'au moins 10'. L'azimut a été déterminé par des observations de l'étoile Polaire et transféré sur le socle de la mine à l'aide de fils à plomb de précision.

L'alimentation est assurée par des stabilisateurs de tension de haute précision utilisés précédemment dans la mine N° 2. Ces stabilisateurs fonctionnent sans interruption depuis 1976 et pas une fois ils ne sont sortis de la référence ce qui témoigne du haut degré de sûreté et de la possibilité de leur application plus large dans l'appareillage géophysique.

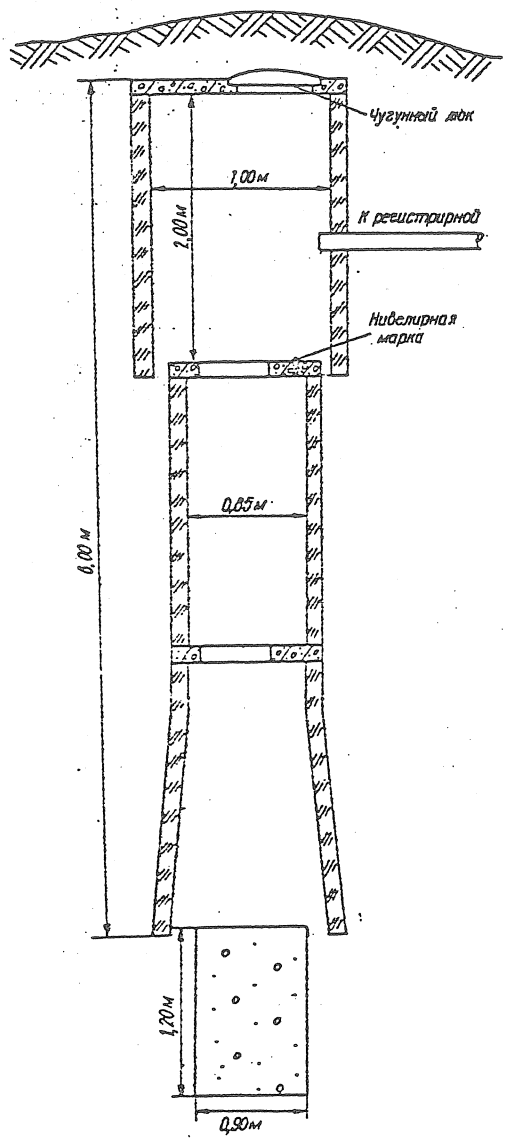

Fig. 2. Coupe verticale du puits

La sensibilité des clinomètres a été maintenue au niveau de 100 à 150 mm/seca pour qu'en cas de nécessité on enregistre sûrement de grandes variations (jusqu'à 1" par jour) signes éventuellement précurseurs d'effondrements.

Pour la période des observations portant sur environ 1,5 an, on a obtenu un enregistrement continu des inclinaisons. Cependant les données expérimentales accumulées ici ne sont pas de même qualité. Au printemps et en automne elles sont utiles non seulement pour l'étude des inclinaisons tectoniques mais aussi pour la détermination des constantes harmoniques des ondes de marées les plus importantes. Dans les autres périodes les inclinaisons thermo-élastiques dominent. Leurs perturbations les plus grandes et presque régulières ont été observées aux fréquences voisines de celle du jour. En outre dans la période d'hiver apparaissaient

des perturbations avec une période de quelques minutes à 1 heure de caractère purement accidentel. Bien qu'elles n'influencent pratiquement pas les résultats de la détermination de l'inclinaison lente ces données ne conviennent tout de même pas pour la séparation des ondes de marées. Il convient de noter que des perturbations analogues ont eu lieu dans les puits N° 2 et N° 4. Les causes en sont probablement les courants de convection de l'air dans la section du puits ou les conditions spécifiques du site des observations. Au nombre des facteurs diminuant la valeur des données expérimentales il faut porter également les interruptions qui, malheureusement, surviennent pour différentes causes. Si leur durée était dans les limites de 1 heure à deux jours, les ordonnées insuffisantes se rétabliraient par interpolation soit par le processus de Lecolazet {7} soit d'après la méthode de Matveyev-Bogdan {4}. Les lacunes plus longues sont complétées par procédé graphique, en utilisant les enregistrements antérieur et postérieur.

Les données initiales continues obtenues de cette façon sont soumises à l'analyse pour déterminer l'allure de l'inclinaison lente dans les deux directions. Pour cela on a appliqué la combinaison de B.P. Pertsev du dix-huitième ordre avec déplacement d'une heure {5} qui élimine avec un degré suffisant de précision les harmoniques à courte période, semi-diurnes et diurnes de n'importe quelle origine. Le processus de détermination de l'allure horaire de l'inclinaison lente est programmé sur ordinateur par B.S. Doubik. Les données ainsi obtenues reflètent l'inclinaison dans les perturbations à longue période thermo-élastiques. Les graphiques pour les directions NS et EW en sont donnés sur la fig. 3. Pour déterminer l'onde annuelle thermo-élastique on a résolu par moindres carrés le système d'équations.

$$X_1 + X_2 t + X_3 \cos \omega t + X_4 \sin \omega t - N_t,$$

où $X_3 = r \cos \phi$, $X_4 = r \sin \phi$; r et ϕ sont l'amplitude et la phase initiale de l'onde déterminée; X_1, X_2 sont les coefficients de la composante linéaire de l'inclinaison; N_t est la moyenne des ordonnées de l'allure de l'inclinaison lente pour 5 jours.

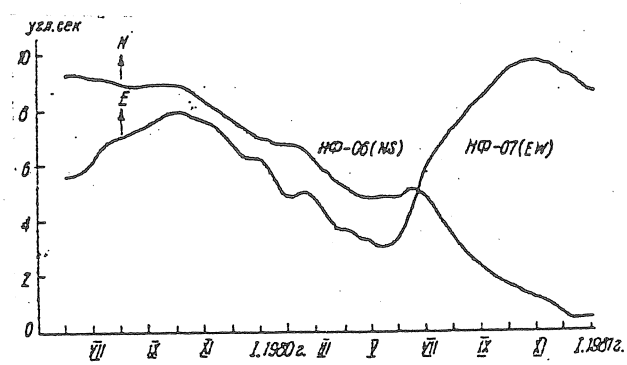

Fig. 3. Allure de l'inclinaison lente au site d'observation.

Les résultats sont donnés dans la table 1 où la phase initiale de l'onde annuelle est donnée au 1er janvier et correspond à un enregistrement de la forme $y = R \cos (t + \phi)$.

Le vecteur inclinaison se détache assez sûrement en indiquant un affaiblissement de la surface de la zone d'effondrement située au sud du point de l'observation ce qui, avec les résultats que nous avons obtenus dans les puits N° 2 et N° 4, donne la possibilité de déterminer le caractère du lieu du centre de la dépression de l'onde étudiée. Dans ce but les vecteurs inclinaisons trouvés aux trois points d'observations sont portés sur la figure I. Comme nous le constatons ils sont dirigés vers le centre de la zone d'effondrement et presque perpendiculaires à la ligne d'axe de l'étendue de la zone. Le vecteur inclinaison dans le puits N° 2 qui est situé presqu'au centre de la dépression est dirigé d'après la sécante des deux autres vecteurs sous un angle de près de 90°. Cela témoigne du fait que la dépression a, dans la région étudiée, la forme d'un chéneau incliné vers le nord-est c'est-à-dire le long de la zone d'effondrement.

La faible amplitude de l'onde annuelle dans la direction NS attire l'attention. En comparaison avec les résultats analogues obtenus dans les puits N° 2 et N° 4 elle est de presque un ordre inférieur. La cause en est probablement l'influence dominante des déformations thermo-élastiques purement locales.

TABLE 1. Résultats de la détermination de l'inclinaison lente et des paramètres de l'onde annuelle pour la période du 4-VI-1979 au 14-XII-1980.

Direction	Inclinaison lente angle/sec/an	Onde annuelle		Vecteur de l'inclinaison	
		Amplitude angle.sec	Phase	Valeur angle.sec	Direction
N-S	$-6,81 \pm 0,22$	$0,22 \pm 0,07$	$275^{2}0 \pm 17,6$	$7,14 \pm 0,21$	$162,6^{o} \pm 1,7$
E-W	$+2,13 \pm 0,24$	$2,81 \pm 0,08$	$4,7 \pm 1,6$		

Remarque. Le signe "+" dans l'inclinaison lente correspond à l'affaissement de la surface vers le nord et vers l'est du point d'observation.

Dans le but de déterminer les constantes harmoniques des ondes les plus importantes de la marée terrestre, les données expérimentales de la meilleure qualité sont soumises à l'analyse harmonique de Matveyev {6}. Le nombre des séries mensuelles indépendantes est respectivement de 16 et 14 dans les

directions NS et EW. γ et $\Delta\phi$ obtenus d'après ces résultats et leurs erreurs quadratiques moyennes, après la moyenne vectorielle, sont données dans la table 2. On observe un grand désaccord dans les paramètres γ et $\Delta\phi$ caractérisant les ondes diurnes. Il est particulièrement grand dans la direction NS. Cela est provoqué non seulement par la faible profondeur du puits mais par le fait qu'à la latitude de Karlo-Libknechtovska dans cette direction les amplitudes des ondes diurnes sont très faibles. Les résultats donnés d'après celles-ci reflètent l'influence des effets perturbateurs. Dans la direction EW on observe pour ce groupe d'ondes des résultats analogues. La précision de la séparation de leurs caractéristiques est également insuffisante. Comme paramètres les plus sûrs il faut prendre les résultats γ et $\Delta\phi$ pour l'onde la plus importante M_2 dont la période diffère de plus avantageusement de celle des influences des facteurs météorologiques.

TABLE 2. Résultats de l'analyse harmonique des observations clinométriques dans

Onde	H_T angle msec.		Direction N-S		Direction E-W	
	N-S	E-W	γ	$\Delta\phi$	γ	$\Delta\phi$
Q_1	0,817	4,892	0,600±1,240	-60,9°±88,5	0,600±0,177	13,9°±14,5
K_1	1,149	6,881	9,101±5,028	62,3±32,3	1,975±0,641	-59,7±25,6
N_2	1,500	2,134	0,598±0,150	-5,1±13,8	0,664±0,124	-10,1± 6,3
M_2	7,834	10,430	0,563±0,034	-1,0± 2,5	0,737±0,016	-5,7± 2,4
S_2	3,645	4,855	0,436±0,306	103,3±40,0	1,205±0,194	-33,9± 9,6

L'attention est attirée par la grande inégalité azimutale du facteur γ, sortant sensiblement des limites des erreurs de mesures. Le déphasage $\Delta\phi$ est voisin de zéro dans la direction NS et atteint 6° dans la direction EW. Pour la composante EW γ ne diffère pratiquement pas de la valeur globale la plus sûre. Nous avons obtenu précédemment des résultats analogues dans le puits N° 2 situé également au bord nord-est de la zone d'effondrement. Dans le puits N° 4 qui se trouve au bord sud-ouest, l'inégalité azimutale en γ a un signe opposé c'est-à-dire $\gamma_N > \gamma_S$. Cela confirme l'existence d'hypothèses de travail sur le mécanisme de l'influence des zones de la malléabilité de l'écorce terrestre sur les inclinaisons de marées et montre la possibilité de son utilisation dans la recherche géophysique ou dans le but de découvrir et de prévoir la constitution des zones d'effondrement et également des phénomènes apparentés.

BIBLIOGRAPHIE

KOUTNII, A.M., Utilisation des inclinaisons de marées dans une zone d'effondrement (Mines N° 2 et 4). Rotation et déformations de marées de la Terre, 1980, Publ. 12, pp. 47 à 50.

KOUTNII, A.M., Observations clinométriques dans une zone d'effondrement. Rotation et déformations de marées de la Terre, 1979, Publ. II, pp. 3 à 8.

OSTROVSKII, A.E., Clinomètre à enregistrement photoélectrique. Etude des marées terrestres. 1961, N° 2, pp. 41 à 75.

MATVEYEV, P.S., BOGDAN, I.D., Interpolation de courtes lacunes dans les observations des marées terrestres. Marées terrestres. Kiev. Naoukova Doumka, 1966, pp. 109 à 117.

PERTSEV, B.P., Sur le calcul de la dérive lors de l'observation des marées élastiques. Izv. Ac. des Sc. URSS. Série Géophys. N° 4, 1959.

MATVEYEV, P.S., Analyse harmonique d'une série mensuelle de marées terrestres. Marées terrestres. Kiev. Naouk. Doum. 1966, pp. 51 à 79.

LECOLAZET, R., Sur la reconstitution des observations par interpolation. Com. Obs. Roy. Belgique, N. 188 (série Geophys. N. 58), 1961, pp. 267-272.

MANIFESTATION OF THE LIQUID CORE RESONANCE EFFECTS IN TIDE STRAINS

L.A. LATYNINA
Institute of Physics of the Earth, Moscow

INTRODUCTION

The discovery of resonance effects of the Earth's liquid core is one of the basic achievements in the studies of the Earth tides. As P. Melchior wrote {1} : "The coupling mechanism between core and mantle is the key of the problem of some Earth rotation anomalies which depend on internal processes. "It was Poincaré {2}, who in 1910 solved in principle the problem of free oscillations of the Earth possessing a liquid core. Possibility of quantitative comparison of theoretically predicted events with the observed ones appeared later when H. Jeffreys and R.O. Vicente {3} and then M.S. Molodensky {4} obtained the solution of the strictly set problem of the rotation of an Earth model with inhomogeneous elastic mantle and compressible inhomogeneous liquid core. At present calculations have been made for a number of Earth models. Following below are the results by Wahr {5} obtained for a version of Gilbert-Dziewonsky model (1066-A). The effects of the ocean and of the mantle viscosity on processes of free and induced nutation are considered by S.M. Molodensky {6}.

Theoretical studies stated the existence of a free nearly diurnal nutation; its period close to 23 hours 56 minutes was defined; disturbances of forced nutations and harmonics of the Earth tides were determined at frequencies close to the resonance. In this paper we shall analyse resonance effects in the Earth tide strains. Tidal variations of gravity, tilts and deformations of the Earth's surface are proportional to a combination of Love numbers h and k and Lambert-Shida number ℓ reflecting integrally the Earth properties. Within the framework of the static theory of tides the values of these numbers are equal for different tidal harmonics. From the dynamic theory of a tide follows a strong frequency dependence of Love and Shida numbers in an area close to the resonance.

For gravity data the amplitude factor δ is defined as equal to $1 + h - \frac{3}{2} k$; from tiltmeter data we obtain the γ factor ($\gamma = 1+k-h$). Registration of linear horizontal strains of the Earth's surface by extensometers allows to define a combination of h and ℓ numbers - let it be called the n -

factors by analogy with the gravity factor :

$$\eta = h - 2\ell\ (1 + \cos^2 \alpha) \qquad (1)$$

where α is the azimuth of the segment whose strain is being measured.

Table I gives the values of h, k, ℓ and δ, γ, for the Earth model II of Molodensky {4} and 1066-A model designated below as the Wahr model {5}. Five models calculated by Wahr {5} differ in distribution of fissure boundaries in the mantle, the inner core structure and the presence of an oceanic layer. For them the differences in h, k, ℓ numbers for large waves are obtained within the interval of 0.2 %.

When comparing theoretical and observed δ and γ factors, O_1 and K_1 waves are used as determined most precisely. The wave O_1 is far from the resonance and the respective Love numbers are close to the statical ones, the K_1 wave frequency equals 15.041°/hour which approaches the resonance equal to 15.073°-15.075°/hour (according to different models). The waves ψ_1 and ϕ_1 disturbed to a greater extent than K_1 are by two orders smaller in amplitude and are determined with low accuracy.

According to Table I the difference of δ for the waves O_1 and K_1, for all the given models, is : $\delta\ (O_1) - \delta\ (K_1) = 0.021$ or 0.020 that is 2 % of the value δ. The difference of γ factor for the same waves : $\gamma\ (O_1) - \gamma\ (K_1)$ = -(0.035 to 0.040) amounts to 5-6 % of the value γ. From the data of N.N. Pariisky and others {7} for tidal gravity stations in the Soviet Union we have obtained on the average :

$$\delta\ (O_1) - \delta\ (K_1) = 0.0225 \pm 0.0011$$

By the data of the world network by Melchior and De Becker {8a} we have :

$$\delta\ (O_1) - \delta\ (K_1) = 0.0160$$

while for Western Europe (Melchior et al. {9}) :

$$\delta\ (O_1) - \delta\ (K_1) = 0.0156$$

Tiltmeter observations have a lower accuracy of determination of tidal harmonics in comparison with gravity measurements but the very effect of horizontal component is two to three times higher. By 14 tiltmeter tidal stations in Western Europe it was obtained (Melchior {8}) :

$$\gamma\ (O_1) - \gamma\ (K_1) = -0.064$$

by the network of the Ukrainian stations (Balenko {10}, Matvéev {11}) :

$$\gamma\ (O_1) - \gamma\ (K_1) = -0.044 \pm 0.009$$

Up to now extensometer data have not often been used when studying the resonance effects of the core. It is explained by the fact that tidal strains are subject to strong disturbing effects due to local topographic and geological inhomogeneities and to the cavity impact. Even the maximum comprehensive consideration of indirect effects performed by Beaumont and Berger {12} for the US stations did not allow to obtain the compatibility of corrected observed deformations with the theoretical ones with the accuracy of up to unities of percent.

Sceptical attitude to the data obtained by extensometers may be justified when we speak about the Earth global parameters h and ℓ. However the problem of resonance effects is in a specific situation : the resonance effect in tidal strains is 10 and 20 times more intense than in gravity variations and tidal tilts.

Theoretical assessment of the η-factor.

Diurnal harmonics of the solid Earth tide for horizontal deformation in the azimuth α are given by the formula :

$$\ell_{\alpha\alpha} = K_i \left[\{h - 2\ell\ (1+\cos^2\alpha)\} \sin 2\theta \cos \omega_i t - 2\ell . \sin 2\alpha . \sin\theta . \sin \omega_i t \right] \qquad (2)$$

where $K_i = D.A_i/ag$, D- being the Doodson constant, A_i - the Doodson or Cartwright decomposition amplitude, a and g - the Earth radius and gravity acceleration, θ - the colatitude, and ω_i the frequence of the i-th harmonics of the tide.

The first term of the right member of (2) has a phase synchronous with that of the corresponding harmonic of the tidal potential and is proportional to the η-factor. For the principal directions N-S (α=0) and E-W ($\alpha=\pi/2$), the second term in (2) turns into zero and $\eta = h - 4\ell$ and $\eta = h - 2\ell$; for the vertical component $\eta = h - 3\ell$.

Table 2 gives the η values for the waves O_1 and K_1 for two models calculated with the data of Table I. The η-factor is larger for the wave O_1 than for the wave K_1 : 1.54 times (Wahr) and 1.45 times (Molodensky II) in the N-S component and 1.25 times (Wahr) and 1.23 times (Molodensky II) for the E-W component. The difference of these factors amounts to 37 % and 43 % of their mean value for the N-S component and 20-22 % for the E-W one.

Thus the effect on tidal strains is 10 and 20 times higher than that on tidal tilts and tidal gravity variations. Therefore the analysis of linear tidal strains opens new possibilities for studying dynamic behaviour of the Earth liquid core.

Comparison of the observed and theoretical values of the factor $\eta=h-2\ell\ (1+\cos^2\alpha)$

A complete research of resonance effects was accomplished by D. Levine's work {13}, which gives the results of an analysis of two-year series of observations by laser extensometer at the station Poorman Mine, Colorado. Results of the analysis shown as curves of dependence of tidal harmonic transfer functions on frequency reveal a high resonance effect for the waves K_1 and P_1. Diurnal waves are also characterized by a linear increase of transfer functions with frequency. Its nature is unclear.

Resonance changes for the waves O_1, P_1, K_1 agreeing with theory are obtained by the data of vertical extensometer at the Walferdange Observatory (Ducarme et al. {14}).

V.G. Bulatsen pointed out the difference in the waves O_1 and K_1 corresponding to the resonance disturbance at a Crimean station in the USSR {15}.

We summarized the results of extensometer observations using the data of the USSR observatories and those of the world known by sufficiently complete publications. Table 3 gives theoretical and observational data R values equal to the ratio of η-factors for the waves O_1 and K_1. Theoretical values correspond to the azimuths of installation of devices at each of the observatories and are calculated for the Wahr model.

In the determination of η, factors amplitudes and phases are used of the observed waves O_1 and K_1 with the account of those indirect effects which are computed for each of the observational sites.

Tidal strains reveal clearly the resonance effect : the η factor for the wave O_1 is larger than that for the wave K_1. The only exception are the strains at the Japanese station Amagase for two directions normal to that of the entry, where the cavity effects are high.

In addition to that a systematic decrease of the observed R values is pointed out in relation to their theoretical meanings. The last column 3 presents the ratio of the observed values to the theoretical ones. Its mean

value is 0.86. A question naturally arises to what extent the obtained result is reliable, whether the difference between the observed and theoretical values is the consequence of errors and ignored indirect effects.

Analysis of errors in determination of $R = \eta(O_1) / \eta(K_1)$ values.

Our aim is to find the sources of errors that could explain the noticed difference of the observed and theoretical values R by 10-15 %.

I. The most essential impact on the value and propagation of tidal strains results from the Earth's crust inhomogeneities - geological structures, faults, relief. Tidal strains in mountain regions, in fault zones, may differ from deformations of laterally homogeneous Earth by tens or even hundreds per cent {16}. However, it is important to say that resonance effects in tidal strains are revealed despite the strong distorting effect of local inhomogeneities since the relative value of distortions is similar for all diurnal waves with an accuracy of up to resonance disturbances. The factor η for each of the waves changes under the effect of local inhomogeneities. But the ratio of these factors R for the waves O_1 and K_1 does not changes much.

Let us assess the R variations under the effect of local inhomogeneities. Let us imagine the local deformation at the observational point $\ell_{\alpha\alpha}$ in accordance with the conceptions of Bilham, King and other {12, 17, 18} as a linear function of surface regional components : meridional $\ell^r_{\theta\theta}$, latitudinal $\ell^r_{\zeta\zeta}$ and the shear one $\ell^r_{\theta\zeta}$:

$$\ell_{\alpha\alpha} = a_{11}\,\ell^r_{\theta\theta} + a_{12}\,\ell^r_{\theta\zeta} + a_{22}\,\ell^r_{\zeta\zeta} \qquad (3)$$

here a_{ij} - are certain constants depending on the point and azimuth of observations.

Let us assume the solid Earth deformation to be regional the oceanic tide is eliminated. Then the impact of deformation shear $\ell^r_{\theta\zeta}$ changing with time according to $\sin \omega_i t$ may be eliminated. We can restrict ourselves with consideration of only the tidal strain component synchronous in phase with the theoretical potential.

The regional deformation component in the azimuth α, synchronous in phase with the theoretical potential, equals :

$$\ell^r_{\alpha\alpha} = \cos^2\alpha \cdot \ell^r_{\theta\theta} + \sin^2\alpha \cdot \ell^r_{\zeta\zeta} \qquad (4)$$

The same component of the local deformation may be written as follows :

$$\ell_{\alpha\alpha} = d\,(\cos^2\alpha.\ell^r_{\theta\theta} + K.\sin^2\alpha.\ell^r_{\zeta\zeta}) \qquad (5)$$

where d and K are the constants which according to (3) are equal to :

$$d = a_{11}/\cos^2\alpha \; ; \quad dK = a_{22}/\sin^2\alpha \qquad (6)$$

R is expressed through the ratio of O_1 and K_1 waves synchronous in phase with the potential :

$$R \cdot \frac{A(O_1)}{A(K_1)} = \frac{\ell_{\alpha\alpha}\,(O_1)}{\ell_{\alpha\alpha}\,(K_1)} = \frac{\cos^2\alpha.\ell^r_{\theta\theta}\,(O_1) + K.\sin^2\alpha.\ell^r_{\zeta\zeta}\,(O_1)}{\cos^2\alpha.\ell^r_{\theta\theta}\,(K_1) + K.\sin^2\alpha.\ell^r_{\zeta\zeta}\,(K_1)} \qquad (7)$$

where $A\,(O_1)/A\,(K_1)$ is the ratio of Doodson and Cartwright decomposition amplitudes equal to 1/1.407.

If the effect of inhomogeneity is expressed in a similar variation of $\ell_{\theta\theta}$ and $\ell_{\zeta\zeta}$, i.e. d = 0, K = 1, then R local equals R regional.

Let us estimate the R value at a significant distortion of the deformation field.

Substituting the following values in (7) :

$$\begin{pmatrix} \ell^r_{\theta\theta} \\ \ell^r_{\zeta\zeta} \end{pmatrix} = DA_i/ag. \begin{pmatrix} h - 4\ell \\ h - 2\ell \end{pmatrix} . \sin 2\theta \, . \cos \omega_i t \qquad (8)$$

where A_i is respectively $A(O_1)$ and $A(K_1)$ (with $\alpha = 45°$) we shall obtain :

$$R = \frac{h\,(O_1)\,(1+K) - 2\ell\,(O_1)\,(2+K)}{h\,(K_1)\,(1+K) - 2\ell\,(K_1)\,(2+K)} \qquad (9)$$

Let K change by 100 % in relation to the undisturbed state : with K equal to 1,2 and 0.5 R respectively is 1.351, 1.313 and 1.400. Thus R varies within the limits of ± 5 % when the contribution of one of the deformation components $\ell_{\zeta\zeta}$ changes by 100 %.

We estimated R for three US observatories located in mountain regions where the relief effect on tidal strains is high. The steepness of the ridge slope at the Poorman Mine station reaches 25°, whereas near the Piñon Flat station it is 40°. Topographic corrections for these points are calculated {12, 19} and consequently the coefficient a_{ij} in (3) and d and K in (5) are

defined. According to (7) we deduce R for these stations.

Table 4 presents theoretical R values for the solid Earth tide and R calculated at these stations with due regard for topographic and geological effects for N-S and E-W directions. For the N-S direction the R difference from the regional value amounts to 2.5 % for E-W it is not more than 1 % whereas topographic corrections to tidal strains at these stations amount to tens per cent.

These examples illustrate the minor impact of inhomogeneities on the R value with their large distorting effect on tidal deformations. But these examples do not exclude the possibility of the existence of such high disturbances of the strain fields that they can essentially change the R value. Such a situation arises when extensometer is installed in the normal to the entry direction. Table 3 takes into account topographic corrections for Poorman Mine, Piñon Flat and Amagase stations for which three-dimensional models were used for calculations.

Table 3 has no corrections for the data of those stations for which the topographic effect was estimated by a two-dimensional model.

II. Ocean-load tide in contrast to indirect tectonic effects not only distorts tidal waves but changes the ratio of individual diurnal waves. In the regions where the ocean-load tide is high it should be eliminated from observational data. We may believe the data of Table 3 not to have any large errors due to oceanic tide. At the Japanese Amagase station the oceanic correction to the wave O_1 amounts to 2 % and is considered in the deformations. At the Kamitakara station a correction is given in the wave M_2-it amounts to 1 %. We may believe that the corrections in diurnal waves should not be higher than this value. Oceanic corrections are introduced to the data of Poorman Mine and Piñon-Flat stations. Evidently the data of the Queensbury station may change essentially after corrections are made.

At the Protvino station near Moscow the correction to the amplitudes of the wave O_1 amounts to less than 1 %, to the phase -0.8°. Estimation of oceanic corrections to the data of Soviet stations of southern regions shows them not to change the R value by more than 3 % and the phase by more than 2°.

III. Corrections for rotation and ellipticity of the Earth are small. According to Wahr ℓ depends on the latitude :

$$\ell = \ell_o + 0.0005\ (3\cos^2\theta - 1)\ ; \qquad \ell_o = 0.084$$

and changes, when shifting from the pole to the equator, from 0.0850 to 0.0835. Maximum change of the R value is about 1 %. At the latitude of 45° this value increases by 0.2 %.

IV. One of the reasons of obtaining reduced R values may be an incomplete splitting of waves $K_1P_1S_1$. For the analysis of data of many Soviet stations, the Pertsev method was used. Let us estimate the error introduced to the factor $\eta(K_1)$ when using this method. In the harmonic analysis of a one month series the amplitude and phase of the sum of waves is defined-of the studied wave K_1 and of waves close to the latter among which the prevailing contribution is made by the P_1 wave. Then from the obtained sum the close harmonics are excluded with the assumption that the coefficient of proportionality between the amplitude of deformation wave and corresponding harmonic of the potential is similar for all close harmonics. When we speak of gravity observations this assumption does not lead to noticeable errors since the factor for the waves P_1 and K_1 differs less than by 2 %. For tidal strains the error may be higher. Using the formulae by which the exclusion of the P_1 wave is made in the Pertsev method {20} we defined what part of the summary wave K_1, P_1 is defined by the wave P_1. For consecutive seven months (I-VII, 1970) the following values are obtained (in fractions of the K_1 wave amplitude) : 0.237, -0.001, -0.260, -0.011, 0.072, 0.270, 0.249. On the mean for six months as it follows from the difference of K_1 and P_1 frequencies, the contribution of P_1 wave to the global amplitude is close to zero. We obtain it as equal to 2 %. When averaging for 7 or 11 months the P_1 wave contribution reaches 3 %. When using the data for 4 months the share of the P_1 wave may reach 8 %. The P_1 wave is ignored with the assumption that its η equals 0.1728, whereas in fact (by Wahr) η is equal to 0.2414; this leads to a change of R value by 0.6 % at P_1 contribution of 2 %, by 2 % at P_1 contribution of 5 %, by 3 % at P_1 contribution of 8 %. Depending on the period of observations this change may be both positive and negative. For the data of Table 3 the maximum possible R variation of the order of 3 % may take place for the stations Garm II and Garm III.

Discussion of the results

Variation of h and ℓ numbers in the area of nearly diurnal resonance causes significant changes of the amplitudinal factor of the linear tidal strain $\eta = h - 2\ell\ (1+\cos^2\alpha)$ for the horizontal component and $\eta = h-3\ell$ for the vertical one. In meridian direction the theoretical value η for the wave O_1 is by 50 % higher than that for the K_1 wave. Such a large resonance changes of the η-factor, if compared with δ and γ factors, and opens new prospects for the use of extensometer data to study the Earth's core-mantle interactions in detail.

Defined from observations the values of η-factor reveal the resonance effect : $\eta\ (O_1)$ is 15-30 % higher than $\eta\ (K_1)$. Summarization of the available data shows a systematic decrease of the ratio $R = \eta(O_1)/\eta(K_1)$ obtained from observations if compared with the theoretical one. This reduction equals 14 % and is defined with the accuracy of ± 3%. The obtained discrepancy was not caused by the considered possible errors of R definition resulting from indirect effects of tectonics and ocean, ellipticity of the Earth, incomplete splitting of K_1 and P_1 waves. However it is possible that not all the systematic errors in definition of linear tidal strains were taken into account. It is also possible that the precise calculation of the oceanic effect in the waves O_1 and K_1 will give more essential correction. These questions require further studies.

We should like to point out that some variation of the resonance curve for h, k, ℓ is possible when the discrepancy of the observed and theoretical values is eliminated and it does not contradict experimentally determined values of the difference of δ and γ factors and their constant nutation ε.

At variation of the resonance parameter β in the Molodensky theory {4} by 12 % the divergence of the observed and theoretical R is eliminated. Being so the difference $\delta(O_1) - \delta(K_1)$ becomes equal to 0.019 instead of the assumed value of 0.022. Its experimental value equals 0,0225-0,0172 {7, 8, 9}. The difference $\gamma(K_1) - \gamma(O_1)$ becomes equal 0,039 instead of the assumed value of 0,035. The value of this difference equal to 0.044 {10, 11}, 0.064 {8} were obtained by observations. The amplitude of constant nutation becomes equal to 9".2062 instead of the assumed 9".2032. Its experimental value equals 9".2069 ± 0".0034 {2}.

Thus, the agreement of theoretical and observed values at some variation of the resonance curve for the Love and Shida numbers is not getting worse.

The first priority task of measurements should be an increase of the accuracy of determination of linear tidal strains and the elimination of indirect effects from observations. The discussed results are obtained by means of averaging the data of 25 points. This bulk of data may apparently be essentially increased. There are several hundred extensometers operating in the world at present. Tide analysis is performed only by individual observatories and mainly the data by M_2 and O_1 waves are published. The use of already existing experimental extensometer data will evidently allow to increase many-fold the list given by Table 3 and doing so to obtain more significant results.

In conclusion I express my deep gratitude to Prof. N.N. Pariisky for his advice and consultations.

TABLE 1. Theoretical values of h, k, ℓ numbers and δ, γ factors for the Molodensky II (A) and Wahr (B) models.

model / harmonic	A	B	A	B	A	B	A	B	A	B
	h		k		ℓ		δ		γ	
O_1	0.614	0.603	0.300	0.298	0.0809	0.0841	1.164	1.152	0.686	0.689
P_1	0.593	0.581	0.290	0.287	0.0817	0.0849	1.158	1.147	0.697	0.700
K_1	0.535	0.520	0.256	0.256	0.0837	0.0868	1.143	1.132	0.721	0.730
ψ_1	0.928	0.937	0.475	0.466	0.0697	0.0736	1.215	1.235	0.547	0.523

TABLE 2. The factor $\eta = h-2\ell(1+\cos^2\alpha)$ for the Molodensky II and Wahr models.

Orientation	Model	The η factor for waves and wave ratios			
		O_1	K_1	O_1/K_1	$(O_1-K_1)/(O_1+K_1)$
α=0	Molodensky II	0.2904	0.2002	1.45	37 %
h=4ℓ	Wahr	0.2666	0.1728	1.54	43 %
α=π/2	Molodensky II	0.4522	0.3676	1.23	20 %
h-2ℓ	Wahr	0.4348	0.3464	1.25	22 %
Vertical	Molodensky II	0.3713	0.2829	1.31	27 %
h-3ℓ	Wahr	0.3507	0.2596	1.35	30 %

TABLE 3. Comparison of the theoretical and observed values $R = \{h-2\ell(1+\cos^2\alpha)\}\ O_1 / \{h-2\ell(1+\cos^2\alpha)\}\ K_1$

Name of station	Coordinates	Azimuth	Number of devices	Duration of a series in months	Amplitudes $\times 10^9$ and phase shifts O_1	K_1	Values R obs.	Values R theoret.	Ratio of R obs. to theoret
1. Poorman Mine USA (13)	40.0 N 105.3 W	173°	1	24	0,80 +3°	0,60 +1°	1,23	1,52	0,81
2. Piñon-Flat USA (12, 21)	33.6 N 116.5 W	0°	1	12	4,03 -2°	4,16 -11°	1,39	1,54	0,90
3. Amagase Japan (22)	34.5 N 135.5 E	107,5°	2	12	4,00 +7,6	4,68 +17,5	1,25	1,27	0,98
4. Kamitakara Japan (23)	36.3 N 137.3 E	45°	1	7	2,81	3,14	1,26	1,35	0,93
5. Queensbury Great Britain (17,24)	53.8 N 1.9 E	45°	5	24	4,25 +4°	5,25 +3°	1,31	1,35	0,97
6. Walferdange Luxemburg (14)	49.7 N 6.1 E	37,8°	5	12	5,92 -22,4°	7,00 +26,3°	1,23	1,38	0,89
7. "	"	7,6°	1	12	5,08 -3°	6,00 +4°	1,19	1,54	0,77
8. "	" vertical		1	30	6,67	7,60	1,23	1,35	0,91
9. Tiefenort GDR (25)	51.0 N 10.2 E	90°	2	6	7,95 0°	9,80 +1°	1,14	1,25	0,91
10. The Crimea (15)	44.6 N 33.6 E	173,5°	1	30	2,71 -2°	2,86 +6°	1,33	1,53	0,87
11. Protvino USSR (28)	54.9 N 37.1 E	0°	1	12	3,35 +2,5°	4,21 -3,5°	1,12	1,54	0,73
12. "	"	90°	1	12	8,30 -3,0	10,30 0°	1,13	1,25	0,91

13. Garm I USSR (27)	39.3 N 70.3 E	2,5°	1	11	3,23 +9°	4,06 +9°	1,12	1,54	0,73	5948
14. "	"	98,5	1	7	1,87 +26°	2,67 -29°	1,00	1,26	0,79	
15. Garm II (16)	39.3 N 70.3 E	177,3	4	4	18,2 +1°	23,0 -18°	1,17	1,54	0,76	
16. Garm III (28)	39.1 N 70.7 E	17,6°	2	4	3,80 -9°	3,90 -9°	1,37	1,49	0,92	
17. "	"	111,1°	2	4	1,98 +18°	2,46 +23°	1,17	1,27	0,92	
18. Varzob USSR (29)	38.8 N 68.8 E	105°	1	12	6,31 +1°	7,94 +4°	1,12	1,26	0,89	
19. "	"	15,0°	2	12	9,80 -14°	11,5 -23°	1,26	1,50	0,84	
20. Talgar USSR (30)	43.2 N 77.2 E	3°	1	12	3,37 +13°	3,82 +16°	1,26	1,54	0,82	
21. Turgen USSR (30)	43.3 N 77.6 E	38,0°	2	12	8,05 -13°	8,97 -22°	1,33	1,38	0,96	
22. "	"	146,6°	2	18	2,06 +27°	2,89 +27°	1,00	1,41	0,71	
23. Zugdidi USSR (31)	42.6 N 41.9 E	172°	2	7	2,50 35°	2,30 15°	1,30	1,52	0,85	
24. Tbilisi USSR (32)	41.7 N 44.8 E	150°	1	10	3,17	3,46	1,29	1,43	0,90	
25. "	"	60°	1	3	3,85	4,66	1,16	1,30	0,89	
								mean	0.86±0.02	

TABLE 4. R values for several USA stations

Azimuth	R			
	theoretical	Stations		
		Boulder	Piñon-Flat	Mine
N-S	1.543	1.583	1.585	1.528
E-W	1.255	1.260	1.255	1.241

REFERENCES

{1} MELCHIOR, P. : Earth Rotation and Nutations in regard to Liquid-Core, Mantle and Ocean-Lithosphere Tidal Interactions.- Proceedings, 4-th Symp. geodesy and Physics of the Earth, GDR, Karl Marx-Stadt, 1980, part. 1, pp. 4-36.

{2} MELCHIOR, P. : Physics and Dynamics of the Planets. Izd. Mir, 1976, tch. II, pp. 484.

{3} JEFFREYS, H., VICENTE, R.O. : The Theory of Nutation and the Variation of Latitude-Monthly Notices. R.A.S. 1957, V. 117, pp. 142-161.

{4} MOLODENSKY, M.C. : Theory of Nutation and Diurnal Earth Tides. In the book : Zemnye prilivy i nutatsia. M., Izd. ANSSSR, 1961, pp. 3-25.

{5} WAHR, J.M. : Body Tides on an Elliptical Rotating, Elastic and Oceanless Earth.-Geophys. J. 1981, V. 64, N. 3, pp. 577-703.

{6} MOLODENSKY, S.M. : Ocean and Mantle Viscosity Effects on the Earth Nutation.- Izv. ANSSSR, Fizika Zemli, 1981, N. 6, pp. 3-17.

{7} PARIISKY, N.N., BARSENKOV, S.N., VOLKOV, V.A. et al. : Tidal Gravity Variations in the USSR, Sb. Izuchenie zemnykh prilivov, Izd. Nauka, M., 1980.

{8} MELCHIOR, P. : Report on the Activities of the International Centre for Earth Tides. Proceedings, 8-th Symp. Earth Tides, Bonn, 1977, pp. 30-43.

{8a} MELCHIOR, P. and DE BECKER, M. : A discussion of world-wide measurements of tidal gravity with respect to oceanic interactions, lithosphere heterogeneities, Earth's flattening and inertial forces. Phys. of the Earth and Planetary Interiors. 31 (1983) 27-53.

{9} MELCHIOR, P., KUO, J.T., DUCARME, B. : Earth Tide Gravity Maps for Western Europe-Physics of the Earth and Planetary Interior, 1976, 13, pp. 184-196.

{10} BALENKO, V.G. : The Study of the Earth's Surface Tilts by Kiev-Artemovsk Profile. Kiev, Naukova Doumka, 1980, p. 174.

{11} MATVEEV, P.S. : Results of Harmonic Analysis of Tiltmeter Observations in Shmakov and Ingults.-Sb. Vrashchenie i prilivnye deformatsii Zemli, 1, 1972, V. 4, pp. 105-170.

{12} BERGER, J., BEAUMONT, C. : An Analysis of Tidal Strain Observations from the United States of America. The Inhomogeneous Tide.- Bull. Seism. Soc. Am., 1976, V. 66, N. 6, pp. 1821-1846.

{13} LEVINE, J. : Strain Tide Spectroscopy and the Nearly Diurnal Resonance of the Earth. Geoph. J.R. Astr. Soc., 1978, V. 54, N. 1, pp. 27-41.

{14} DUCARME, B., FLICK, J., MELCHIOR, P., VAN RUYMBEKE, M. : Tidal Deformations Measured with Gravimeters, Clinometers and Extensometers at the Underground Laboratory of Geodynamics at Walferdange. Proc. 8-th Symp. Earth Tides, Bonn, 1977, pp. 661-677.

{15} BULATSEN, V.G. : Tidal and Slow Earth's Crust Deformations by the Data of Extensometer Observations in Inkerman (the Crimea), Sb. Vrashchenie i prilivnye deformatsii Zemli YII, 1975, pp. 9-15.

{16} LATYNINA, L.A., SHISHKINA, T.P. : On the Intensity of Tidal and Tectonic Movements in the Zone of the Surkhob Fault. Izv. ANSSSR, Fizika Zemli, 1978, N. 6, pp. 87-93.

{17} ITSUELY, U.J., BILHAM, R.G., GOUTLY, N.R., KING, G.C.P. : Tidal Strain Enhancement Observed across a Tunnel. Geoph. J.R. Astr. Soc., 1975, V. 42, pp. 555-564.

{18} BEAVAN, J., BILHAM, R., EMTER, D., KING, G. : Observations of Strain Enhancement across a Fissure. Deutsche Geod. Komm. Akad. Wiss. Rech. B., Munchen, 1979, 231, pp. 47-58.

{19} LEVINE, J., HARRISON, J.C. : Earth Tide Strain Measurements in the Poorman Mine near Boulder, Colorado, J. Geoph. Res., 1975, V. 81, pp. 2543-2555.

{20} PERTSEV, B.P. : Harmonic Analysis of Elastic Tides.- Izv. ANSSSR, ser. geofiz., 1958, N. 8, pp. 946-958.

{21} BERGER, J., WYATT, F. : Some Observations of Earth Strain Tides in California. Phil. Trans. R. Soc. Lond. A., 1973, 274, pp. 267-277.

{22} TAKEMOTO, S., Effects of Local Inhomogeneities on Tidal Strain Measurements. Bull. Disast. Prev. Res. Inst. Kyoto Univ. 1981, V. 31, part. 4, N. 284, pp. 211-237.

{23} NAKAGAWA, I., DOI, H., OIKE, K. SHIDA'S Number Obtained by Extensometric Observations in Kamitakara, Japan. Symp. Marées Terrestres, Strasbourg, 1969. Observatoire Roy. Belgique, 1970, pp. 150-153.

{24} BILHAM, R.G., KING, G.C.P., MCKENZIE, D.P. : Inhomogeneous Tidal Strains in Queensbury Tunnel, Yorkshire-Geoph. J. Astr. Soc., 1974, 37, pp. 217-226.

{25} LATYNINA, L.A., KARMALEEVA, R.M., HARWARDT, H., SIMON, D. : Uber die Ergebnisse von Straimetervergleichsregistrierungen in Tiefenort. Proceedings 4-th Symp. Geodesy and Physics of the Earth, GDR, Karl-Marx-Stadt, 1980, Part. III, pp. 676-692.

{26} KARMALEEVA, R.M., LATYNINA, L.A. : Results of Observations of the Earth's Surface Tidal Deformation at the Protvino Station (Russian Platform). Bull. Inf. Marées Terrestres, 1979, N. 82, pp. 5143-5149.

{27} LATYNINA, L.A., KARMALEEVA, R.M. : Tidal Strains at the Garm Observatory, Tadjik SSR. Izv. ANSSSR, Fizika Zemli, 1981, N. 12, pp. 84-87.

{28} LATYNINA, L.A. : On Tidal Strains at the Chusal Station, Tadjik SSR. Sb. Izuchenie Zemnykh Prilivov, Nauka, M., 1980, pp. 207-214.

{29} LATYNINA, L.A., RIZAEVA, S.D. : On Tidal Strain Variations before Earthquakes. Tectonophysics, 1976, 31, pp. 121-127.

{30} LATYNINA, L.A., KARMALEEVA, R.M., TIKHOMIROV, A.V., KHASILEV, L.C. : Secular and Tidal Deformations Recorded in the Fault Zone of the North-Eastern Tien-Shan. Proceedings Eauropean Seism., Comm. and European Geoph. Society, 1978, Strasbourg, V. 5, pp. 407-420.

{31} BALAVADZE, B.K., ABASHIDZE, C.G., ZHARINOV, N.A. et al. : Analysis of the Earth's Crust Tidal Strains by Extensometer Observations at the Inguri Hydro-Power Station. Bull. Acd, Sci. Georgian SSR, 1980, 98, N. 3, pp. 573-576.

{32} KARTVELISHVILI, K.Z. : Investigation of the Earth Tides by Observations in Tbilisi. Izd. Metsniereba, Tbilisi, 1978, p. 168.